SITE SPECIFIC OPTIMIZATION OF ROTOR / GENERATOR SIZING OF WIND TURBINES

A Thesis
Presented to
The Academic Faculty

by

Kirk Martin

In Partial Fulfillment
of the Requirements for the Degree
Master of Science in the
School of Mechanical Engineering

Georgia Institute of Technology
December 2006

SITE SPECIFIC OPTIMIZATION OF ROTOR / GENERATOR SIZING OF WIND TURBINES

Approved by:

Dr. Sam V. Shelton, Advisor
School of Mechanical Engineering
Georgia Institute of Technology

Dr. Susan W. Stewart
Strategic Energy Institute
Georgia Institute of Technology

Dr. William J. Wepfer
School of Mechanical Engineering
Georgia Institute of Technology

Date Approved: August 24, 2006

ACKNOWLEDGEMENTS

I'd like to thank several people who have made this work possible. First, I'd like to thank my advisor, Dr. Sam V. Shelton. It was through a random set of events that led to my work for him at the Strategic Energy Institute, but I could not have chosen an advisor better suited to my interests, personality, and working style. His guidance and insight, both with regards to this thesis and to the wider field of energy and energy technologies, have been invaluable to me. Our shared passion for energy and energy related issues has made working for him a pleasure.

I'd also like to thank Dr. Susan Stewart. It was her analysis of the Georgia coastal wind resource that eventually led to this thesis, and her advice regarding wind and other topics has been helpful in completing this work. Michael Schmidt was helpful with data checking and other tasks.

Finally, I want to thank my family and friends. It is through their support that I have been able to focus on my work. My parents taught me that value of learning early on, and have always been supportive of my various decisions to continue my education.

TABLE OF CONTENTS

LIST OF TABLES

LIST OF FIGURES

NOMENCLATURE

A	Area
AWEA	American Wind Energy Association
AR	Aspect Ratio
BE	Blade Element
BEM	Blade Element Momentum Theory
c	Chord Length
C_D	Coefficient of Drag
C_L	Coefficient of Lift
C_p	Coefficient of Performance
CF	Capacity Factor
D	Drag
EES	Engineering Equation Solver
GE	General Electric Corporation
Gen Cap	Generator Capacity
h	Weibull Probability Function
H	Height above the Surface of the Earth
k	Weibull Probability Shape Parameter
kg	Kilogram(s)
kW	Kilowatts
kW-hr	Kilowatt-hours
l	Weibull Probability Scale Parameter
L	Lift
m	Meter(s)
$\dot{m}$	Mass Flow Rate
MW	Megawatts
MW-hr	Megawatt-hours
N_{BLADES}	Number of Rotor Blades
NREL	National Renewable Energy Laboratory
P	Pressure
P_0	Ambient Pressure
P_R	Static Pressure at the Plane of the Rotor
PURPA	Public Utility Regulatory Policies Act of 1978
Q	Torque
r	Width of a Blade Element
R	Distance from the Rotor Hub to a Blade Element
RPM	Revolutions per Minute
s	Second(s)
SA	Specific Area, Rotor-to-Generator Size
t	Time
T	Thrust
TSR	Tip Speed Ratio
u	Change is Swirl Velocity from Upstream to the Plane of the Rotor
v	Change in Air Velocity from Upstream to the Plane of the Rotor

V	Relative Air Velocity due to Wind Speed and Rotation at a Blade Element
V_0	Wind Speed
V_{avg}	Average Wind Speed for a Wind Resource
V_{in}	Velocity of Incoming Air entering the Plane of the Rotor
V_{rot}	Linear Velocity of a Blade Element due to Rotation
V_{rmc}	Root-Mean-Cubed Velocity
$\dot{W}$	Power
α	Angle of Attack
α_{stall}	Stall Angle
€	Euro
Γ	The Gamma Function
Ω	Angular Velocity of the Rotor
ρ	Air Density
Φ	Angle between the Plane of the Rotor and V
Θ	Angle between the Plane of the Rotor and the Blade Element Chord
λ_1	Thrust Coefficient
λ_2	Torque Coefficient

SUMMARY

Wind is increasingly being used to provide a share of the world's electricity. Advantages of wind generated electricity include zero emissions and zero fuel cost. However, because the velocity of the wind varies on a daily and hourly basis, the maximum amount of power produced by a wind turbine at a given time cannot be controlled by the operator. This leads to a different criterion for optimum design than that used for other equipment where the rate of electricity production can be controlled up to the equipment maximum rating. The optimum design for a wind turbine operating in a given wind resource is the design that produces the most electrical energy for a given capital cost.

The purpose of this study was to develop a methodology to determine the optimal rotor-to-generator size for a given wind resource; and to determine how this optimum varies as the wind resource varies. In each of the trials, the total cost of the rotor plus electrical system was held constant, and the rotor-to-generator size was varied with this cost constraint. Generator capacity was gradually increased as rotor diameter was gradually decreased, keeping the combined cost constant. Annual electrical energy output was calculated for each rotor-to-generator size, and the rotor-to-generator size with the highest annual electricity produced was determined to be the optimum. The relationship was studied at wind resources defined by average wind speeds of 6, 7.25, and 8.4 m/s representing a class 2, 4, and 6 wind resource, and Weibull probability shape parameters , *k,* of 1.8, 2, and 2.2. At each wind resource, cost constraints of $50,000, $200,000, $500,000, $1,000,000, and $2,000,000 (manufacturing costs) were examined.

Generator sizes were allowed to vary from 500 kW to 20 MW, and rotor diameters from 20 m to 200 m. A total of 45 trials were run representing 5 cost constraints at 9 different wind resources.

A model was developed to predict total annual electrical production from a wind turbine of given design characteristics at a wind resource defined by the Weibull probability parameters. The blade element momentum method was used to determine power output of a given wind turbine configuration at a given wind speed, and the Weibull probability function was used to determine total hours-per-year at that wind speed. Total annual electrical energy was calculated, and the results for individual rotor-to-generator configurations were compared. The blade element momentum technique used is an iterative process, so Engineering Equation Solver (EES) software was used as the platform on which the model was developed.

Results show that the optimum relationship of rotor-to-generator size is a function of the cost constraint in addition to a function of the wind resource. This is a product of the differing cost relationship between the rotor and the generator. Whereas the cost of the generator scales linearly with the size of the generator (power capacity), the cost of the rotor is a cubic function of the diameter. This leads to a shift in the rotor-to-generator relationship in favor of the generator as total cost, and therefore turbine size, increases. It also leads to a corresponding reduction in optimal capacity factor as cost increases.

Other trends observed show a shift toward a lower rotor-to-generator size as the average speed of the wind resource increases, and a shift toward a higher rotor-to-generator size as the k value of the resource increases. The shift toward the rotor at higher k values is slight and appears to be diminishing in some of the cases examined.

This is to be expected as theory indicates the relationship should approach a constant ratio as k moves toward infinity, which represents a resource with a constant wind velocity. Optimal capacity factor was shown to rise with average wind speed for the range of parameter values studied. Likewise, optimal capacity factor was shown to increase with Weibull shape parameter *k* within the range of values studied. The behavior of optimal capacity factor with increasing *k* mirrored closely to that of the optimal rotor-to-generator size. Theory indicates optimal capacity factor should approach unity as *k* approaches infinity; i.e., a constant velocity wind resource.

In each of the trials an optimal capacity factor was found to exist that was well below unity. Optimal capacity factors for the conditions examined range from a low of 0.23 to a high of 0.48. Higher capacity factors than these result in less electricity being produced.

An interesting implication of the analysis is to show that, at large turbine sizes, there is an advantage in having multiple generator size options available for a given rotor. The analysis shows that at wind sites with high average wind speeds and low *k* values, the ideal generator size for a given size rotor is significantly larger than at sites with low average wind speeds and high k values.

Wind farm developers can use the results from this analysis, and the methodology presented, as a tool in terms of selecting ideal turbines for a known wind site. Design graphs show the optimal relationships between rotor and generator sizes at a range of wind conditions. Lines of constant capital cost direct the user to the best configuration for a given turbine size range. There are many factors involved in turbine selection and

this methodology is one tool amongst many that planners can use to determine the best equipment design for their application.

CHAPTER 1

INTRODUCTION

1.1 Background

Wind power is the fastest growing technology for producing electricity in both the United States and the world. In 2005 alone installed capacity in the U.S. grew from 6,718 to 9,149 megawatts[2]—an increase of 36% percent. Increases in 2006 are projected to be over 3000 MW[2]. Table 1.1 shows the increase in worldwide installed capacity over the past decade.

Table 1.1: Worldwide Installed Wind Capacity[1]

Region	***Installed Capacity (MW)***				
	End-1995	End-1999	End-2003	End-2004	End-2005
Europe	2,518	9,307	28,706	33,660	40,504
North America	1,676	2,619	6,677	7,241	9,550
South & Central America	11	87	139	208	232
Asia & Pacific	626	1,403	3,034	4,698	6,782
Middle East & Africa	13	39	150	241	256
TOTAL World Wide	4,844	13,455	38,706	46,048	57,324

1.1.1 History

Humankind's harnessing of wind energy to do useful work has a long history. Some of the landmarks in the history of wind energy are as follows:

Circa 5000 B.C. - Use of wind power for transportation. Oldest record of a sailing vessels is from an Egyptian vase dated to about 3100 B.C[24]. There is reason to believe that the invention of sailing pre-dates this[12,21,24].

500 to 900 A.D. - Wind turbines appear in Persia. First machines were vertical axis devices that relied primarily on drag as the operating principle. They were used for pumping water. There is some evidence the

invention actually came from China, and may date to as early as the B.C. era[6,12,25].

1200's - Horizontal axis windmills appear in Europe. Earliest documentation is from 1270 A.D. for a machine used for grinding[6].

1200 to 1870 - Windmills spread throughout Europe. There were 600 years of gradual improvements in the vertical axis design. Improvements included shift from drag oriented to lift oriented machines, ability to "yaw" into the direction of the wind, and changes in blade shape that vastly improved efficiency. Machines were used for a variety of purposes including grinding, milling, cutting, and pumping water[6].

1888 - First use of a wind turbine to generate electricity by Charles Brush of Cleveland, OH. The machine had a rotor size of 17 m and a power capacity of 12 kW. It was in operation for 20 years[6,11,25].

1970's & 1980's - Oil crisis prompts R&D into alternative energy sources. Department of Energy sponsored a series of projects exploring wind. Federal Law signed in 1978 (PURPA) required utilities to purchase power from wind farms at avoided cost. Additionally, federal investment tax credits were established encouraging investment in wind turbines. This lead to significant investment, particularly in California (which also offered state level incentives). Over 1500 MW of capacity was installed. The federal tax credits were withdrawn in the early 1980's, and investment stopped[25].

1990's - Center of activity moved to Europe, spurred by concerns about global warming and nuclear energy. By 2001, Europe had 11,831 MW of installed capacity (compared to 2,568 in the U.S.)[9]. The average size of turbines grew substantially (see Figure 1.1 below)[10].

2000 to present - A combination of factors caused a rapid expansion of wind development in the U.S. and in the world. These factors included government incentives of various types (production tax credits, renewable portfolio standards, etc), but also included significant advances in turbine design and manufacturing[9,25]. The cost of electricity from wind decreased to within the range of other forms of electricity production (around 5 cents per kW-hr in the U.S.)[4]. Worldwide capacity increased more than four-fold, from 13.5 GW to 57.3 GW[1]. The largest machines reached 5 MW in power output, with rotor sizes larger than 120 meters in diameter[28].

Figure 1.1 summarizes the modern history of wind turbines as a means of electricity generation.

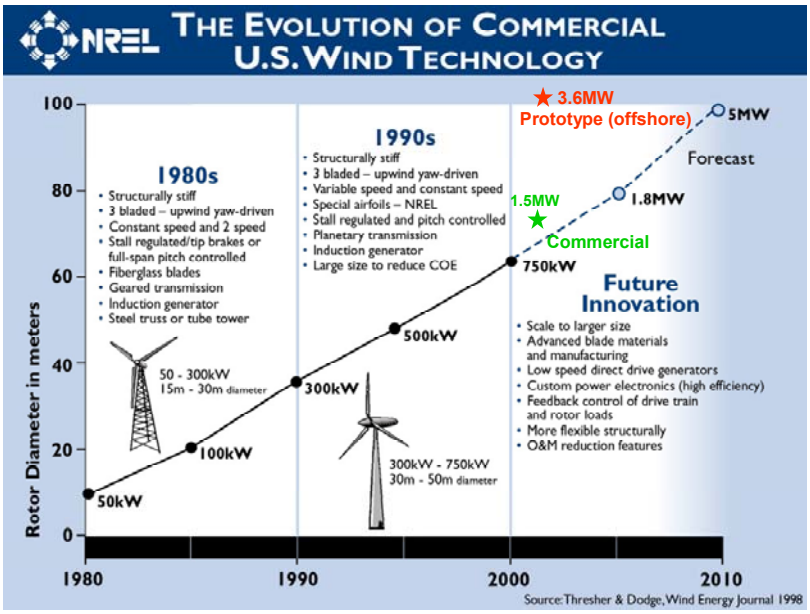

Figure 1.1: The Evolution of Commercial Wind Energy Technology[10]

1.1.2 Types of Wind Turbines

Figure 1.2 shows the various types of wind turbines that have been built over the years. While most people think of upwind facing, horizontal axis machines when they think of wind turbines, this is only one of many possible configurations. However, it is the configuration that has thus far proved to be the most efficient and economical. Virtually all modern machines have this configuration.

Most modern machines have rotors with three blades. Machines in the past have been built with as few as one blade and with numbers approaching 20 or more. An early 20th century water pumping turbine seen on farms throughout the U.S. is an example of a many-bladed turbine. Increasing the number of blades increases starting torque, which is desired in the water pumping application. There is also a slight efficiency gain with added blades, but this gain is small and diminishes with each blade added. Cost, however, goes up substantially with each blade. The three blade turbine has been

adopted as a good optimum in terms of efficiency, cost, and the balancing of rotational forces[27].

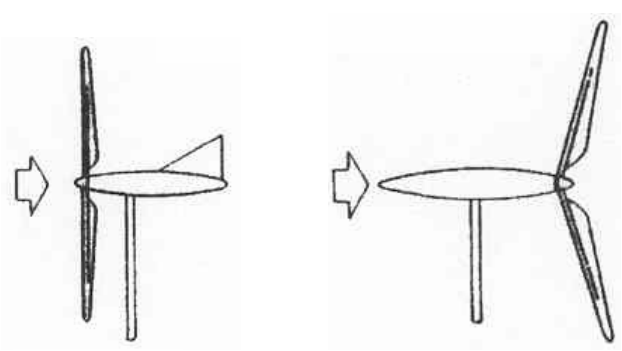

Upwind vs. Downwind Designs

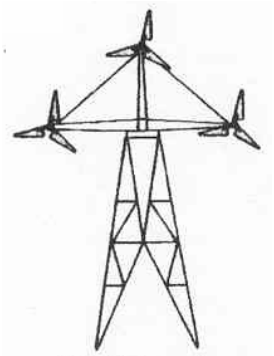

Multiple Rotor Machines

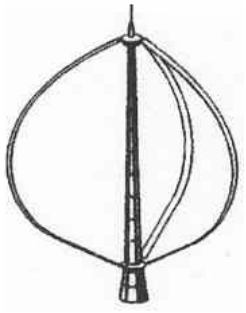

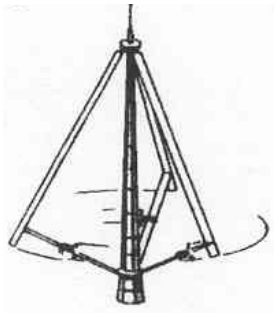

Vertical Axis Turbines

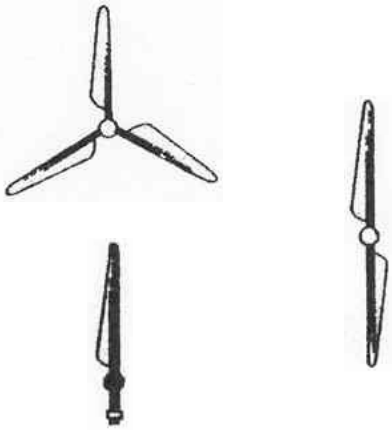

3, 2, & 1 Bladed Designs

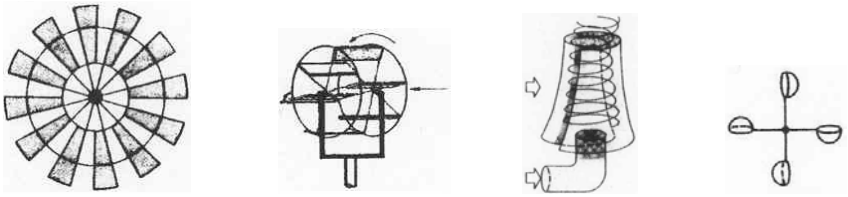

Other

Figure 1.2: Various Wind Turbine Configurations[25]

1.1.3 Increase in Size

Figure 1.3 shows the growth in size of wind turbines over the past twenty-five years. The largest turbine commercially available today is the REpower 5M. It has a rotor diameter of 126 meters (diameter) and a maximum power output of 5 MW[28]. General Electric,s GE 3.6sl is the largest machine from an American manufacturer with a rotor size of 111 meters and a 3.6 MW generator[14]. Because power is a function of the swept rotor area, which is a function of the diameter squared, increasing rotor size makes sense in terms of significantly increased output.

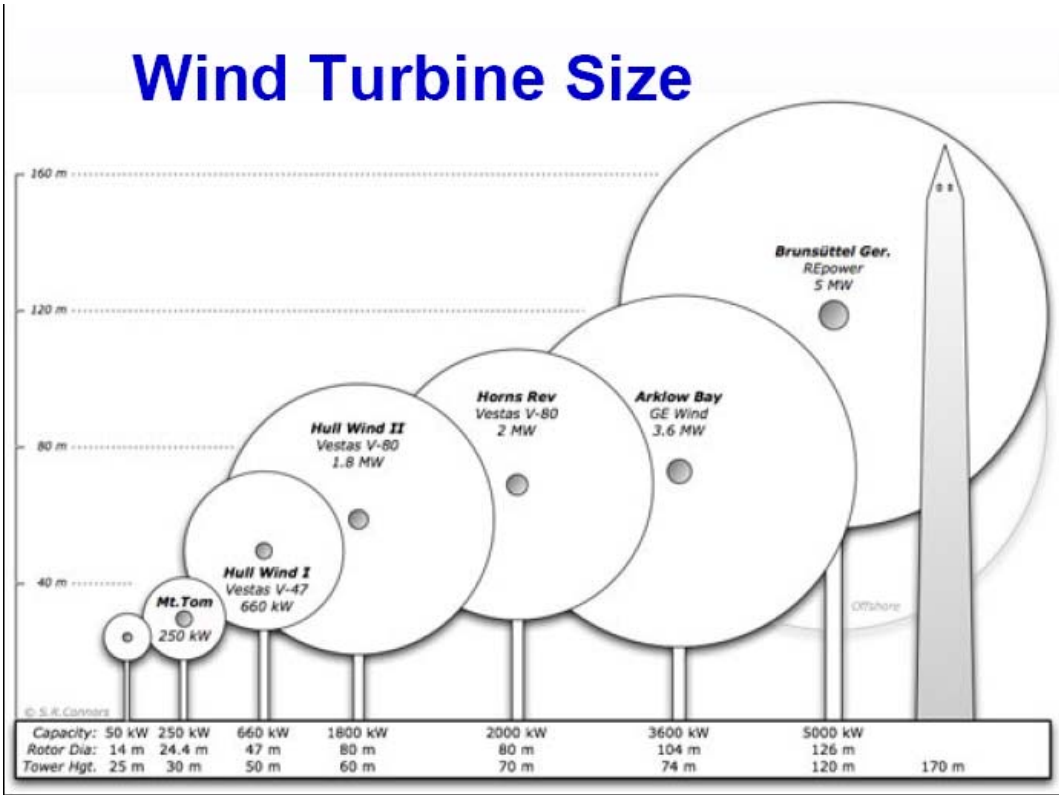

Figure 1.3: Growth in Wind Turbine Size over the past 25 Years [1]

1.2 Modern Wind Turbines

Figure 1.4 shows the layout of a modern wind electric generating machine (commonly referred to as wind turbines). Figure 1.5 shows a cut-away view of the nacelle, the housing situated at the top of the tower which contains the generator, gearbox, and other equipment, and from which the rotor hub extends. Besides the rotor blades, the majority of the components that make the wind turbine functional reside within the nacelle.

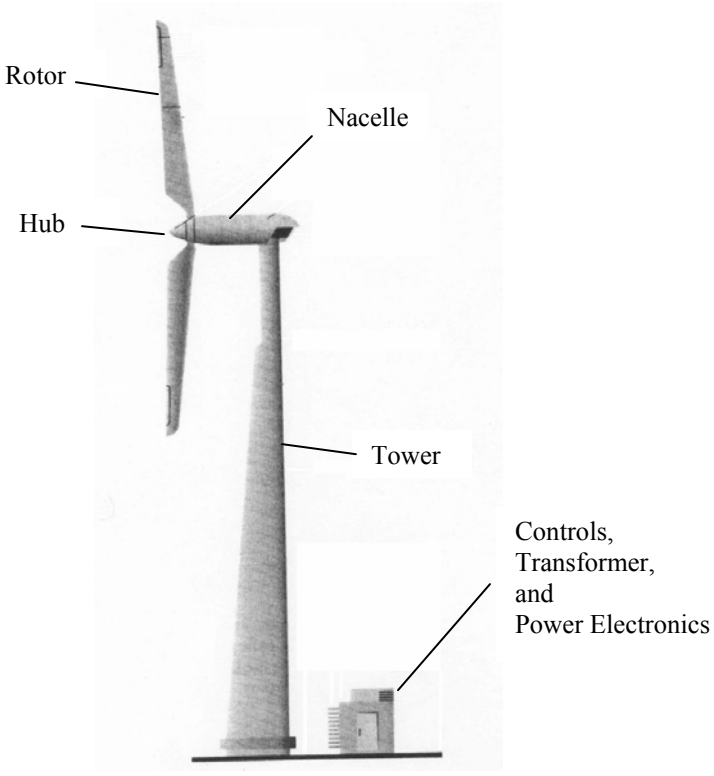

Figure 1.4: Wind Turbine Layout[27]

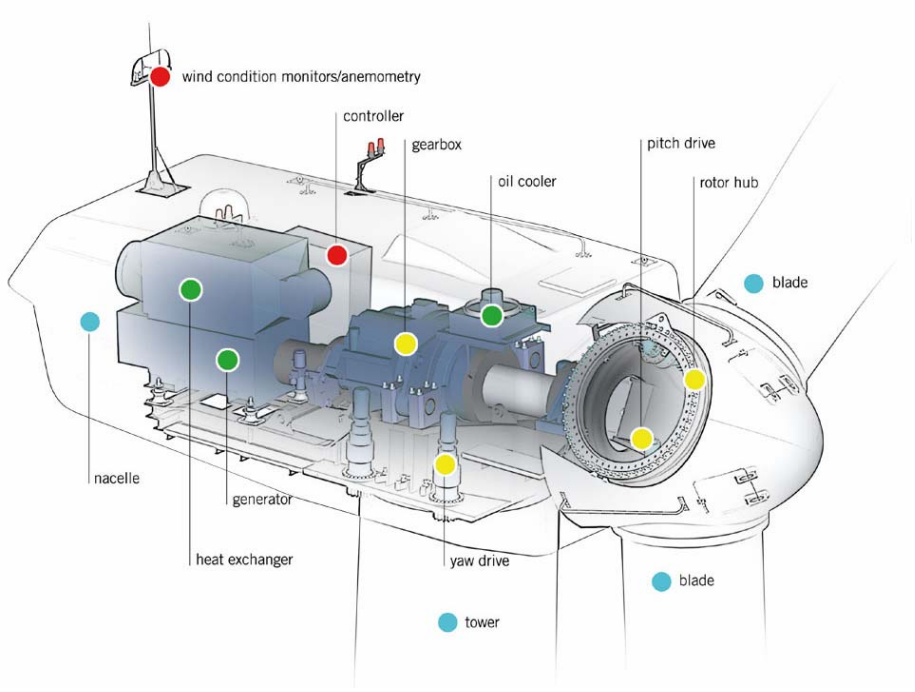

Figure 1.5: Wind Turbine Nacelle[14]

1.2.1 Control Mechanisms

Yaw Control – "Yaw" refers to the ability of the nacelle and rotor to rotate into the wind. The nacelle sits on a vertical pivot point such that it can rotate clockwise or counter-clockwise as viewed from a point directly above. Small turbines used for remote, off-grid residences (< 1 kW) often use a passive yaw control system—namely a tail-fin (a wind vane) that aligns itself (and therefore the rotor) with the wind. Large modern machines use wind sensing equipment and electric motor drives to align the nacelle and rotor into the wind[9,25,27].

Pitch Control – Most modern turbines are able to adjust the pitch of the rotor blades within a certain range in order to improve the efficiency of the device. At a given wind speed and a given RPM, there exists an ideal pitch angle for a rotor blade of a given design to extract as much wind energy as possible. Also, at high wind speeds the blades are feathered in order to not over-power the generator (the generator has constant output at maximum capacity above a certain wind speed). At very high wind speeds, the blades are pitched to stop the rotor, which is done to protect the equipment from damage[9,25,27].

Speed Control – In the past, most turbines operated at a fixed RPM. Some modern turbines have the ability to adjust RPM within a given range[14,34]. This is important because for a given rotor design there exists an ideal RPM that varies according to wind speed. This relationship is defined by a tip speed ratio (TSR). TSR refers to the ratio of the linear speed of the rotor tip compared to the speed of the incoming wind. Every turbine has an optimum tip speed ratio that is fixed, and generally this falls somewhere between 4 to 6[25,27].

1.3 Wind Resource

The power generated by wind turbines varies with the cube of the velocity—doubling the speed of the wind results in an eightfold increase in power. Location of a wind farm therefore is extremely important in terms of the profitability of the farm.

The American Wind Energy Association (AWEA) has devised a scale that rates potential wind generating sites on a scale from 1 to 7[3]. This is based on the average wind power density at the site, which can approximately be related to average wind speed.

Table 1.2 shows the AWEA wind class scale at heights of 10 meters and 50 meters above the surface of the Earth.

Table 1.2: Wind Resouce Power Classes at 10 m and 50 m^3

Wind Power Class	Wind Power Density (W/m^2)	Wind Speed (m/s)	Wind Power Density (W/m^2)	Wind Speed (m/s)
1	<100	<4.4	<200	<5.6
2	100 - 150	4.4 - 5.1	200 - 300	5.6 - 6.4
3	150 - 200	5.1 - 5.6	300 - 400	6.4 - 7.0
4	200 - 250	5.6 - 6.0	400 - 500	7.0 - 7.5
5	250 - 300	6.0 - 6.4	500 - 600	7.5 - 8.0
6	300 - 400	6.4 - 7.0	600 - 800	8.0 - 8.8
7	>400	>7.0	>800	>8.8

However, since the distribution of winds at a given site can follow a variety of forms, Table 1.2 only tells part of the story. The distribution of wind speeds at a site is not normal and tends to follow a Weibull distribution[9,25,27]. The nature of the Weibull distribution is discussed in detail in Chapter 2. Figure 1.6 shows the distribution of wind speeds for a site off the Georgia coast near Savannah with a correlated Weibull distribution curve.

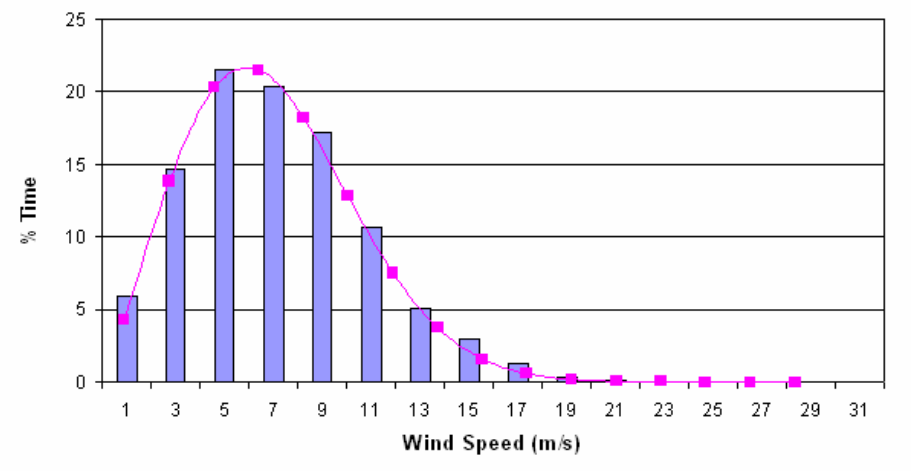

Figure 1.6: Wind Speed Distribution for Coastal Georgia Site[32]

1.4 Optimal Design

1.4.1 Dispatchable vs. Non-dispatchable Energy Resources

With most forms of electricity production, the primary fuel is "dispatchable". This means it can be converted to electrical energy at a rate which is controlled by the operator. This is important because it allows the electric utilities industry to adjust power output to meet demand as it fluctuates throughout the day. Wind power is not dispatchable. An operator cannot simply turn up the speed of the wind when more electricity is needed.

Traditional power plants generally fall into one of two categories: base load plants and "peaking" plants. Baseload plants provide a steady supply of power that is at, or less than, the lowest demand on the system. Peaking plants fluctuate their output to make up the difference. Due to the non-dispatchable nature of the resource, wind plants don't fit well into either category. It is impossible for a wind plant to provide a steady supply of power, and it is impossible for them to provide extra power "on demand". One advantage of wind plants, however, is that the energy resource is free. Once a plant is built, its operating costs are very low and are more-or-less limited to maintenance. Because of this, the objective of a wind plant is to always capture as much energy as possible. Other plants, particularly peaking plants, can then adjust output to match demand.

1.4.2 Optimal Rotor/Generator Sizing and Capacity Factor

Capacity factor is defined as energy produced during a given period (usually a year) divided by the amount that would have been produced if the equipment was driven

at capacity the entire time. It is often desirable in purchasing electric generating equipment to try to select devices that will operate at a high capacity factor. This is driven by economics. Equipment represents a significant investment, and there is considerable incentive not to purchase more machinery capacity than is absolutely necessary. Because of the non-dispatchability of the wind resource, capacity factor should **not** be an important consideration in selecting wind turbines. The reason for this is explained by Figure 1.7.

Figure 1.7 shows two possible configurations of rotor and generator for a given fixed cost. Figure 1.7-a shows a very large rotor on a very small generator. This machine will have a very high capacity factor because even at relatively low wind speeds the rotor will be able to drive the generator at or near its capacity. At higher wind speeds, however, the blades will be feathered so that the generator is not overpowered. This is energy that could have been captured with a larger generator, and represents electricity that is not being produced.

Figure 1.7-b shows the opposite extreme—a small rotor on a large generator. This machine will also have a low production of electricity, but this time it is the rotor that is the limiting factor. Regardless of how fast the wind blows, the rotor will not overpower the generator and the energy will be captured. However, this configuration will almost certainly not be optimal. The generator represents a significant expense, and it would never be driven near its capacity. Its capacity factor would be very low. Simply put, in this configuration too much money has been spent on the generator.

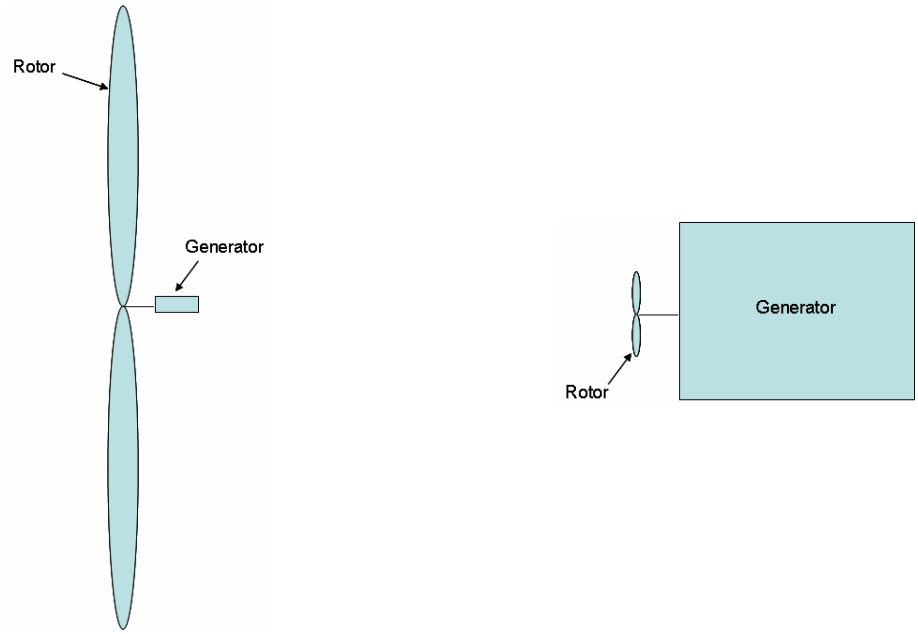

Figure 1.7: Two Possible Rotor / Generator Sizing Relationships at a given Fixed Capital Cost

The optimal configuration will fall somewhere between these two extremes. It will vary from site to site and will be a function of the wind speed distribution at a given site. The purpose of this study is to analyze this relationship. It is to determine the optimal relationship of rotor to generator size (at a fixed capital cost) at wind sites of differing Weibull distributions, to document general trends regarding this relationship, and to establish a methodology for carrying out this type of analysis at sites with parameters that fall outside the range of values looked at in this study.

1.5 Literature Review

A number of studies have been published concerning the site specific design of wind turbines. These studies are outlined below with a brief description of their nature

given. Many seem to look at capacity factor as the variable being optimized, with the objective of maximizing capacity factor. Due to the non-dispatchable nature of the wind resource, this is the wrong parameter to optimize in designing the rotor-to-generator size. Total electricity produced for a given capital investment is a better measure of the cost effectiveness of a project.

Optimum Windmill – Site Matching (Z.M. Salameh, I. Safari)

This study matched existing turbines with existing wind sites. It used the published performance coefficients (performance coefficients are explained in Chapter 2) to calculate electricity generated at two separate wind sites during four different months. The best turbine for the site was determined to be the one with the highest capacity factor[29].

Site-Specific Design Optimization of 1.5 – 2.0 MW Wind Turbines (P. Fuglsang, K. Thomsen)

Cost of energy (a function of energy production and manufacturing + installations costs) was optimized in this study. Numerous wind turbine characteristics were varied to see the affect on performance using wind data from two wind sites, one offshore and one onshore. An aero-elastic load prediction model was used to determine performance. Rotor size was varied between 60 m and 74 m (dia.), and generator capacity was limited to two values, 1.5 and 2.0 MW. Hub height, RPM, and other features were also investigated, as well as wind phenomenon such as turbulence and shear. In total, 20 degrees of freedom were monitored. This seems to be a very complex analysis that

considers rotor / generator sizing to some degree, but does not look explicitly at the optimum relationship for various wind characteristics[13].

Optimum Siting of Wind Turbine Generators (S.H. Jangamshetti, V.G. Rau)
This study looked at 54 potential wind sites around India and predicted the performance of 12 existing turbines at those sites. The machine with the highest predicted capacity factor was determined to be the best machine for a given site[23].

Wind Turbine Generator Trends for Site-specific Tailoring (K. Jackson, C.P. van Dam, D. Yen-Nakafuji)
This study matched a 1 MW generator with four rotor sizes—50, 60, 70, and 90 meters (dia.). Performance was modeled with blade element momentum theory (discussed in Chapter 3) using data from specific wind sites in California. It looked at both long and short term wind variations—seasonal and time of day—and attempted to match electrical production with electrical demand (for the State of California). A metric called "value factor" was created as a general measure of the necessity of electricity generated at a given time (how well it matched loads), and a "revenue factor" was defined as the product of value factor and capacity factor. The configuration with the highest predicted revenue factor was chosen as the optimum[22].

Risk Based Optimum Site-Matching Wind Turbine Analysis (R. Billington, H. Chen)
This was a statistical analysis of the ability of wind turbines at known wind sites to meet electrical load. A Monte Carlo simulation was used to assess 'loss of load' occurrences, which was essentially a measure of a machines failure to meet its share of the load. Seven turbine designs were examined at two wind sites. While characteristics such as

cut-in and cut-out speeds were looked at, physical parameters such as rotor size were not addressed. Several performance measuring indices were introduced, and a methodology was presented around selecting an optimum turbine for a given situation (which includes wind data, as well as load data). No single measure was chosen as an optimizing parameter, although some were deemed more significant. All of the parameters pointed to a machines general ability to meet its share of the load. The purpose of the study seems to be to present a methodology and guidelines for selecting a turbine based on several parameters[8].

On the Prediction of Capacity Factor and Selection of Size of Wind Electric Generators – A Study based on Indian Sites (K. Sasi, S. Basu)

This study presented a method for selecting a rotor and generator size for a given wind site. A Weibull distribution is fitted to a series of sites in India, and for each site an optimal rated wind velocity is determined using a mathematical method. This optimal rated velocity is then used to select and/or design a turbine for the site. Figure 1.8 shows a normalized power curve for a generic wind turbine. Rated velocity is the velocity at which a turbine *begins* to produce its maximum power. Total electricity produced is looked at as one of the output parameters, and this is incorporated into a cost of electricity parameter that is optimized around[30].

Of the studies reviewed, only the study by Sasi and Basu[30] considered total electrical production as an indicator of optimal design. This was also the only study that explicitly looked at the optimal relationship between generator and rotor size. The study used a mathematical method to approximate an optimal "rated speed" for wind turbines at

a series of sites, and then stated that turbines should be designed for this optimal rated speed. "Rated speed" refers to the wind speed at which a turbine begins to produce power at its rated capacity. At any higher wind speed, the turbine will continue to produce power at its rated capacity until the "cut-out speed" is reached (and the machine stops producing power). This is shown in Figure 1.8 using a normalized power curve for a generic wind turbine. The method for determining the sizing relationship is to select a generator, and then select a rotor that will drive the generator at its capacity when the wind is blowing at this optimal rated speed (assuming other parameters, such as RPM). Or the technique can be applied in reverse by first selecting a rotor, and then choosing the generator based on rated speed. This is different than the methodology that was employed in the current study and seems to produce somewhat different results. In particular, this method seems to predict a smaller rotor size (for a given generator) than is predicted in the current study, and that is seen on existing equipment.

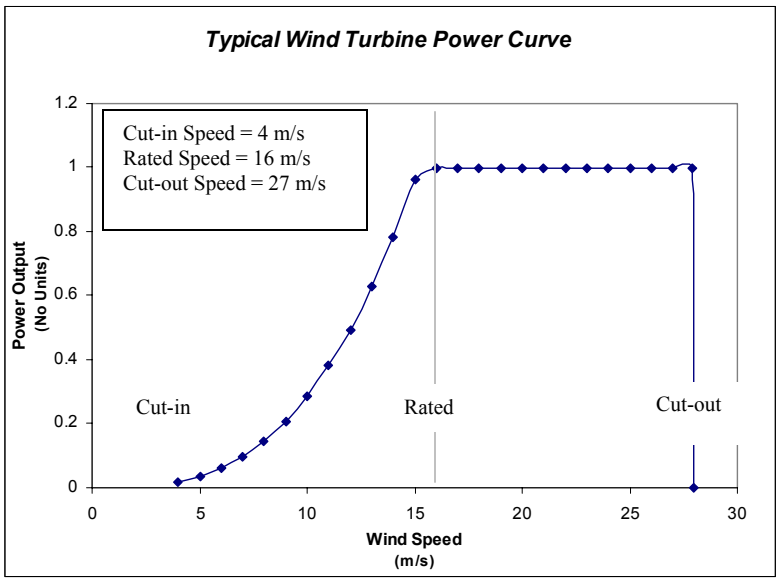

Figure 1.8: Typical Wind Turbine Power Curve

CHAPTER 2

TECHNICAL BACKGROUND

2.1 Wind Energy Fundamentals

2.1.1 Energy Available from the wind

The purpose of a wind turbine is to convert the kinetic energy of the wind into work and/or electricity. The power available in a horizontal column of wind is equal to:

$$\dot{W} = \tfrac{1}{2}\dot{m}V_0^2 \tag{2.1}$$

where:

V_0 = velocity of wind
$\dot{m}$ = mass flow rate (flux) of wind through the column

However,

$$\dot{m} = \rho A V_0 \tag{2.2}$$

where:

ρ = density of the air
A = cross-sectional area of the column

So the equation for power becomes,

$$\dot{W} = \tfrac{1}{2}\left(\rho A V_0\right)V_0^2 \rightarrow \dot{W} = \tfrac{1}{2}\rho A V_0^3 \tag{2.3}$$

This is important because it shows that the power produced is a function of the cube of the wind speed. Doubling the speed of the wind results in an eightfold increase in available power.

2.1.2 Energy Extracted by a Wind Turbine

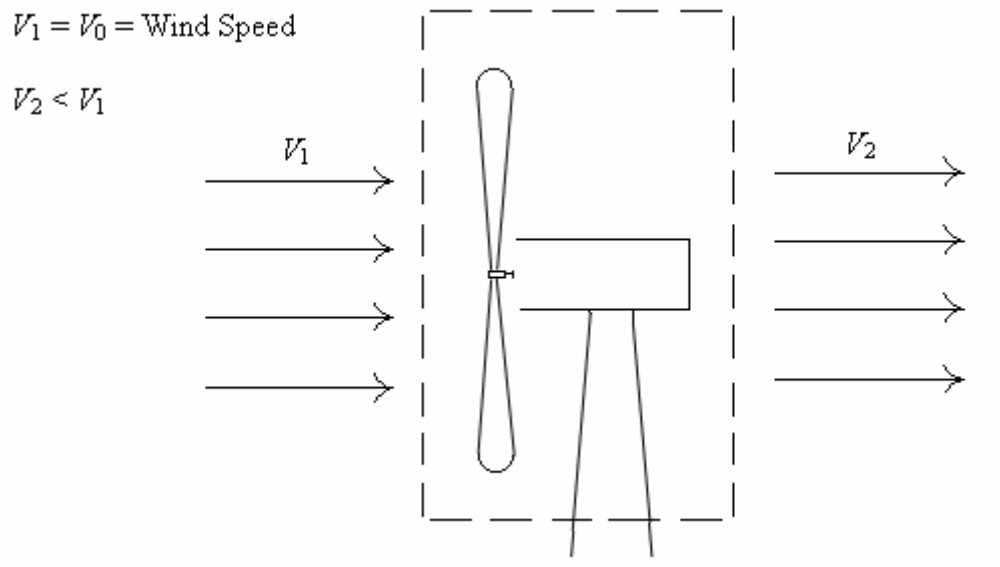

Figure 2.1: Wind Turbine Control Volume

Figure 2.1 shows a control volume drawn around a turbine rotor. The power extracted from the wind is:

$$\dot{W} = \tfrac{1}{2}\dot{m}(V_1^2 - V_2^2) \tag{2.4}$$

$\dot{m}$ must be evaluated using the velocity at the plane of the rotor. This is the average of V_1 and V_2. Area, A, is the swept area of the rotor

$$\dot{W} = \tfrac{1}{2}\left[\rho A\left(\frac{V_1 + V_2}{2}\right)\right](V_1^2 - V_2^2) \tag{2.5}$$

This can be rearranged to produce,

$$\dot{W} = \tfrac{1}{2}\rho A V_1^3 \frac{(1+\frac{V_2}{V_1})\left[1-\left(\frac{V_2}{V_1}\right)^2\right]}{2} \tag{2.6}$$

or

$$\dot{W} = \tfrac{1}{2}\rho A V_0^3 C_P \tag{2.7}$$

with C_P being a function of V_1 and V_2. C_P is the coefficient of performance of the wind turbine, and represents a measure of efficiency for the system. In 1919, German physicist Albert Betz showed that there is an ultimate limit to this factor of 16/27 (about 59%)[9,25,27]. This occurs when V_2 is equal to 1/3rd the value of V_1. Figure 2.2 shows the value of C_P vs. V_2/V_1. This result may seem surprising, but has a valid, physical reason that will be discussed in the following section.

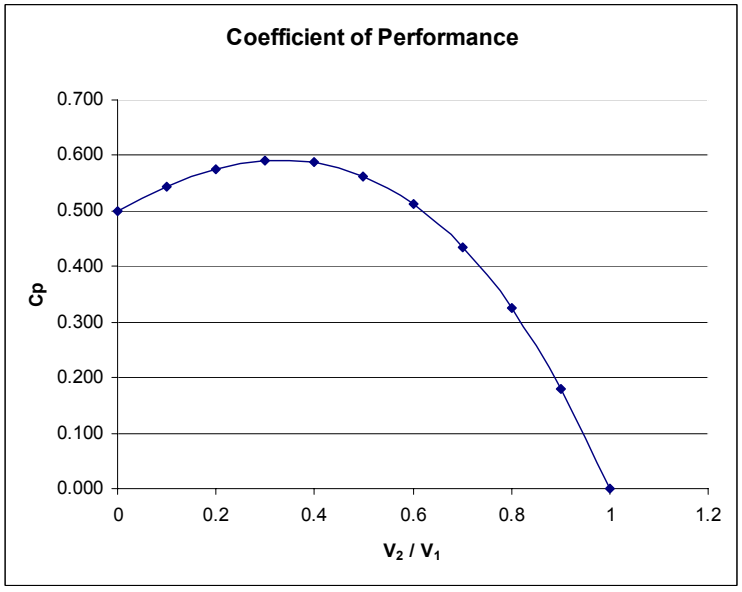

Figure 2.2: Wind Turbine Efficiency as Function of V_{in}/V_{out}

2.1.3 Actuator Disc Theory

Figure 2.3 shows the path followed by air molecules as they travel through the plane of a wind turbine rotor. This is well established both by wind tunnel tests and theory. If the air passing through this plane is treated as an incompressible substance (a valid assumption in this case as long as it is not moving near the speed of sound), it must follow a path similar to this because of the loss of kinetic energy that occurs as the air molecules make this journey. The air leaving the rotor will have a slower velocity than the air entering, and therefore the cross-sectional area of the air entering must be less than that of the air leaving[18,25,27,31].

The Betz limit is a consequence of this phenomenon. As the efficiency of the turbine increases, the upstream cross-sectional area of the wind that intersects the rotor decreases. This means that the mass flow rate decreases. More energy is being extracted from each elemental air mass, but less air mass is coming into contact with the rotor. The Betz limit represents the transitional point whereby further increases in efficiency are more than offset by the decrease in the mass flow rate. This occurs at 59% of the total power in the column of wind.

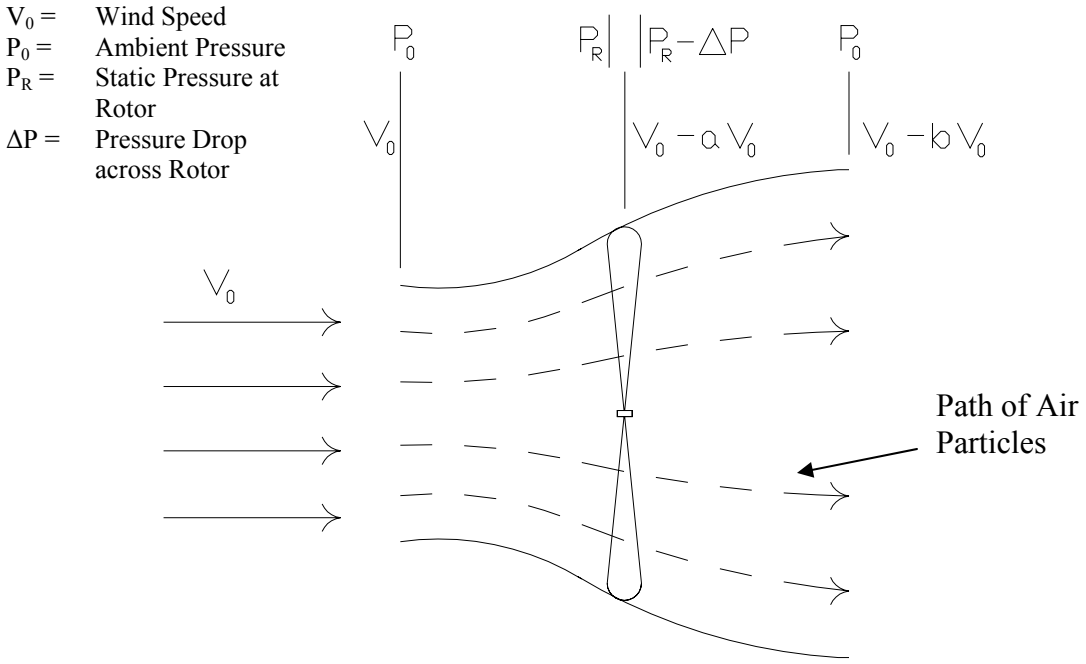

Figure 2.3: Actuator Disc Flow

Actuator disc theory treats the rotor as a disc that causes a pressure drop across the plane of the rotor[18,25,31]. This assumption, combined with the Bernoulli principle, states that ½ of the decrease in velocity must occur ahead of the plane of the rotor, and ½ must occur behind the plan of the rotor. The proof of this is presented below.

Referencing Figure 2.3 and applying the Bernoulli Equation, which assumes reversibility and incompressibility:

Initial Pressure

$$P_{initial} = \underbrace{P_0 + \frac{\rho}{2} V_0^{\,2}}_{\text{Free Stream}} = \underbrace{P_R + \frac{\rho}{2}\left(V_0 - aV_0\right)^2}_{\text{Just Ahead of Rotor}} \tag{2.8}$$

Final Pressure

$$P_{final} = \underbrace{\left(P_R - \Delta P\right) + \frac{\rho}{2}\left(V_0 - aV_0\right)^2}_{\text{Just Behind Rotor}} = \underbrace{P_0 + \frac{\rho}{2}\left(V_0 - bV_0\right)^2}_{\text{Far Behind Rotor}} \tag{2.9}$$

Using the free stream definition for $P_{initial}$ and the far-field definition for P_{final}

$$\Delta P = P_{initial} - P_{final} = \left(P_0 + \frac{\rho}{2} V_0^{\,2} \right) - \left[P_0 + \frac{\rho}{2} \left(V_0 - bV_0 \right)^2 \right] = \rho V_0^{\,2} b \left(1 - \frac{b}{2} \right) \quad (2.10)$$

Rotor thrust is the change in momentum from far ahead of the rotor to far behind it

$$T = \dot{m} \left[V_0 - \left(V_0 - bV_0 \right) \right] = \dot{m} \left(bV_0 \right) = \left[\rho A \left(V_0 - aV_0 \right) \right] \left(bV_0 \right) = \left[\rho V_0^2 b \left(1 - a \right) \right] A \quad (2.11)$$

Thrust is also equal to $\Delta P \cdot A$, so

$$\Delta P = \rho V_0^2 b \left(1 - a \right) = \rho V_0^{\,2} b \left(1 - \frac{b}{2} \right) \rightarrow a = \frac{b}{2} \quad (2.12)$$

2.2 Wind Distribution

2.2.1 Weibull Distribution

Wind patterns at a given site tend to be consistent on an annual basis, and can be described using the Weibull probability density function[9,25,27]. This is defined as follows:

$$h\left(V_0 \right) = \left(\frac{k}{l} \right) \left(\frac{V_0}{l} \right)^{(k-1)} e^{-\left(\frac{V_0}{l} \right)^k} \quad \text{for } 0 < V_0 < \infty \quad (2.13)$$

where:

V_0 = wind velocity

k is the shape parameter, l is the scale parameter, and

$$h = \lim_{\Delta V_0 \rightarrow 0} \left\{ \frac{\text{Fraction of time wind speed is between } V_0 \text{ and } \left(V_0 + \Delta V_0 \right)}{\Delta V_0} \right\}$$

Parameters k and l relate to the average wind speed in the following manner:

$$V_{avg} = l \times \Gamma \left(1 + \frac{1}{k} \right) \quad (2.14)$$

where Γ represents the Gamma function.

Integrating h between two different velocities gives the percentage of time in a given year the winds can be expected to fall within this velocity range. Integrating h between 0 and ∞, by definition, is equal to unity (there is a 100% probability the wind speed will be between 0 and ∞ in a given year).

$$\int_{V_0=0}^{\infty} h \times dV_0 = 1 \tag{2.15}$$

Figure 2.4 shows the effect of varying shape parameter k while keeping scale parameter l constant. As k increases, the distribution becomes narrower and more uniform. As can be seen in the graph, k=3 implies a distribution that is relatively close to a normal distribution. Wind site data tend toward a k value of 2, but sites with values as low as 1.5 and as high as 3 have been investigated[23,30]. In this study, sites with k values between 1.8 and 2.2 are considered. The majority of wind sites considered for projects fall within this range.

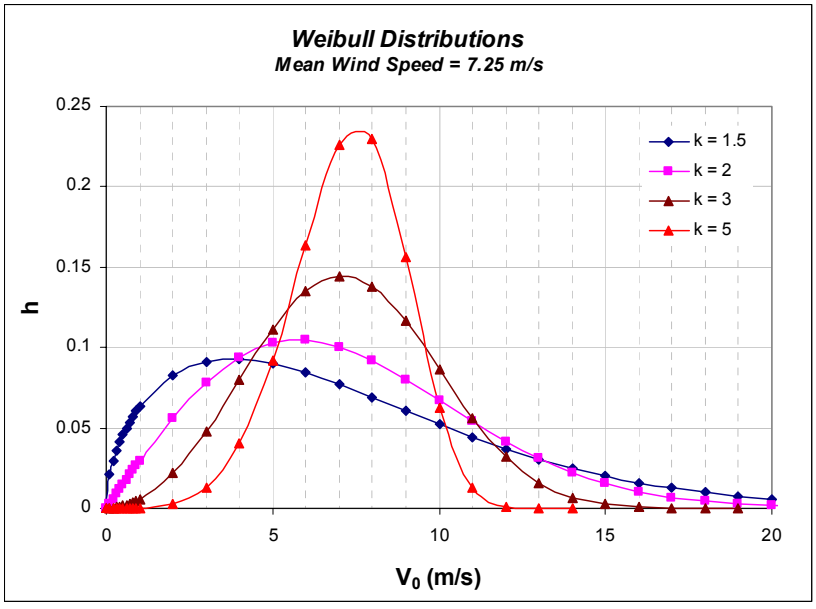

Figure 2.4: Effect of Varying Value of Shape Parameter *k* on Weibull Distribution

Figure 2.5 shows the effect of varying the average wind speed while keeping the shape parameter constant.

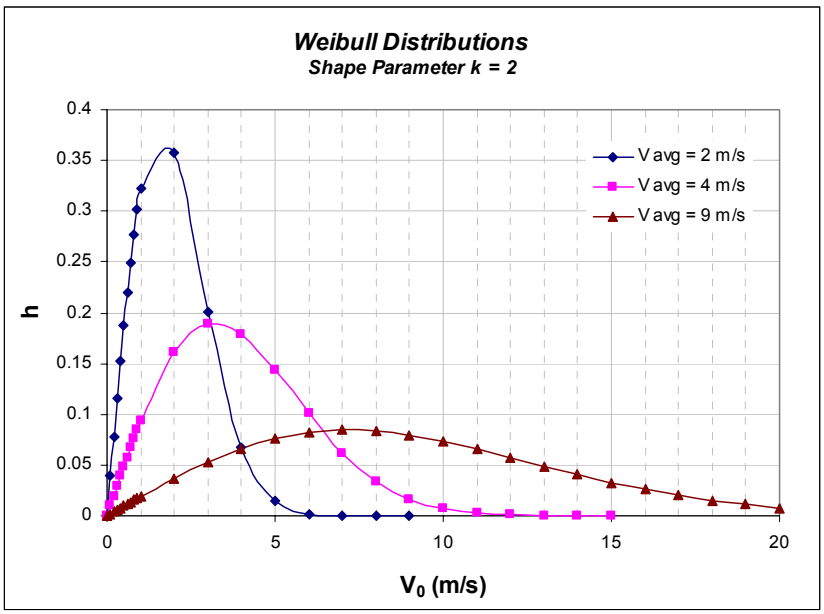

Figure 2.5: Effect of Varying Value of Average Wind Speed on Weibull Distribution

Figure 1.6 in section 1.3 shows the measured wind data for an offshore site near Savannah Georgia. The data has been curve fitted to a Weibull distribution with a shape factor of k=2 and a mean wind speed of 7.356 m/s.

2.2.2 Wind Classes

Table 1.2 in Chapter 1 shows the classes of winds as defined by AWEA (American Wind Energy Association) at 50 meters height. Wind classes are defined by the average power density (W/m^2) through a vertical plane, perpendicular to the direction of wind flow, at 50 meters above the surface*. Except for Class 1 and Class 7 wind sites,

* Power densities defining the classes are calculated assuming a wind site with a Weibull shape parameter k = 2

the value corresponds to the first digit of the initial power density value that defines the class. A site that averages 200 W/m^2 is a Class 2 site, a site that averages 300 W/m^2 is a Class 3 site, and so on. This is at 50 meters. These values closely correspond to wind speed values, and can be extrapolated to any height typically using the 1/7th power law[3,27].

$$V_2 = V_1\left(\frac{H_2}{H_1}\right)^{\frac{1}{7}} \tag{2.16}$$

where:

H_1 = 50 meters above the Earths surface
V_1 = wind speed at 50 meters
H_2 = new height
V_2 = wind speed at new height

This formula can be used to approximate the change in wind velocity between any two heights at a given wind site, but is only a very rough correlation[27]. Also, different exponents are used to reflect different types of surrounding ground terrain.

For this study sites with mean wind speeds of 6, 7.25, and 8 m/s were investigated, representing class 2, 4, and 6 sites.

CHAPTER 3

BLADE ELEMENT MOMENTUM THEORY

3.1 Thrust & Torque as Functions of Lift & Drag

Blade element momentum (BEM) theory is a tool for modeling the performance of wind turbines and propeller driven aircraft. The first applications of BEM were to model the performance characteristics of propellers[†]. BEM models treat rotor blades as a series of aerofoil sections. They calculate thrust and torque exerted on each aerofoil section, and then sum the results. Power is computed by taking the product of torque and angular velocity.

Whether a wind turbine or propeller, transfer of energy between rotor and air is a function of the velocity of the incoming air, the angular velocity of the rotor, and the aerodynamic properties of the rotor blades. Under certain conditions, energy is transferred from the rotor blades to the air. This represents the propeller situation. Under other circumstances, energy is transferred from the incoming air to the blades. This represents the wind turbine situation. Namely, at a fixed pitch angle and RPM, a given rotor will transfer energy to the air below a certain incoming air speed. Above that air speed, energy is transferred from the air to the rotor.

Aerodynamic rotors are essentially rotating wings that operate on the principles of lift and drag. Figure 3.1 shows a cross section of a typical aerofoil, with vectors drawn representing lift and drag. The aerofoil in the diagram represents a standard airplane wing moving in the **x** direction. Shifting the reference frame to the wing (aerofoil),

[†] BEM theory is based on equations originally developed by Glauert[18].

incoming air is moving in the *negative* **x** direction. Lift is produced in the **y** direction, and drag occurs in the direction of the incoming air (opposite of that which the wing is moving). The amount of lift and drag produced is generally proportional to the angle of attack, α.

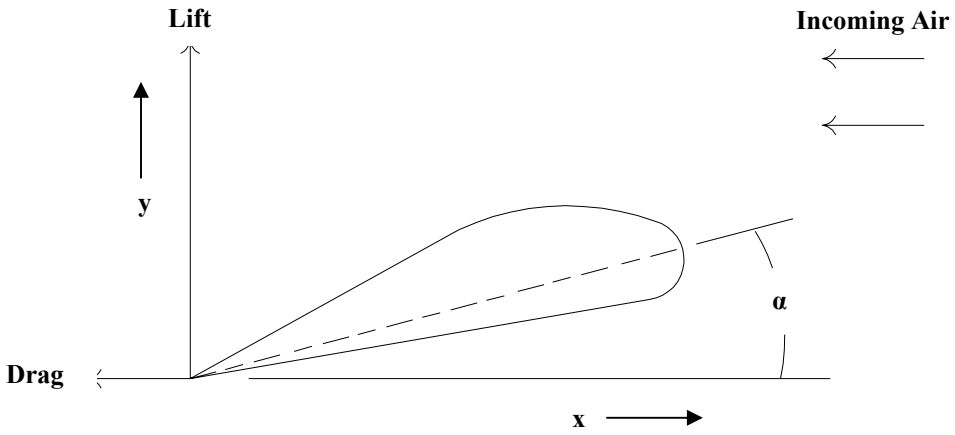

Figure 3.1: Aerofoil Section

Figure 3.2 shows typical curves from experimental data for coefficient of lift, C_L, and coefficient of drag, C_D, for an aerofoil. While there are theories that explain the general nature of the relationship of C_L and C_D to angle of attack, the published curves are products of experimentally determined data for existing aerofoils[5,31]. Lift and drag are directly measured in wind tunnel tests. As seen in the lift graph, the relationship is fairly linear up to a certain angle at which the slope begins to decrease. The point where the slope is horizontal is referred to as the stall angle. In order to maximize lift, an angle of attack near stall—but without reaching stall—is typically desired. After stall, flow separation occurs and behavior becomes unpredictable[25,31].

When the angle of attack is negative, the coefficient of lift is also negative. This results in negative lift. The drag is fairly negligible to up a certain angle (about 8 deg in the graph shown), but then begins to have a noticeable effect. Regardless of whether the angle of attack is positive or negative, the coefficient of drag is always positive.

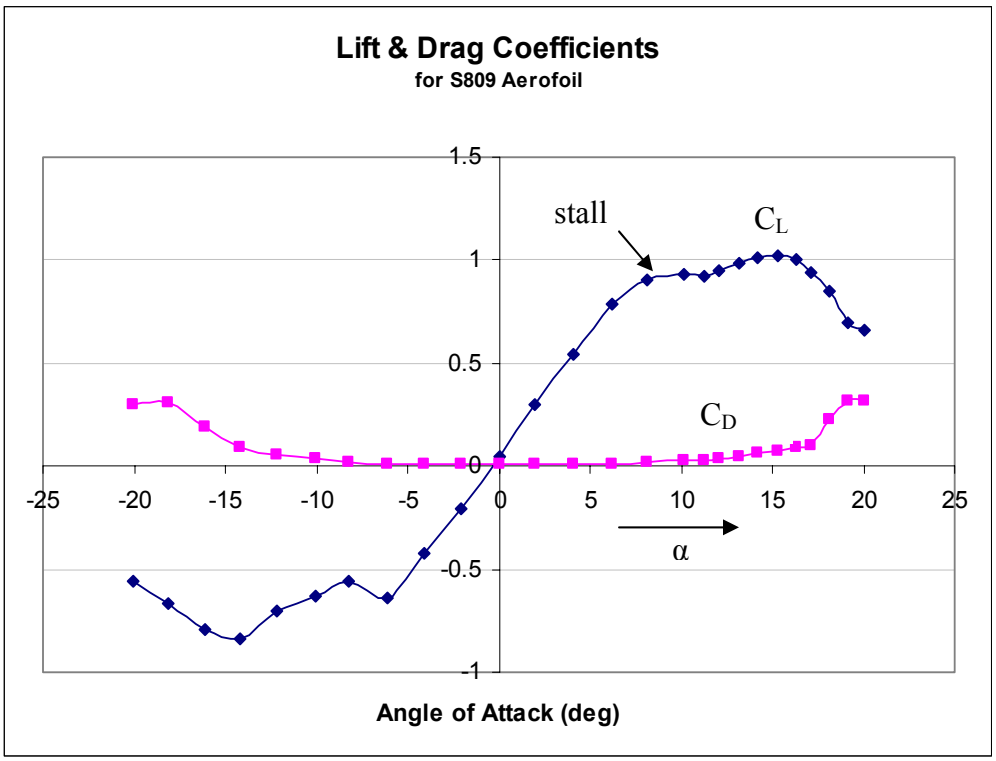

Figure 3.2: Coefficients of Lift and Drag vs. Angle of Attack for S809 Aerofoil[26]

The relationship between lift and drag forces and their coefficients is shown in equations (3.1) and (3.2).

$$L = C_L \frac{1}{2} \rho V^2 S \tag{3.1}$$

$$D = C_D \frac{1}{2} \rho V^2 S \tag{3.2}$$

where:

L = lift force on the wing (per unit of chord length)
D = drag force on the wing (per unit of chord length)
ρ = density of air
V = velocity of air over the wing
S = span (length) of wing

These equations give lift and drag per unit of chord length, and must be multiplied by the chord length to give lift and drag forces. Since chord length typically varies from the root to tip on a wing, the equations are generally presented in the above format.

A technique for approximating total lift and drag forces is to divide the wing up into segments, treat each segment as an individual aerofoil, and sum up the results. The chord can be assumed to be constant for the segment, and can be included in the equations. Equations (3.3) and (3.4) show the lift & drag produced by each blade segment, equations (3.5) and (3.6). show the total lift and drag for the wing.

$$L_i = C_L \frac{1}{2} \rho V^2 c_i \cdot r_i \tag{3.3}$$

$$D_i = C_D \frac{1}{2} \rho V^2 c_i \cdot r_i \tag{3.4}$$

where:

L_i = lift force on the i *th* wing segment
D_i = drag force on the i *th* wing segment
r_i = width of the i *th* wing segment
c_i = chord length of the i *th* wing segment

$$\text{Lift} = \sum_{i=1}^{n} L_i \tag{3.5}$$

$$\text{Drag} = \sum_{i=1}^{n} D_i \tag{3.6}$$

Figure 3.3 and Figure 3.4 show the above concept applied to a rotor blade. The principle is the same, but the details are a bit more complex. With a rotor blade, the incoming air velocity *relative to the aerofoil segment* (not to be confused with air entering the plane of the rotor) is a function of both the air entering the plane of the rotor and the rotational velocity of that segment. This is shown in Figure 3.4, where V is the incoming air "seen" by the blade segment. As before, α is the angle of attack, lift is perpendicular to V, and drag is parallel and in the direction of V.

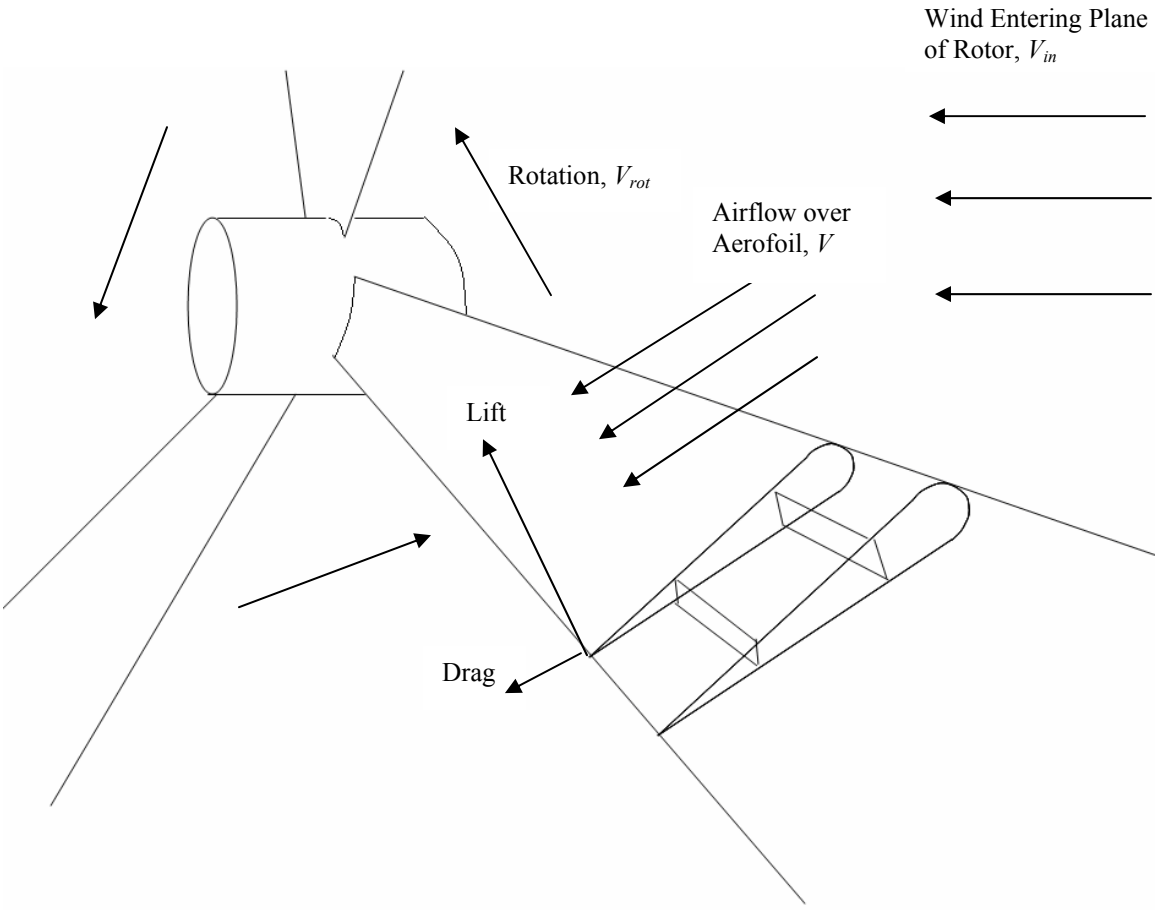

Figure 3.3: Rotor Blade Element

V_0 = Wind Speed

$V = \sqrt{V_{in}^2 + V_{rot}^2}$

V_{in} = Wind Speed + v

V_{rot} = $\Omega \cdot R - u$

where:

v = change in velocity from upstream to plane of rotor

u = change in swirl from upstream to plane of rotor

R = radial distance of blade segment

Ω = Angular Velocity of rotor

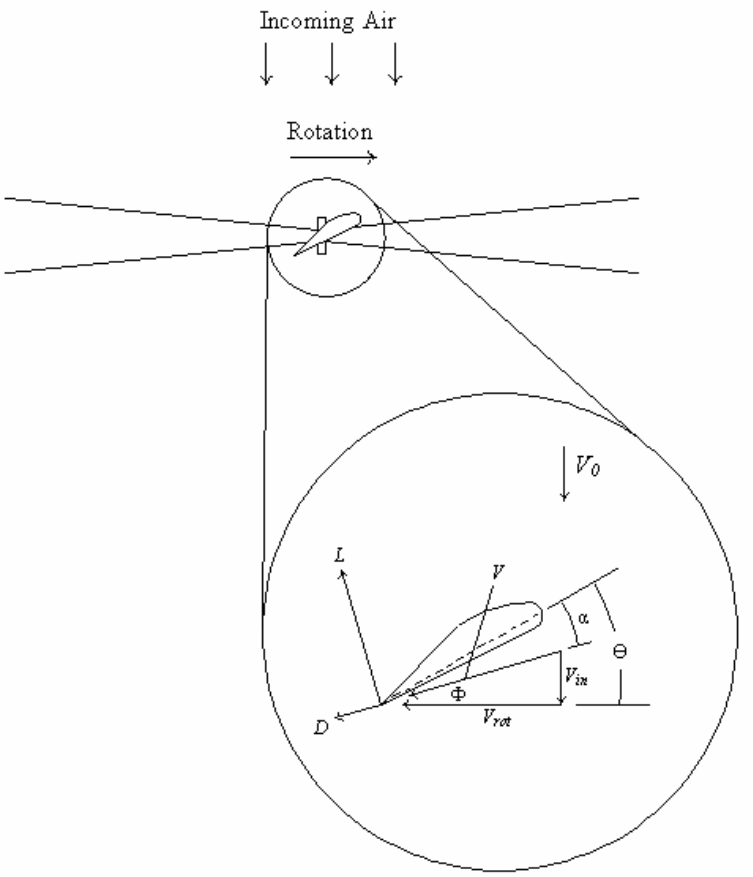

Figure 3.4: Airflow and Forces at Blade Element

It was shown in Chapter 2 that ½ of the change in velocity occurs upstream of the rotor, and ½ occurs downstream. This means that the incoming axial air velocity, V_{in}, is the upstream velocity, V_0, plus a ΔV. For a propeller this ΔV will be positive, and for a wind turbine it will be negative. From this point onward, the axial ΔV between upstream and the plane of the rotor will be referred to as v. So the total change in velocity from far upstream to far downstream is $2v$. There is an equivalent situation to this in the plane of rotation. As the rotor turns, it induces a velocity in the direction of rotation known as swirl. As with the incoming axial air velocity, it can be taken that ½ of the total swirl occurs upstream of the plane of rotation and ½ occurs downstream. The change in swirl

from upstream to the plane of the rotor will be designated as u. Therefore, $2u$ is the change in rotational velocity from upstream to downstream. Figure 3.4 defines these relationships. Each blade segment has different values of V_{in}, V_{rot}, v, and u, but tend to be similar to those of the adjacent elements. The changes in V_{rot} and u along the blade radius are more pronounced.

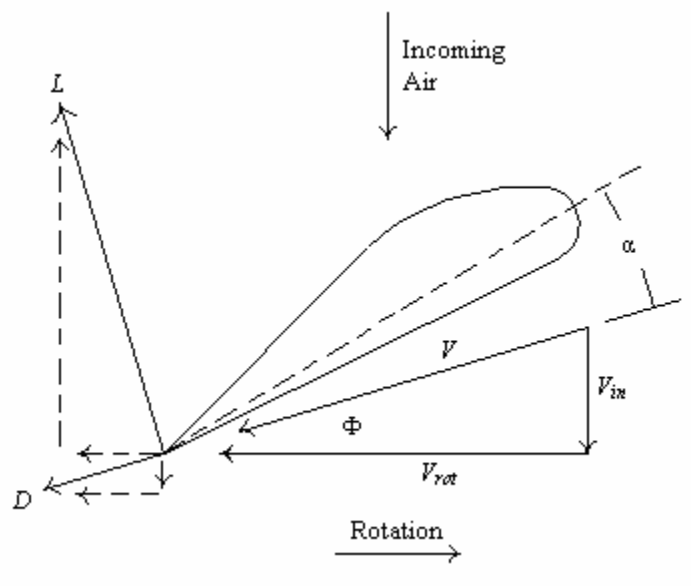

Figure 3.5: Components of Lift and Drag acting on a Blade Element

With a rotating aerofoil both lift and drag have components in the rotational direction, and in the axial direction; i.e., the direction perpendicular to the plane of the rotation. This is shown in Figure 3.5. The axial components contribute to thrust, and the rotational components contribute to torque.

$$\lambda_{1,i} = C_{L,i}\cos\phi_i - C_{D,i}\sin\phi_i \tag{3.7}$$

$$\lambda_{2,i} = C_{L,i}\sin\phi_i + C_{D,i}\cos\phi_i \tag{3.8}$$

$$T_i = \lambda_{1,i}\frac{1}{2}\rho V_i^2 c_i \cdot r_i \tag{3.9}$$

$$Q_i = \lambda_{2,i} \frac{1}{2} \rho V_i^2 c_i \cdot r_i \cdot R_i \tag{3.10}$$

where:

T_i = Thrust on i *th* blade element
Q_i = Torque on i *th* blade element
ρ = Air density
c_i = Chord length of i *th* blade element
R_i = Distance of i *th* blade element from center of rotation
r_i = Width of i *th* blade element (= effective "span" of element)

With an airplane propeller the objective is to maximize thrust and minimize torque, and with a wind turbine the objective is to maximize torque and minimize thrust. Power produced by the turbine is the product of torque and rotational velocity.

Figure 3.5 showed the details of this principle for an airplane propeller, and now Figure 3.6 extends it to a wind turbine. Because of significantly lower angular velocity (compared to a propeller), Φ (the angle between the plane of rotation and the relative wind) is greater than Θ (the angle between the plane of rotation and the chord of the blade segment), resulting in a negative angle of attack, which results in negative lift (based on the coordinate system used here). As long as the component of lift in the rotational direction is greater than the component of drag that opposes rotation, torque and power will be transferred to the shaft (as opposed to from the shaft as is the case for a propeller). In order to achieve maximum lift, the shape of the aerofoil is inverted such that the cambered edge faces away from the incoming wind. This has the effect of mirroring the C_L curve of Figure 3.2 diagonally, such that quadrants 2 and 4 switch position, and mirroring the C_D curve vertically such that quadrants 1 and 2 switch position.

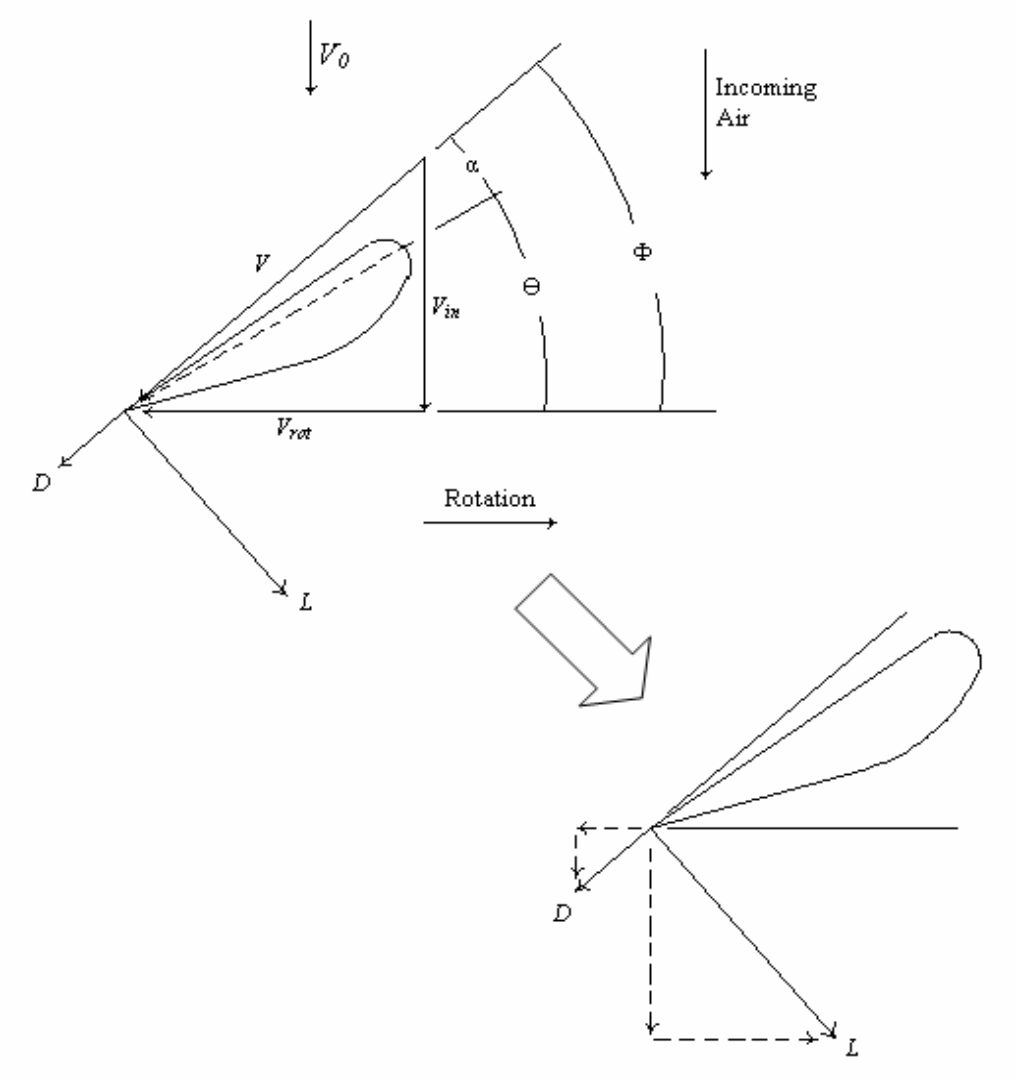

a

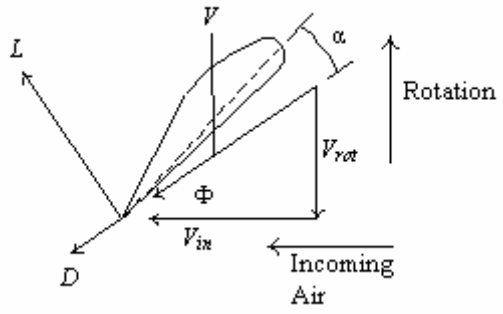

b

Figure 3.6 Wind Turbine Blade Element Airflow and Forces

Figure 3.6-b shows the same information as Figure 3.6-a except with the reference frame reversed. The horizontal axis shows the incoming wind and the vertical axis is the axis of rotation. The angle of attack and the lift force, however, can now be treated as positive. This provides a clearer view of the geometry of the various flows and forces at the blade element. The reference frame of Figure 3.6-a makes the most sense when analyzing a propeller, and the reference frame of Figure 3.6-b makes the most sense when analyzing a wind turbine rotor. The information provided, however, is the same.

3.2 Thrust & Torque as Functions of Momentum Change

A second method for determining thrust and torque is to perform a momentum balance on the air that passes through annuli defined by the areas swept out by the blade elements. This is shown visually in Figure 3.7.

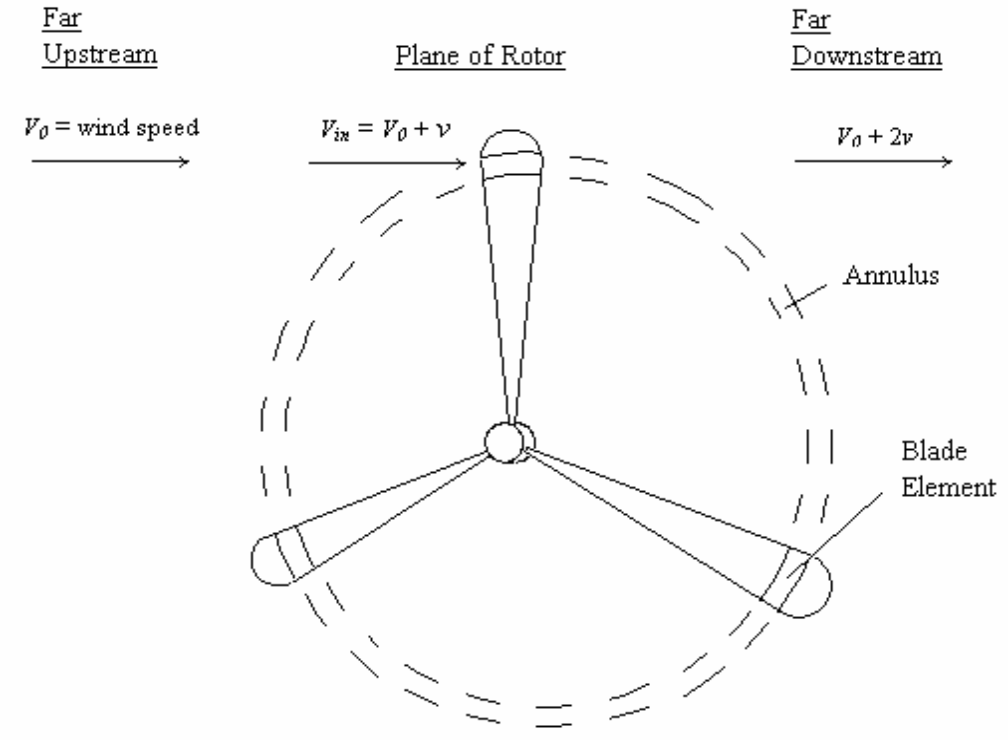

Figure 3.7: Change of Momentum through Annulus formed by Blade Element

For each blade element, thrust is equal to the change in momentum from far upstream to far downstream.

$$T_i = \dot{m}_i V_{upstream} - \dot{m}_i V_{downstream} = \dot{m}_i \left[V_0 - \left(V_0 + 2v_i \right) \right] \tag{3.11}$$

$$= \dot{m}_i \cdot 2v_i$$

where:

T_i = Thrust on the i *th* blade element
V_0 = Wind Speed
v_i = Change in velocity from upstream to plane of rotation through the i *th* annulus
$\dot{m}_i$ = mass flow rate through the i *th* annulus

The mass flow rate is evaluated at the rotor, and is a product of air density, the velocity of the air at the rotor, and the area swept out by the blade element.

$$\dot{m}_i = \rho A_i (V_0 + v_i) = \rho \left(2\pi R_i \cdot r_i \right) \left(V_0 + v_i \right) \tag{3.12}$$

where:

ρ = Air density
A_i = Area of i *th* annulus
R_i = Distance of i *th* blade element from center of rotation
r_i = Width of i *th* blade element (= width of i *th* annulus)

Since torque is nothing more than force in the direction of rotation times the radial distance, a similar angular momentum balance can be carried out to produce

$$Q_i = \dot{m}_i \cdot 2u_i \cdot R_i \tag{3.13}$$

where:

Q_i = Torque on the i *th* blade element
u_i = Change in swirl velocity from upstream (zero) to the plane of rotation through the i *th* annulus

The mass flow rate is the same as defined above.

The above equations are neutral with regards to the function of the rotor. If the rotor is a propeller, *v* will have a positive value. If it is a wind turbine, it will be negative. Likewise, u will also have a negative value for a wind turbine.

3.3 Iterative Solution for Thrust and Torque

Equations (3.9) and (3.11) each give values for thrust on a given blade element, and equations (3.10) and (3.13) each give values for torque. Solving for values of *v*, and *u* will produce values for thrust and torque. However, these are non-linear equations and a non-iterative solution is not possible. An iterative routine is necessary, and software written for Engineering Equation Solver (EES) was used to perform the task for this study.

CHAPTER 4

COST MODELING

The following formulas were used to estimate the costs of the components being analyzed.

$$\text{Electrical System Cost} = 99 \cdot \text{Generator Capacity} \quad (4.1)$$

$$\text{Rotor Cost} = N_{BLADES} \cdot 1.304 \cdot \text{Radius}^{3.03} \quad (4.2)$$

where:

N_{BLADES} = Number of Blades

Generator Capacity (kW)

Radius (m)

Electrical System Cost ($)

Rotor Cost ($)

The model for electrical system cost came from Harrison et. al.[20] which stated a general formula of 90 € per kW of generator capacity. This study was published in 2000. The average exchange rate for the year 2000 was 1.1 $ per €, which was used to obtain equation (4.1) above.

The model for rotor cost came from a 2001 NREL study[19]. An additional model from Harrison et. al.[20] was used to compare with the NREL model. The NREL paper stated a cubic relation between rotor cost (per blade) and radius. The paper does not give a formula, but gave the following data points:

Radius (m)	Per Blade Cost
23.3	$19,215
32.9	$52,370
38.0	$80,200
40.8	$98,815
46.6	$147,260
53.8	$228,800
60.2	$323,770

Curve fitting this data produced equation (4.2). This formula has a standard error of $770, which is less than 1% of the average cost listed.

Harrison et. al.[20] listed a cost range for rotor blades of 8 to15 € / kg. Using the conversion rate shown above for the year 2000 of 1.1 $ / €, this is $8.8 to $16.5 per kg. The Vestas V90 wind turbine has a rotor radius of 45 m and a rotor weight of 38 metric tons[34]. Using the NREL formula, a per blade rotor cost is determined to be $133,000. Using this value with the Harrison formula, a cost of about $10.5 per kg is computed. This falls within the range expected.

Because both the electrical system and rotor cost models came from sources published at roughly the same time, they were not adjusted for inflation. Any inflation would impact both equally. The cost formula for the electrical system encompasses more than just the generator and includes installation, cabling, and control (soft starters). However, this cost scales linearly with the capacity of the generator and is therefore sufficient for the purposes of the optimization as it puts an effective constraint on the cost of the two items.

CHAPTER 5

METHODOLOGY

5.1 General Methodology

The general approach used to determine the optimum relationship of rotor to generator size—for a given wind site at a fixed capital cost—is as follows:

1. Set capital cost (rotor + electrical system), and wind conditions (Weibull parameters) for the wind resource.
2. Begin with a small generator and a large rotor, and calculate total electricity produced by this configuration at the wind resource.
3. Gradually increase the size of the generator and decrease the size of the rotor (under the total cost constraint). Calculate electrical energy output for each configuration.
4. Analyze results to see which configuration that has the maximum electrical output.
5. Repeat this process with a variety of cost constraints, and with a variety of characteristic wind parameters.
6. Analyze the data to see how the optimum is affected by Weibull parameters, and fixed cost.

Software models were created for steps 2 and 3 using Engineering Equation Solver.

5.1.1 Engineering Equation Solver

Engineering Equation Solver (EES) software was used for all aspects of the optimization. EES was chosen for the following reasons:

- Iterative Solver – EES is an iterative equation solver. The primary calculations involve a BEM analysis to predict power output by various rotor sizes in various wind speeds. This is by nature an iterative process. EES is designed to quickly perform this iteration and produce results with errors less than 10^{-9}.

- Tables — EES has the ability to present results in the form of tables. This made it easy to analyze the data — both in terms of detecting convergence errors and in terms of finding trends in the final results

- Other – EES also has the ability to look up thermodynamic properties. Other than air density, none are used in these models. However, one can easily change temperature and pressure values (and therefore density) to see their effect on performance.

5.2 Software Modules

Figure 5.1 is a flow diagram showing the general working of the software. Three main modules were created: a Primary Optimizer module, an Electrical Production module, and a Power Produced module.

The majority of the calculations occurred in the Power Produced module where BEM was used to calculate rotor power. The Electrical Production module used the power values, along with the wind resource data, to determine annual electrical output for wind turbines of various configurations; i.e., rotor-to-generator sizes. The Primary Optimizer passed a series of configurations to the Electrical Production module and selected the optimal configuration based on the feedback. Sub-modules included Wind Time and Costing. Wind Time calculated the hours per year spent at individual wind speeds, and the Costing module calculated generator and rotor costs.

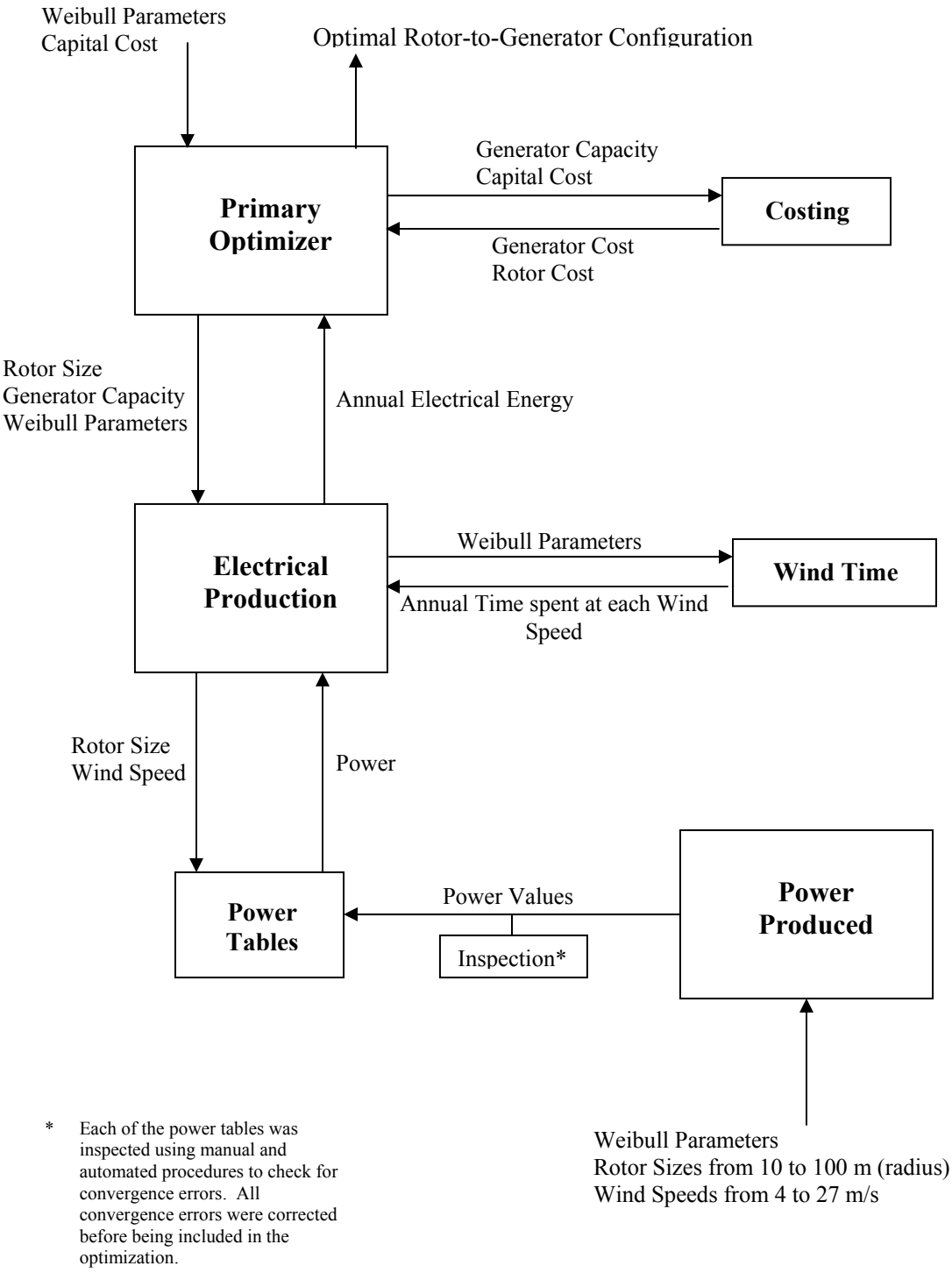

* Each of the power tables was inspected using manual and automated procedures to check for convergence errors. All convergence errors were corrected before being included in the optimization.

Figure 5.1: **Optimization Software Flow Diagram**

The following gives descriptions of the inner-workings of each of the modules:

5.2.1 Primary Optimizer Module

This module performed the overall optimization. It works in the following manner.

1. User sets the fixed cost for rotor plus the electrical power generation system.
2. User sets the Weibull parameters to define the wind speed distribution.
3. Begin with small generator size. 500 kW was used as the starting point in most of the trials.
4. Call electrical system costing model which returns the cost of the electrical system and the cost of the rotor.
5. The size of the rotor is calculated using equation (4.2).
6. Send rotor size, generator size, & Weibull parameters to Electricity Production model to determine total electricity produced in a year.
7. Calculate additional parameters such as capacity factor and *SA* = rotor area / generator capacity.
8. Repeat process from step 4, increasing generator size by a small amount. As capital is fixed, rotor size decreases as generator size increases. Generator size was increased from 500 kW to 5000 kW in most cases.

This process was repeated for each wind resource at capital cost constraints of:

- $50,000
- $200,000
- $500,000
- $1,000,000
- $2,000,000

The entire process was repeated using 9 different wind resources defined by all combinations of the following parameters:

$$k = 1.8, 2.0, 2.2$$

$$\text{mean wind speed} = 6, 7.25, 8.4 \text{ m/s}$$

The shape parameter values were chosen as representative of typical wind sites considered for project development. Average wind speeds were chosen as median values (at 50 m) representing class 2, 4, & 6 wind sites.

The final results were plotted on a graph of ideal rotor-to-generator size, for each of the wind resources examined. The ideal rotor size is defined as the one that produces the most electrical energy at the given capital cost constraint. A series of additional graphs were created to explore how this relationship changes with the various parameters involved.

5.2.2 Electrical Production Module

The Electricity Production module calculates the total electricity produced by a rotor of a given configuration at a given wind site in a year. It works in the following manner:

1. Rotor size, generator size, and Weibull parameters are input by the main module.
2. Weibull parameters are sent to the Wind Time module. The Wind Time module returns a set of values for the amount of time, in hours, that the wind is expected to blow at each speed from 4 to 27 m/s in a typical year.
3. A reference average wind speed is set for each wind characteristic case based on the wind speed distribution. The root-mean-cube speed was used, defined as

$$V_{rmc} = \sqrt[3]{\frac{\sum V_i^3 t_i}{\sum t_i}} \tag{5.1}$$

where:

V_i = a given wind speed
t_i = time spent, in hours, at that wind speed

The root-mean-cube speed is the speed that represents the distribution at a given site in terms of total electrical output. If the wind at the site blew constantly at this speed, the annual energy available would be the same as the distribution produces.

4. Begin with a minimum tip-speed-ratio (TSR). This varied from trial to trial (based on the expected value which would produce the optimum electrical output).

5. Tip speed and angular velocity are set based on rotor size, V_{rmc}, and TSR.

6. Set the generation cut-in wind speed. 4 m/s was used in trials.

7. Send wind speed, generator size, and rotor size to Power Produced model. Power produced by the turbine is returned.

8. Electricity produced by the turbine at that wind speed is calculated by taking the product of power and annual time corresponding to that wind speed.

9. Wind speed is increased by 1 m/s and the process returns to step 7. This repeats until the generator cut-out speed is reached, which was taken as 27 m/s in the trials.

10. Total electrical output is calculated by summing the individual electrical outputs at each of the wind speeds.

11. TSR is incremented by 0.1 and process returns to step 5. This occurs a set number of times. 10 iterations were used in most of the trials.

12. Electrical output is compared for each of the TSR's, and the maximum is chosen as the electrical output of the machine.

13. Capacity factor is calculated.

14. Values of electricity produced, capacity factor, and RPM are returned to the main routine.

5.2.3 Power Produced Module

The Power Produced module calculates the power output of a turbine of a given configuration at a given wind speed. It works in the following manner:

1. Rotor size, generator size, and wind speed are input by the Electrical Production module.
2. Blade pitch is selected based on wind speed.
3. BEM analysis is used to determine the power output of the rotor at the given wind speed.
4. Power output of the rotor is compared to generator capacity. Lesser of the two is determined to be power output of wind turbine.
5. Power output of rotor is compared to zero. Greater of the two is determined to be the power output of the wind turbine.
6. Power value is returned to Electricity Routine.

The Power model uses BEM modeling to calculate the power produced by a rotor of a given size and a given angular velocity at a given wind speed. For each wind speed examined, an optimum pitch was selected. Pitch is defined as the angle between the plane of rotation and the chord of the blade element at the 75% point (as measured outward from the hub). This was blade element 15 in the model (there were 19 blade elements total).

Originally an iterative optimization routine was planned, but this was determined unnecessary. It was found that an open loop approach that selected pitch solely on wind speed worked sufficiently well. The reason for this relates to the geometry diagramed in Figure 3.6 and the methodology used to select the fixed speed (RPM) for the wind resource. If RPM and rotor diameter are held constant, an optimum pitch angle exists for each wind speed at which the turbine operates. This will be the pitch that produces the maximum torque (as per figure 3.6) over the sum of the blade elements. If the tip-speed-ratio, based on root-mean-cube wind velocity, is held constant, then the geometry will

remain constant regardless of rotor diameter. Pitch becomes solely a function of wind speed.

Figure 5.2 shows the relationship between pitch and power for a 20 meter rotor operating at 21 RPM. For a $k = 2$, $V_{avg} = 8.4$ m/s wind resource, this corresponds to a 4.1 TSR (relative to V_{rmc}). Notice that pitch angles that produce maximum power at high wind speeds actually produce negative power at low wind speeds. This is a function of the geometry of Figure 3.6.

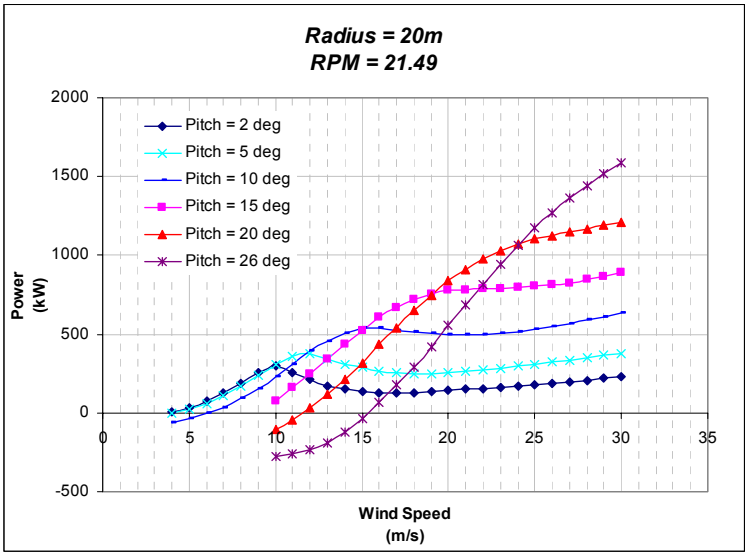

Figure 5.2: Relationship of Pitch to Power

Optimum pitch angles for individual wind speeds were selected based on the results shown in Figure 5.2. These can be seen in Appendix A. Each of the optimizations used this set. This open-loop approach had a small impact on the trials but brought the advantages of a substantially simplified model and significantly improved calculation speed.

5.2.4 Wind Time Module

The Wind Time module calculates the hours the wind is expected to blow at each speed from cut-in to cut-out in a year. The range used in the optimization trials was 4 to 27 m/s. It works in the following manner:

1. Weibull Parameters are input by the Electrical Production module.
2. The Weibull function, equation (2.13) is used to calculate the amount of time spent at each wind speed from cut-in to cut-out in a year.
3. The time values are returned to the Electrical Production module.

5.2.5 Costing Module

The Costing module calculates the cost of the generator and cost of the rotor. It works in the following manner:

1. Generator capacity and fixed capital cost are input by the Primary Optimizer module.
2. Equation (4.1) is used to calculate the cost of the electrical system.
3. Rotor cost is calculated by taking the difference between the fixed capital cost and the cost of the generator.
4. Values for the cost of the rotor and the cost of the generator are returned to the Primary Optimizer module.

5.3 Implementation

5.3.1 Multiple Sets of Code

The original intent was to create a single piece of software that ran the main module and each of the supporting sub-modules to give the optimum configuration for a given cost and a given wind resource. However, a desire to examine "internal data" led

to a decision to divide the software into several independent segments. "Internal data" is defined as data that is generated, used internally, and then discarded—but from which the foundation for the final result is built. EES is a powerful tool that seems ideally suited to perform a BEM analysis. This is primarily because EES is an iterative solver and BEM is by nature an iterative process. However, there are occasions when EES fails to converge on a solution for individual blade elements, and this affects the final result.

5.3.2 Power Tables and Verification of Power Values

An extremely useful feature of EES is its ability to produce results in the form of a table. Table 5.1 is an example of a table produced with a single run of the Power Produced module at a given rotor size, RPM, and wind speed. With each run, values for every parameter of each blade element are accessible and can be monitored. By separating the power module from the primary optimizing routine, it was possible to check thousands of pieces of data for computational errors before incorporating them into the main routine. This was accomplished by having EES generate tables of power produced for each circumstance of V_{RMC} (which is a function of wind speed distribution) and TSR investigated. Each table showed the power produced at each wind speed (from 4 to 27 m/s) for rotors ranging from 10 to 100 meters in radius. Ultimately 90 such tables were generated, 10 for each of the nine Weibull configurations. The tables contained additional information, most importantly the power produced by each blade segment for each variation in rotor size. These tables were then transferred to a Microsoft Excel spreadsheet that had measures to look for computational errors. In particular, it was found early in the creation of the model that when EES would fail to converge on a

Table 5.1: Blade Element Parameter Values at Radius = 50 m, RPM = 8.93, Wind Speed = 10 m/s[‡]

Blade Element	R (m)	Chord (m)	twist (deg)	*r* (m)	V_{in} (m/s)	*v* (m/s)	V_{rot} (m/s)	*u* (m/s)	*V* (m/s)
1									
2									
3	8.975	5.375	28.8	1.25	8.918	-1.082	9.371	-0.9746	12.94
4	11.05	6.525	23.82	2.9	8.661	-1.339	11.31	-0.9735	14.25
5	13.83	6.275	17.05	2.65	8.455	-1.545	13.82	-0.8886	16.2
6	16.5	6.025	11.86	2.7	8.247	-1.753	16.26	-0.8246	18.23
7	19.25	5.775	8.21	2.8	8.098	-1.902	18.75	-0.7427	20.43
8	22.03	5.525	5.795	2.75	8.005	-1.995	21.29	-0.6882	22.75
9	24.75	5.275	4.16	2.7	7.962	-2.038	23.78	-0.6219	25.07
10	27.5	5.025	2.94	2.8	7.942	-2.058	26.29	-0.5637	27.46
11	30.25	4.775	1.955	2.7	7.932	-2.068	28.82	-0.5161	29.89
12	32.98	4.525	1.135	2.75	7.923	-2.077	31.32	-0.4764	32.31
13	35.75	4.275	0.425	2.8	7.893	-2.107	33.89	-0.4448	34.8
14	37.33	4.025	0.045	0.35	7.922	-2.078	35.34	-0.4216	36.22
15	38.68	3.775	-0.275	2.35	7.961	-2.039	36.58	-0.4007	37.44
16	41.23	3.525	-0.83	2.75	7.888	-2.112	38.95	-0.3858	39.74
17	44	3.275	-1.33	2.8	7.709	-2.291	41.54	-0.3824	42.25
18	46.75	3	-1.695	2.7	7.294	-2.706	44.13	-0.3966	44.73
19	49.05	2.725	-1.92	1.9	5.992	-4.008	46.32	-0.4327	46.71

Blade Element	Φ (deg)	Θ (deg)	α (deg)	C_D	C_L	Mass Flow	Thrust (kN)	Torque (kN·m)	Power (kW)
1									
2									
3	43.58	32.8	10.79	0.02968	1.085	744.3	1610	13021	12.18
4	37.44	27.82	9.622	0.02498	1.002	2065	5529	44415	41.55
5	31.45	21.05	10.41	0.02859	1.059	2304	7118	56603	52.95
6	26.89	15.86	11.04	0.03265	1.101	2733	9574	74321	69.53
7	23.36	12.21	11.15	0.03913	1.104	3247	12333	92704	86.72
8	20.6	9.795	10.81	0.02975	1.087	3607	14349	109047	102
9	18.51	8.16	10.35	0.02843	1.055	3958	16050	121228	113.4
10	16.81	6.94	9.869	0.02656	1.02	4549	18554	139754	130.7
11	15.39	5.955	9.436	0.02379	0.9882	4820	19617	148081	138.5
12	14.19	5.135	9.059	0.02138	0.9604	5345	21603	163398	152.9
13	13.11	4.425	8.686	0.01949	0.9384	5878	23638	178406	166.9
14	12.63	4.045	8.59	0.01903	0.933	769.9	3001	22723	21.26
15	12.28	3.725	8.552	0.01885	0.9309	5383	20176	153332	143.4
16	11.45	3.17	8.278	0.01753	0.9156	6653	24496	184444	172.5
17	10.51	2.67	7.843	0.01606	0.8899	7066	25528	187542	175.4
18	9.384	2.305	7.079	0.01537	0.8411	6849	23957	164134	153.5
19	7.371	2.08	5.291	0.01453	0.6886	4154	13736	72740	68.05

solution for an individual blade element, the resulting power (as well as Φ and α) for that blade element would be assigned a value of essentially zero ($< 10^{-20}$). Not only was this

[‡] The innermost two elements, representing the hub and root, were not used in the BEM calculations.

result extremely unlikely (while negative values of varying magnitude were both possible and likely under certain conditions, a value of zero was extremely improbable), it was physically impossible (as it produced impossible inconsistencies with the adjacent blade elements). Verification through a variety of measures (manual calculations, comparison with other models, and real world turbine data) showed that when EES produced a non-zero solution it was essentially accurate. This observation made it easy to test the data for errors. The Excel spreadsheets were set up to scan the power produced by each blade element and throw up a flag when one of these extreme near-zero values was found. Ultimately, the occurrence of this computational error was much lower than expected. Of the roughly 45,000 data points produced showing power values at the different configurations (of rotor size, wind speed, V_{RMC}, and TSR) only 22 were shown to fail to converge. Furthermore, the error was the result of an incorrect value of (essentially) zero being assigned to only a small number of blade elements (usually just one), so the overall result (power produced for that configuration) was only slightly lower than it should have been. In each case the errors were corrected with single runs of the model that only looked at that configuration. Manual manipulation of guess values allowed for convergence. Correcting these errors, however, had essentially no effect on the overall optimization.

In addition to the features incorporated into the excel spreadsheet, a manual random sampling of the data in the power tables was performed. Roughly 10 combinations of rotor size and wind speed were chosen from each table and an independent single run of the power program was performed to validate the listed power value. In each case, the power value was shown to be correct.

It is likely that there would have been substantially more errors if it weren't for the methodology that was used to create the power tables. As an iterative solver, EES relies on guess values of all variables as a starting point in order to converge upon a solution. The quality of these guess values (meaning how close they are to the final solution values) are critical in terms of obtaining convergence. In a BEM model, the values of the parameters associated with a given blade element will be close to those associated with adjacent elements. So the model was set up such that the iteration for each element would use the solutions of adjacent elements for its initial guess values. In particular, a solution was first obtained for the blade element at the 75% point (radially). Neighboring elements (both toward the center and toward the tip) used this solution to obtain guess values, and this process worked its way down (and up) the blade.

The guess values for the 75% element were set in the following manner. A base case was solved for a given radius and wind speed (at a given TSR); e.g.,10 meters and 10 m/s. EES would begin a series of runs that temporarily kept wind speed constant but increased rotor size in increments of 5 meters. With each run, the solution from the previous run was used as the new guess values. When the radius reached 100 meters and a solution was obtained, the wind speed was increased by 1 m/s. Then the process began to work inward. With each successive run the radius was decreased by 5 meters until a 10 meter radius was obtained. Then wind speed was increased by 1 m/s, and the process began to work outward again. With each run, the conditions (rotor size and wind speed) were only incrementally different from those of the previous run. Each time, the solutions from the previous run provided the guess values for the current run. It was this overall process that kept convergence errors to a minimum.

The process used to generate the power tables required a great deal of manual work. However, this process produced tables in which there is a tremendous amount of confidence. These BEM calculations represent the most complex part of the overall model, and their validity is critical to the success of the analysis. As will be discussed in chapter 6, the model was shown to approximate real-world turbine performance fairly accurately.

5.3.3 Interpolation

In the various software models, a fair amount of information was looked up from tables. This includes the values of C_L and C_D, the optimal pitch for a given wind speed, the amount of twist for a given blade element (the angle between the chord of the element and the plane of rotation when the pitch, the angle of the 75% element, is set to zero), and the power values (for rotors of various sizes and TSR's at different wind speeds). Whenever a model was required to estimate a value that fell between table values, linear interpolation was used.

5.3.4 Fixed Speed

Some modern commercially available wind turbines have the ability to adjust their angular velocity within a certain range. For instance, the Vestas V90 2.0 MW wind turbine can operate from 9 to 14.9 RPM, depending on wind speed[34]. This can lead to an improvement in efficiency. However, a decision was made not to try to model variable speed operation for the following reasons:

- Unknowns regarding the exact nature of implementation of variable speed control strategy in individual turbine models

- Differences between the various models of turbines available with regards to the implementation of variable speed control.

- Complexity is added to the model. Ideal 100% variable speed is relatively easy to model, but variable speed within a limited range adds complexity

- Unnecessary. Comparisons between the output of currently available turbines presumably operating with some degree of variable speed matched closely with the output of the model used in this paper. Matches of total electrical output for a year were at or less than 5.1%, which was deemed sufficiently accurate to perform the analysis.

5.4 Rotor Data

5.4.1 C_L, C_D Values used in the Optimization

Rotors based on the S809 aerofoil shape have been used extensively for research by NREL and others, and closely approximate those of commercially available wind turbines[15,16,33]. The optimization carried out in this study used a rotor based on the S809 aerofoil with modified C_L and C_D values based on the results of a 2004 NREL study[33]. Figure 5.3 shows the standard C_L and C_D curves for an S809 aerofoil along with the modified values. As shown in the figure, C_L and C_D values corresponding to angles of attack below 10 degrees are not affected by the modification. Above 10 degrees, two separate techniques were used to determine the values of C_L and C_D, depending upon the value of α. The following summarizes the selection of C_L and C_D. values used in this optimization:

- Below 10 degrees published C_L and C_D values for the S809 aerofoil were used.

- Between 10 and 20 degrees, C_L and C_D values obtained experimentally in the NREL study[33] were used.

- Above 20 degrees, a set of equations, first introduced by Viterna and Corrigan in the early 1980's, were used[33].

A drawback of BEM theory is that it treats flow over the aerofoil as a two dimensional phenomenon[15,33]. This is correct when the aerofoil being analyzed is a standard wing moving in a linear direction. However, this assumption produces inaccuracies when the aerofoil is a rotating wing. With a rotating wing, 3-D flow develops due to forces acting in the spanwise direction (radially). In particular, it has been shown that the 2-D assumption begins to breakdown as the angle of attack reaches and exceeds α_{stall}. This was first addressed by Viterna and Corrigan in the early 1980's when they showed that at high angles of attack it is no longer sufficient to treat each blade element as an independent entity[15,33]. They concluded that the entire geometry of the blade must be considered. They offered the following equations to modify C_L and C_D at angles of attack in the post-stall region[33]:

$$C_{D_{MAX}} = 1.11 + 0.018 \cdot AR \qquad (\alpha = 90°) \qquad (5.2)$$

where:

AR = aspect ratio of the blade

$$C_D = B_1 \sin^2 \alpha + B_2 \cos \alpha \qquad (\alpha = 15° \text{ to } 90°) \qquad (5.3)$$

where:

$$B_1 = C_{D\max}$$

$$B_2 = \frac{C_{D,stall} - C_{D\max} \sin^2 \alpha_{stall}}{\cos \alpha_{stall}}$$

$$C_L = A_1 \sin 2\alpha + A_2 \frac{\cos^2 \alpha}{\sin \alpha} \qquad (\alpha = 15° \text{ to } 90°) \qquad (5.4)$$

where:

$$A_1 = \frac{B_1}{2}$$

$$A_2 = \left(C_{L,stall} - C_{D\max} \sin \alpha_{stall} \cos \alpha_{stall} \right) \frac{\sin \alpha_{stall}}{\cos^2 \alpha_{stall}}$$

The 2004 NREL[33] study compared the Viterna equations with test data from a rotor based on the S809 aerofoil. The rotor used had a 5.03 m radius, had an aspect ratio of 11 (based on chord length at the 80% point), and a fixed velocity of 72 RPM. The study concluded that the Viterna equations provide a good fit above angles of attack of 20°, but that using an AR of 14 provided a better fit. Below 10° no modifications to C_L or C_D were necessary, as expected. Between 10° and 20°, C_L and C_D were estimated from pressure measurements taken from a series of sensors along the blade.

The C_L and C_D values used in the rotor-to-generator optimization were set according to the results of the NREL[33] study. Above 20 degrees, the Viterna equations were used with AR set to 14. Between 10 and 20 degrees, the values experimentally obtained with the 5.03 m rotor were used[33]. The C_L and C_D values are shown in Figure 5.3 and are listed in Appendix B.

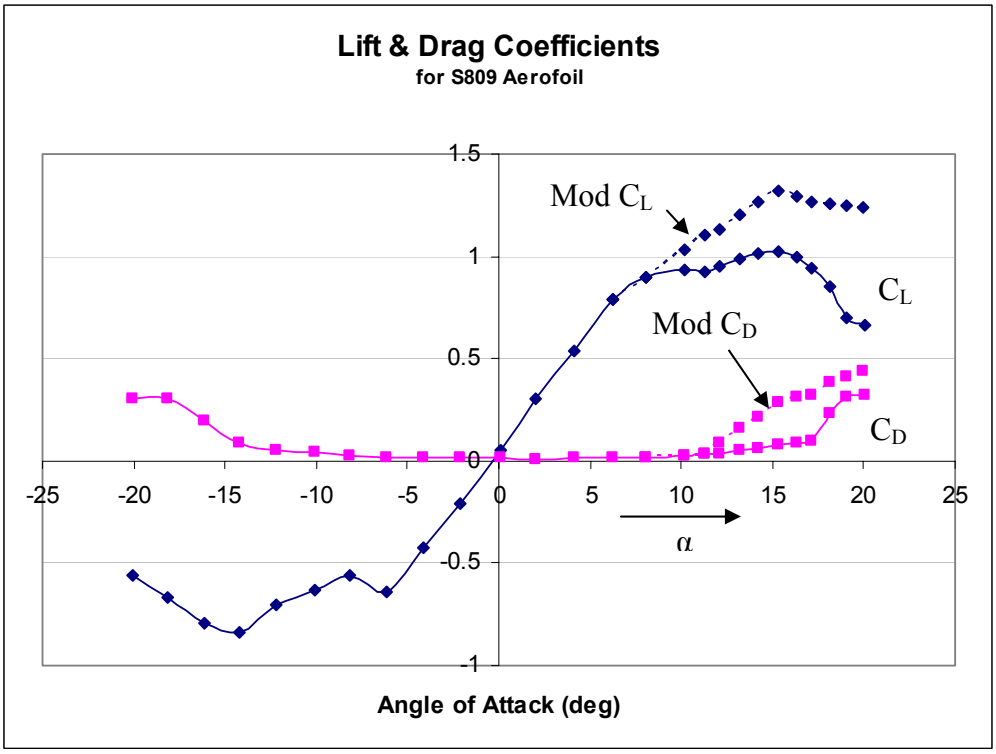

Figure 5.3: Standard and Modified Lift and Drag Coefficients for an S809 Aerofoil

5.4.2 Rotor Dimensions and Twist

The specifications for the rotor blade used in the NREL 3-D flow study[33] mentioned above are described in a 1999 NREL report[16]. The report lists chord length, twist angle, and radial distance (from the center of the hub) at 20 separate locations from root to tip (with the first directly at the root blade and the last directly at the tip). Following this report, the BEM analysis in the rotor-to-generator optimization divided the rotor blades into 19 elements. Values of dimensionless chord length and dimensionless radial distance were computed from the information given and are defined as chord length divided by radius and radial distance divided by radius respectively. These values were then used to set the chord length and radial distance for each of the blade elements in the rotor-to-generator optimization as the rotor size was varied. Twist is defined as the

angle between the plane of rotation and the blade element chord when the pitch is set to zero. The twist values required no modification and were used directly. The specifications for the 19 blade elements used in the rotor-to-generator optimization are shown in Appendix B.

CHAPTER 6

VALIDATION

6.1 Vestas 90 2.0 MW Turbine

The Vestas V90-2.0 MW wind turbine has a 45 meter rotor, a 2 MW generator, and operates between 9 and 14.9 RPM[34]. Figure 6.1 shows the power output of the Vestas turbine compared to that of the model developed for the optimization study. The power output of the Vestas machine was from Vestas literature[34]. The power output from the model was calculated using a 45 meter rotor, a 2 MW generator, and a fixed speed of 10.7 RPM.

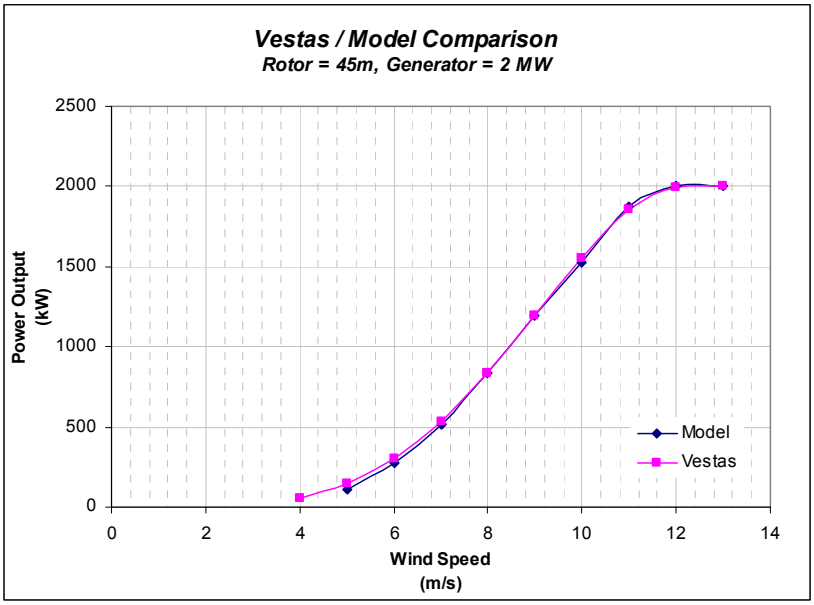

Figure 6.1: Optimization Model compared with Vestas-V90 Wind Turbine

Software was written to determine the total electrical output of the Vestas machine at the sites examined in this optimization study. This software used the

published power relationship shown in Figure 6.1. Column 1 in Table 6.1 shows the annual electrical output for the 9 wind resources examined in the optimization study. Column 2 shows the annual electrical output from a turbine of matching rotor size and generator capacity, using the model developed for the optimization study.

Table 6.1: Optimization Model compared with Vestas-V90 Wind Turbine

		1	2	3
	Average Wind Speed (m/s)	Electricity - Vestas (MW-hr)	Electricity - Model 45m, 2MW (MW-hr)	Model / Vestas
k = 1.8	6	4687	4533	0.967
	7.25	6606	6470	0.979
	8.4	8118	8001	0.986
k = 2.0	6	4574	4412	0.965
	7.25	6656	6513	0.979
	8.4	8334	8215	0.986
k = 2.2	6	4449	4281	0.962
	7.25	6671	6523	0.978
	8.4	8492	8372	0.986

The model used a separate fixed speed optimized for each of the wind resources. The cut-in and cut-out speeds were 4 and 25 m/s respectively, which matched the published values for the Vestas machine[34]. The results show a good match at each of the wind resources. In all cases the error is less than 4%.

6.2 General Electric 3.6sl Turbine

Figure 6.2 and Table 6.2 show the comparison to a GE 3.6 MW machine performed in the same manner as above. The model used the GE turbine design with a rotor size of 55.5 m, and a generator capacity of 3.6 MW. The GE turbine reportedly

operates between 8.5 and 15.3 RPM[14]. A fixed RPM of 8.05 was used to produce the power curve from the optimization model shown in Figure 6.2. For each case of Table 6.2, a separate resource-optimized fixed RPM was calculated and used. The cut-in and cut-out speeds were 4 and 27 m/s respectively, matching the GE published data[14].

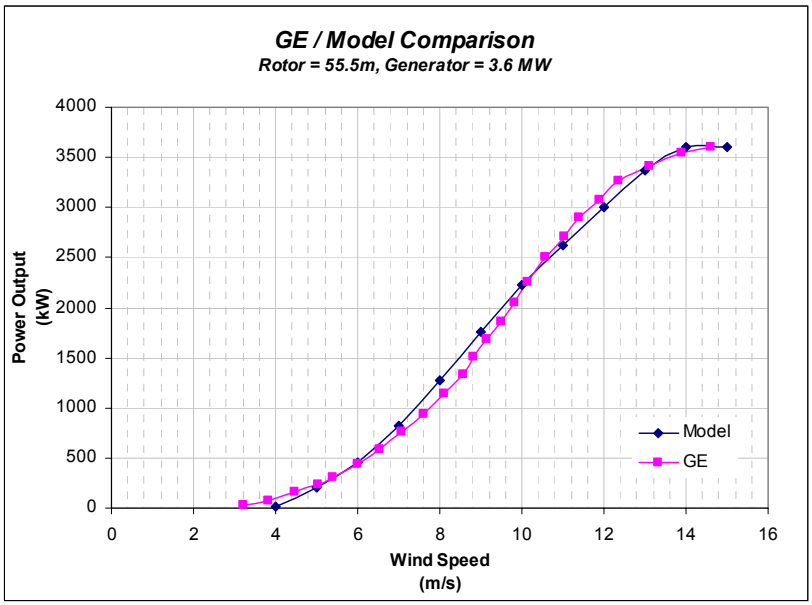

Figure 6.2: Optimization Model compared with GE-3.6sl Wind Turbine

Table 6.2: Optimization Model compared with GE-3.6sl Wind Turbine

		1	2	3
	Average Wind Speed (m/s)	Electricity - GE (MW-hr)	Electricity - Model 55.5m, 3.6MW (MW-hr)	Model / GE
k = 1.8	6	6910	7181	1.039
	7.25	10078	10512	1.043
	8.4	12717	13273	1.044
k = 2.0	6	6639	6913	1.041
	7.25	10015	10484	1.047
	8.4	12926	13517	1.046
k = 2.2	6	6369	6646	1.043
	7.25	9905	10411	1.051
	8.4	13038	13682	1.049

Again the optimization model results are a good match. The largest error in Table 6.2 is 5.1 %.

A great deal of confidence was obtained with each of the above results. It was determined that the fixed speed model was adequate to carry out the rotor/generator optimization.

CHAPTER 7

RESULTS AND DISCUSSION

7.1 Results

7.1.1 Optimal Rotor to Generator Size Relationship

Figure 7.1 shows optimization runs for 2 separate cost constraints at 3 different wind resources. This same type of analysis was performed for a total of 45 cases, representing five different cost constraints, each analyzed at nine wind conditions. A new parameter is introduced, *SA*, which is defined as follows:

SA = Swept Rotor Area / Generator Capacity

SA signifies *specific area* and is a measure of the general relationship between rotor and generator size. Figure 7.3 thru Figure 7.5 examines the relationship between this variable and the other parameters investigated.

Appendix C shows similar graphs for each of the circumstances analyzed. Table 7.1 shows the general results for each of the optimizations.

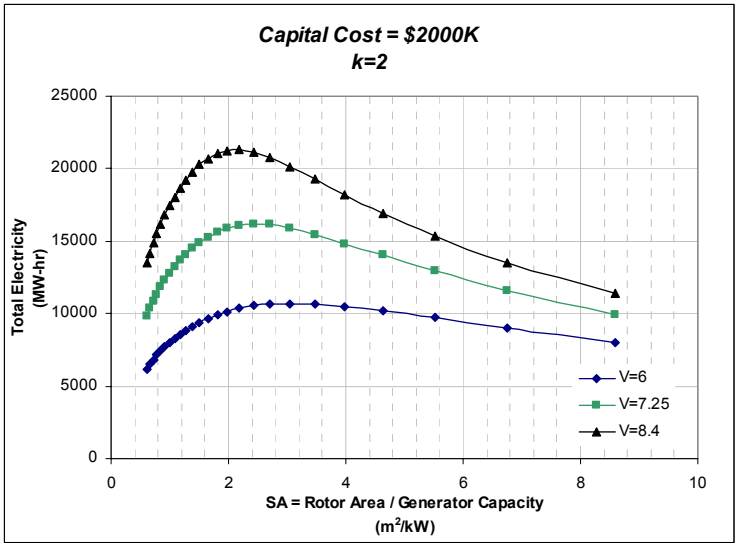

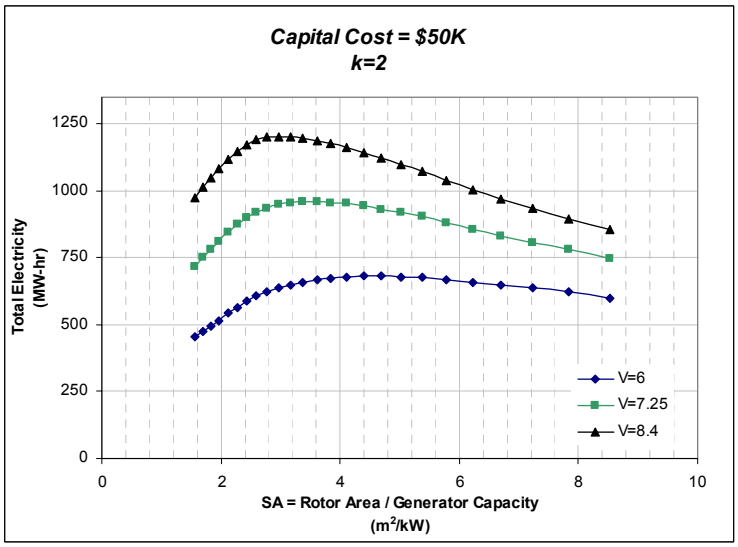

Figure 7.1: Total Annual Electricity from various Rotor-to-Generator Configurations in a $k = 2$ Wind Resource

Figure 7.1 above shows how total electricity varies with the relationship of rotor-to-generator size, SA. In each case (of those shown above), there is an optimum that falls somewhere between 2 and 4. Perhaps a more important graph is presented in Figure 7.2. It shows the relationship between capacity factor and total electricity for the same turbines and same wind resources. As can be seen, the optimum capacity factor falls between 0.2 and 0.45 in each case shown. Higher capacity factors result in less

electricity being produced. In all of the trials investigated, the highest optimal capacity factor demonstrated was 0.48.

Table 7.1 shows the general results for each of the optimizations. Nine separate Weibull distributions were examined under five capital cost constraints. A $50,000 wind turbine represents a very small machine, and $2,000,000 represents wind turbines larger than those currently available.

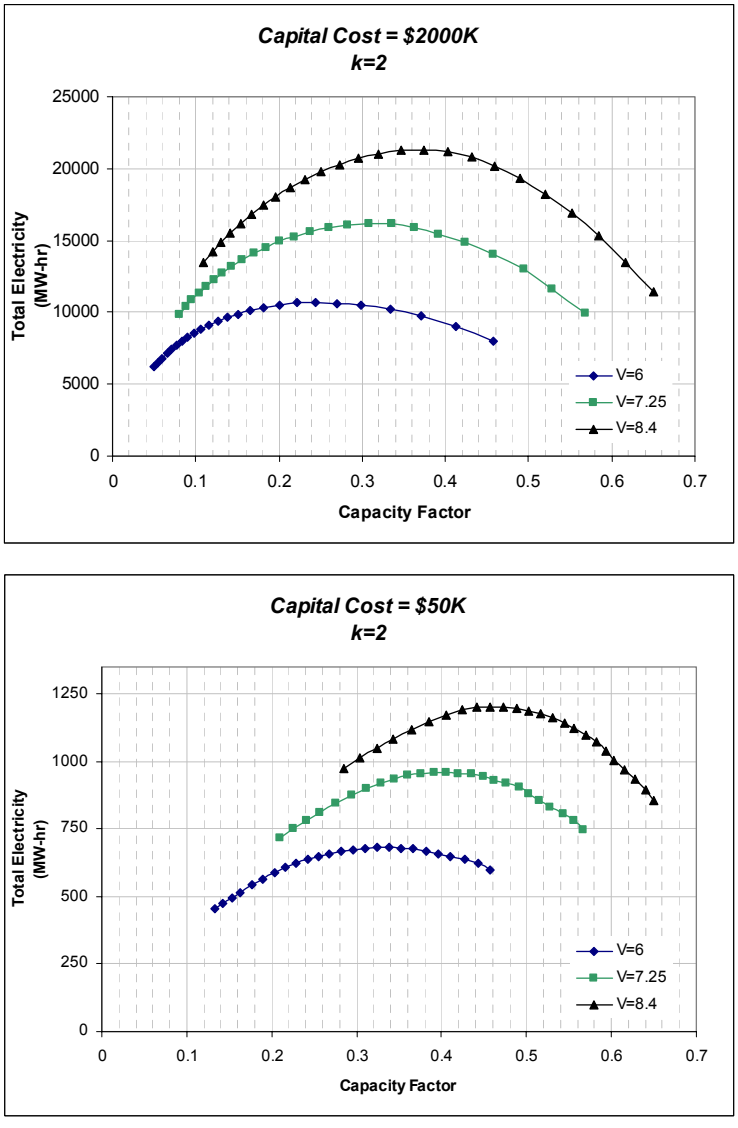

Figure 7.2: Total Annual Electricity vs. Capacity Factor in a $k = 2$ Wind Resource

Table 7.1: Optimal Rotor/ Generator Sizing for Turbines at various Wind Resources and Capital Cost Constraints

	Fixed Cost ($)	V_{avg} (m/s)	Gen Cap (kW)	Radius (m)	Capacity Factor	SA (m^2/kW)	Electricity (MW-hr)
k = 1.8	$50K	6	240	18.32	0.326	4.39	685.7
		7.25	280	17.36	0.387	3.38	949.9
		8.4	300	16.83	0.446	2.97	1172
	$200K	6	800	30.32	0.284	3.61	1989
		7.25	950	29.04	0.342	2.79	2849
		8.4	1000	28.58	0.412	2.57	3606
	$500K	6	1800	41.9	0.253	3.06	3982
		7.25	2000	41.03	0.330	2.64	5784
		8.4	2200	40.12	0.383	2.30	7372
	$1000K	6	3100	53.97	0.245	2.95	6663
		7.25	3600	52.67	0.310	2.42	9779
		8.4	4000	51.57	0.358	2.09	12559
	$2000K	6	5600	68.79	0.225	2.65	11061
		7.25	6200	67.84	0.301	2.33	16371
		8.4	6900	66.7	0.350	2.03	21182
k = 2	$50K	6	230	18.54	0.339	4.70	682.1
		7.25	280	17.36	0.391	3.38	959.5
		8.4	300	16.83	0.458	2.97	1203
	$200K	6	750	30.73	0.298	3.96	1959
		7.25	900	29.48	0.361	3.03	2850
		8.4	1000	28.58	0.418	2.57	3666
	$500K	6	1600	42.73	0.277	3.59	3889
		7.25	1900	41.47	0.347	2.84	5769
		8.4	2100	40.58	0.406	2.46	7473
	$1000K	6	3000	54.22	0.246	3.08	6459
		7.25	3400	53.19	0.326	2.61	9719
		8.4	3700	52.4	0.391	2.33	12689
	$2000K	6	5100	69.56	0.239	2.98	10693
		7.25	6000	68.16	0.308	2.43	16211
		8.4	6800	66.87	0.358	2.07	21300
k = 2.2	$50K	6	230	18.54	0.336	4.70	677.3
		7.25	270	17.61	0.409	3.61	966.2
		8.4	290	17.1	0.482	3.17	1225
	$200K	6	700	31.12	0.315	4.35	1934
		7.25	900	29.48	0.361	3.03	2848
		8.4	950	29.04	0.445	2.79	3705
	$500K	6	1500	43.13	0.290	3.90	3811
		7.25	1900	41.47	0.345	2.84	5746
		8.4	2100	40.58	0.410	2.46	7536
	$1000K	6	2600	55.21	0.277	3.68	6306
		7.25	3200	53.71	0.344	2.83	9641
		8.4	3700	52.4	0.394	2.33	12764
	$2000K	6	4300	70.75	0.275	3.66	10368
		7.25	5700	68.63	0.322	2.60	16059
		8.4	6200	67.84	0.394	2.33	21380

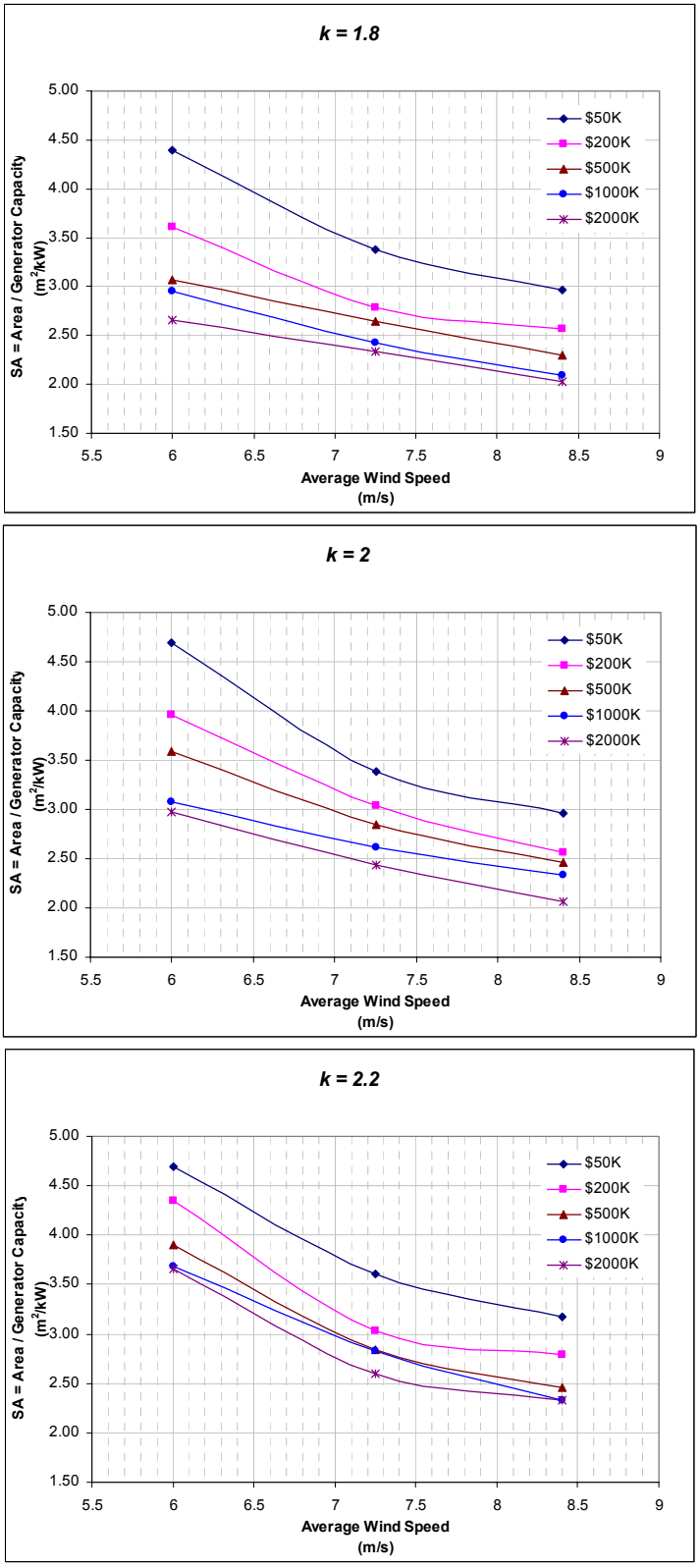

Figure 7.3: Optimal *SA* vs. Average Wind Speed at Constant *k*

Figure 7.3 shows that for a wind distribution with a constant shape parameter k, optimal *SA* tends to fall as the average wind speed rises. This means that as average wind speed decreases, rotor size becomes more important. As average speed increases, the balance shifts in favor of the generator.

Figure 7.4 shows that at a fixed average wind speed, optimal *SA* rises as *k* rises. Rising *k* means that the distribution of winds is moving toward more annual hours closer to the average wind speed. At a site with $k = \infty$, winds would blow at a single speed constantly. The ideal configuration for that site would be one with a rotor whose power output (at that wind speed) matched generator capacity. While the relationship between optimal *SA* and *k* for the cases examined show *SA* rising with *k*, the rise is slight and appears to be leveling in some instances. It is possible that *SA* reaches a peak and then begins to decline with higher *k* values. Ultimately, however, it seems that for a site with a constant average wind speed, the optimum *SA* must approach the value designed for V_{avg} discussed above.

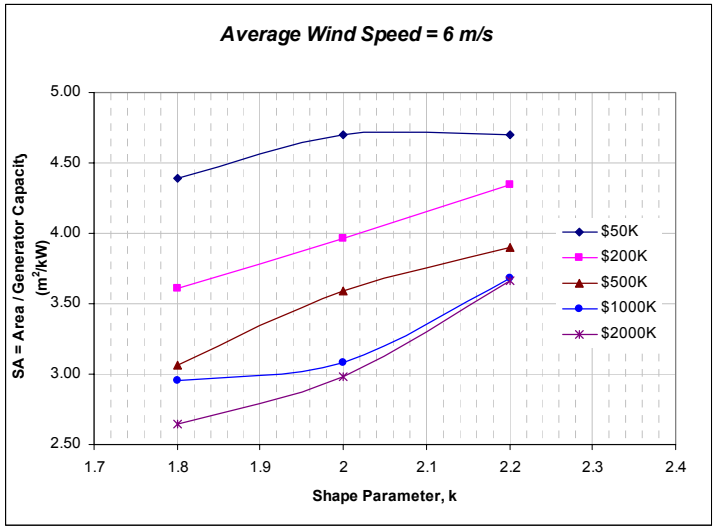

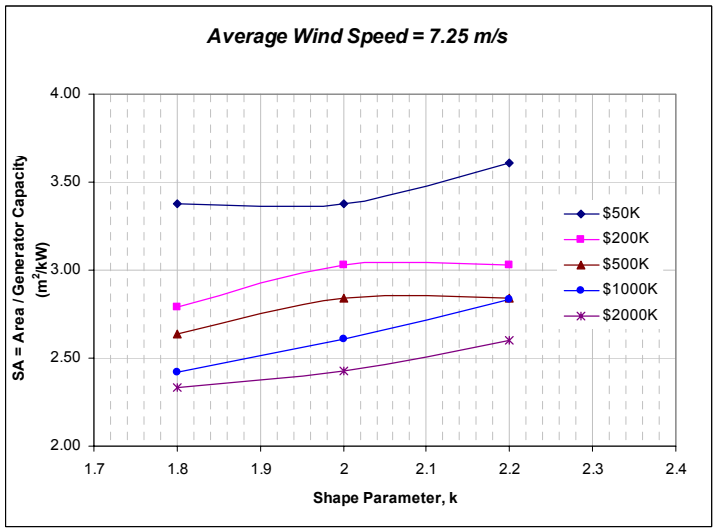

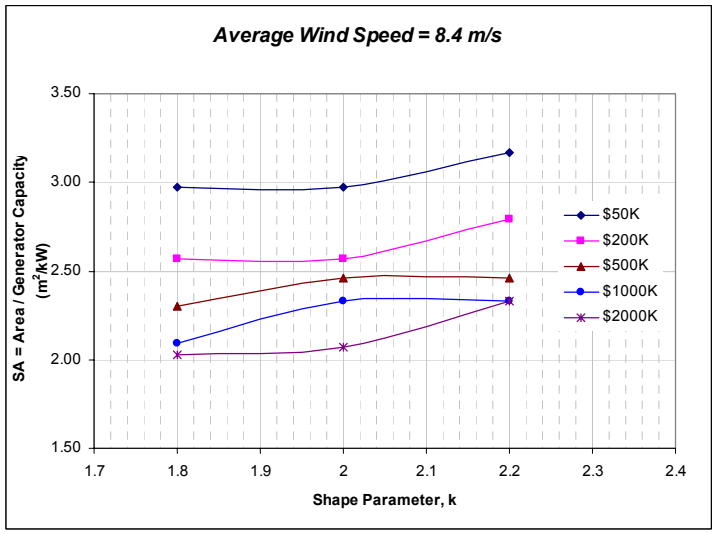

Note: Increasing value of k means the distribution is becoming more uniform and the variance is growing smaller.

Figure 7.4: Optimal *SA* vs. *k* at Constant Average Wind Speed

Figure 7.5 shows that for a given wind resource (constant k & V_{avg}), optimal SA decreases with an increase in capital cost. In other words, as capital cost increases the balance falls in favor of the generator. This is a result of the scaling differences in the rotor and generator costs. The cost of the generator scales linearly with size. The cost of the rotor is a function of the cube of the radius. As the rotor gets larger, small increases in size come at greater and greater expense.

A definite leveling is seen at the higher capital costs. Each wind condition seems to have a different asymptote point. This result indicates that as wind turbines become larger, there may be an optimum ratio that more or less holds steady above a certain size.

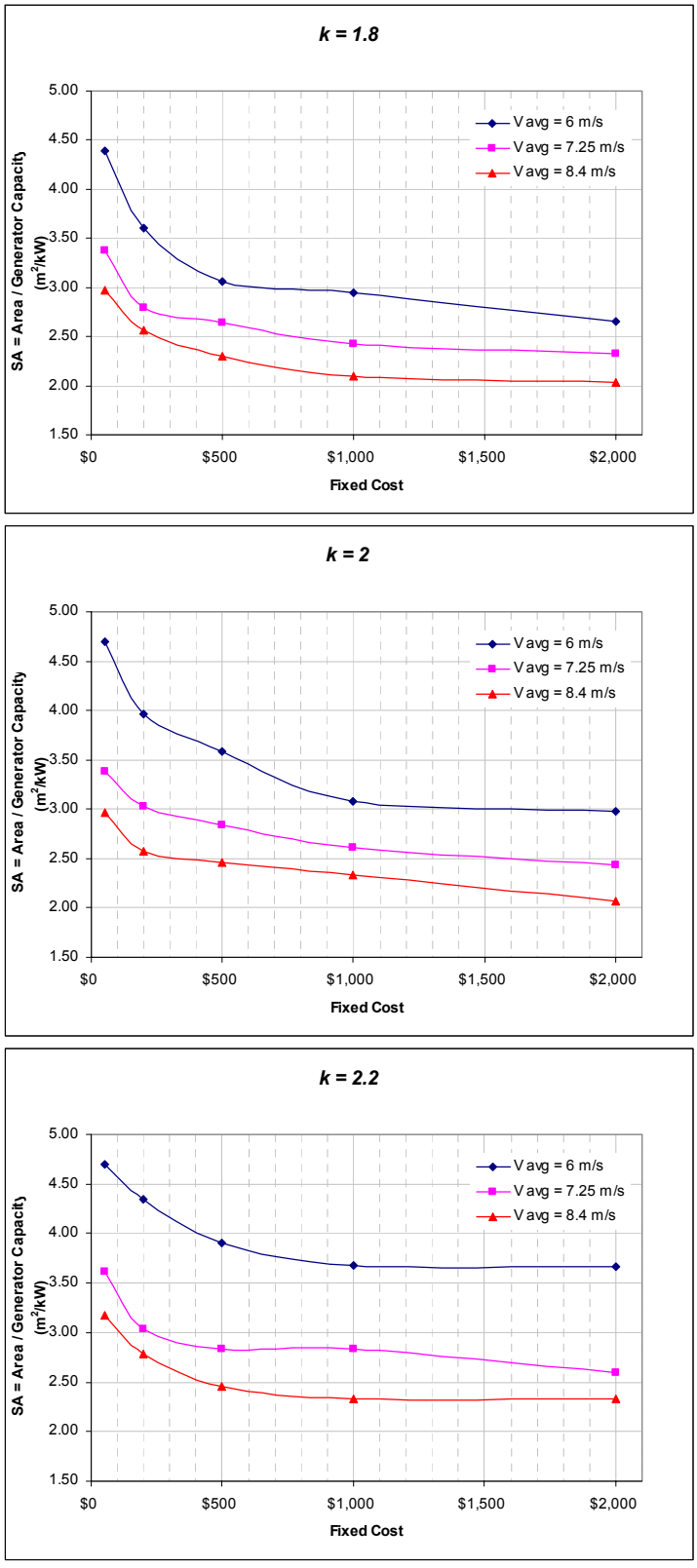

Figure 7.5: Optimal *SA* vs. Fixed Cost at a Constant Wind Resource

7.1.2 Optimal Capacity Factor

The middle column of Table 7.1 shows the capacity factor for each configuration. This represents the optimum capacity factor for the wind site at the given capital cost. A higher or lower capacity factor will result in less electricity being produced. Figures 7.6 thru 7.8 show the effect each of the parameters has on optimal capacity factor.

Figure 7.6 shows that as average wind speed rises, so does the optimum capacity factor. This is a bit unexpected as it was shown earlier that an increase in average wind speed leads to the *SA* ratio decreasing. However, the relationship between wind speed and power is cubic. At a constant k, increasing V_{avg} leads to significantly more power from the rotor. This increase in power, at least in the range of cases examined, raises electrical output sufficiently to overcome the effect of a smaller rotor and increase capacity factor even as generator capacity rises.

Figure 7.7 shows an increase in optimal capacity factor as k increases. This is to be expected. As was discussed in the previous section, $k = \infty$ is a site with a constant wind speed. In such a site, one could design a turbine with a capacity factor at or near 1 (neglecting maintenance, etc). Higher values of k means a narrower distribution of wind speeds. The narrower the distribution, the higher the theoretical capacity factor.

Figure 7.8 shows a decrease in optimal capacity factor with increased capital cost. This is to be expected and is due to of the different cost relationships of the two components as discussed in the previous section. At a given wind resource, capacity factor will always rise or fall along with SA.

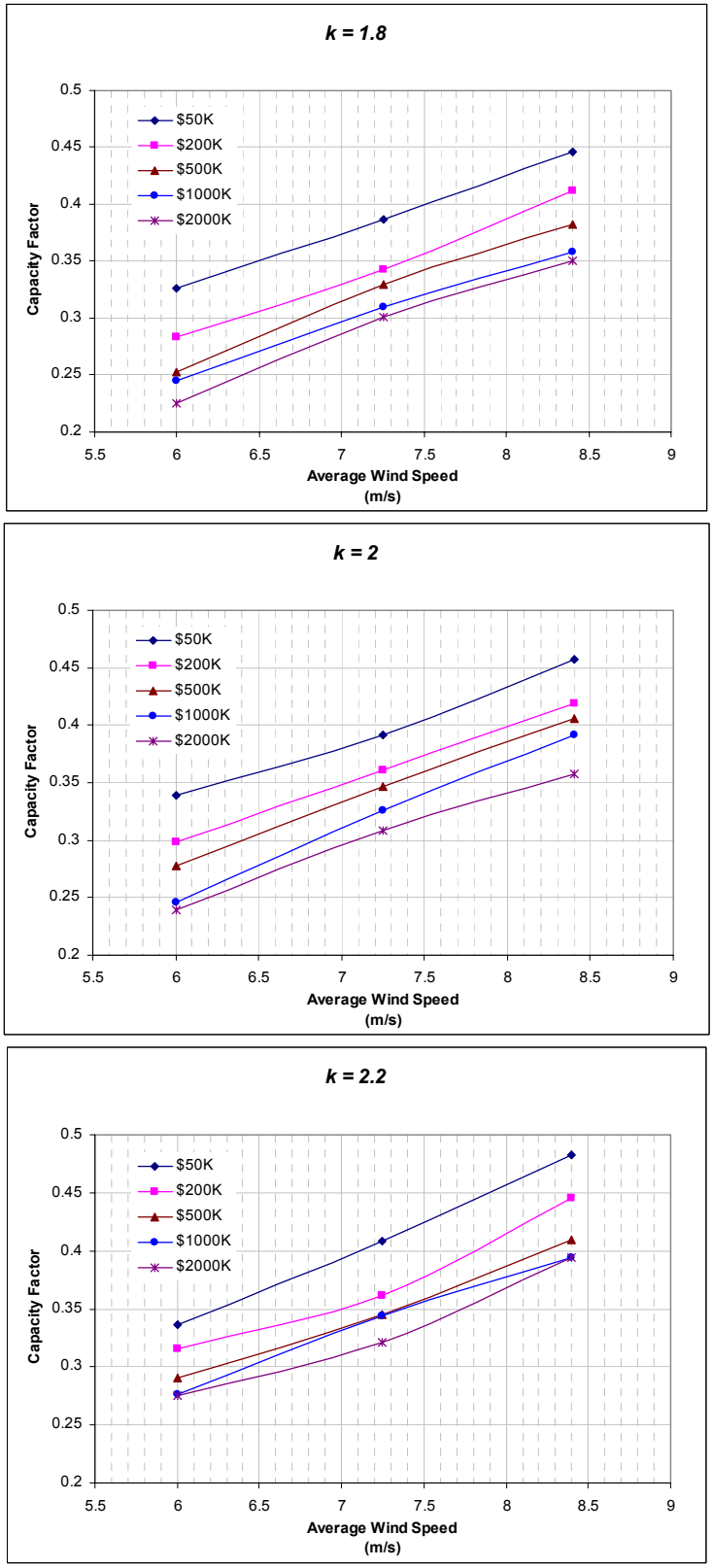

Figure 7.6: Optimal Capacity Factor vs. Average Wind Speed at Constant *k*

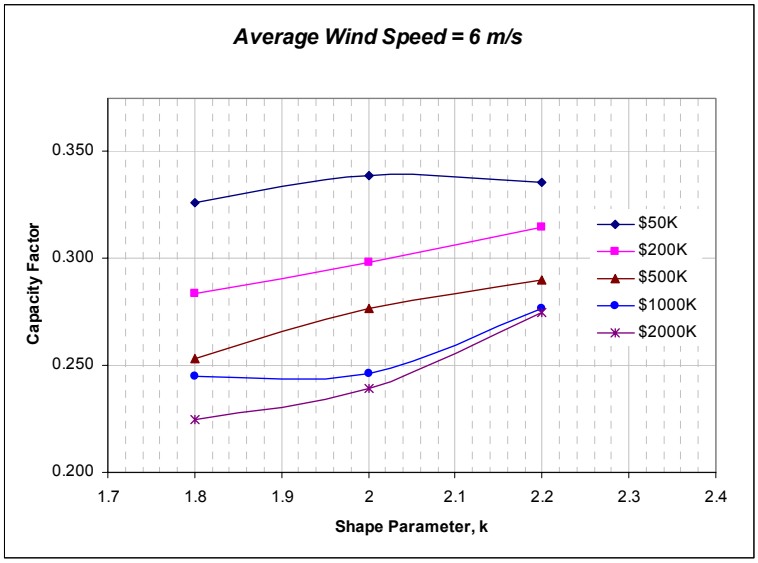

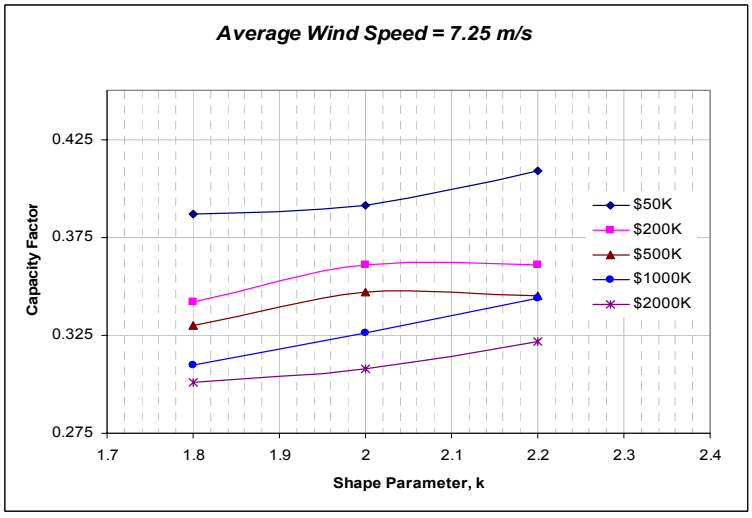

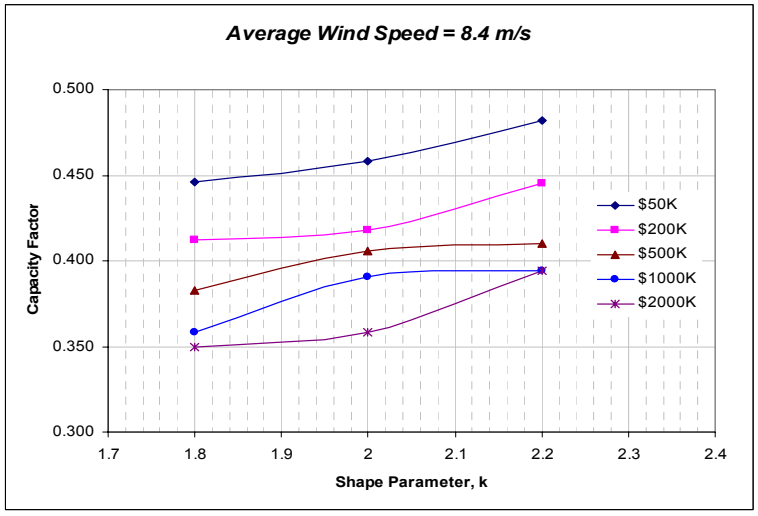

Figure 7.7: Optimal Capacity Factor vs. *k* at Constant Average Wind Speed

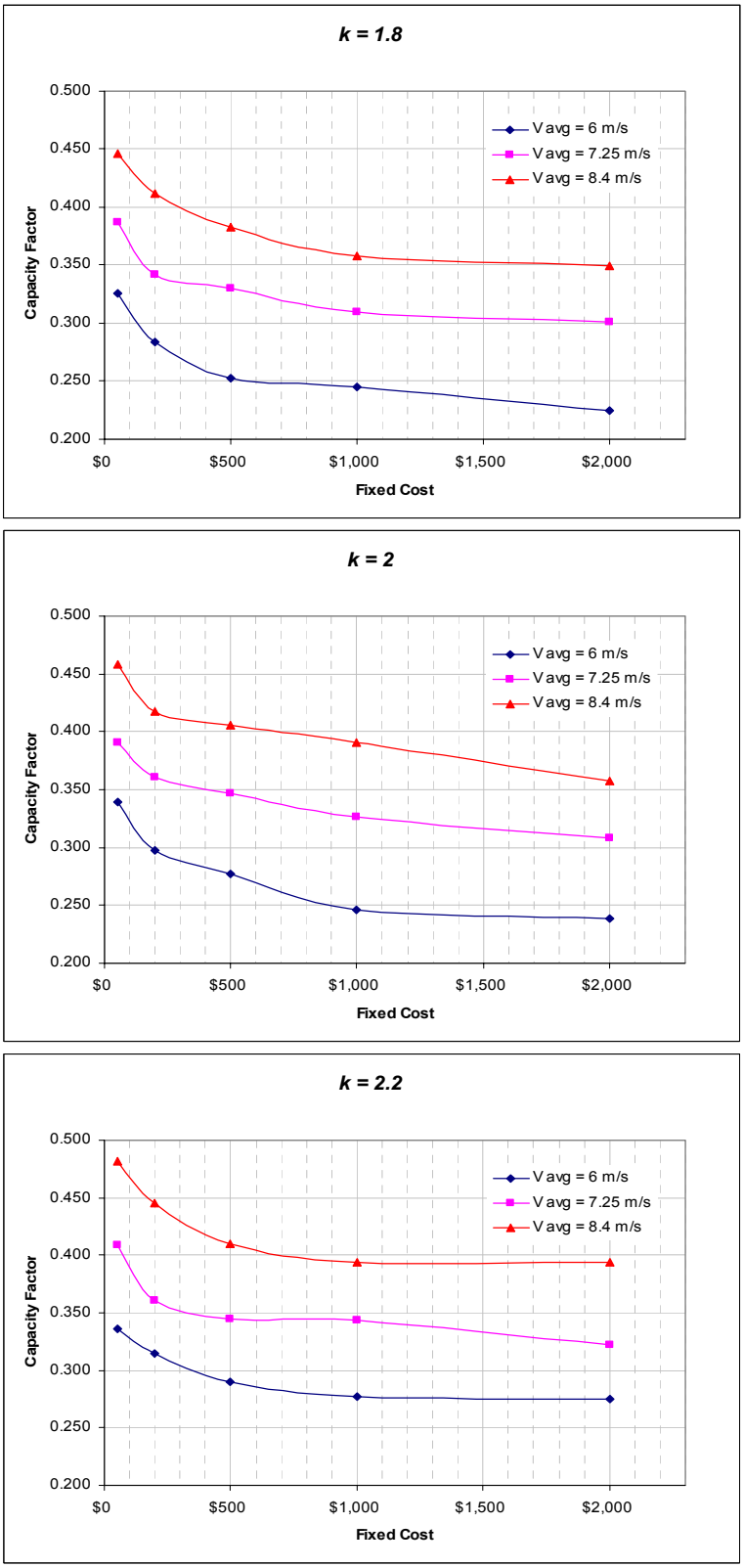

Figure 7.8: Optimal Capacity Factor vs. Fixed Cost at a Constant Wind Resource

7.2 Example Cases

Table 7.2 and Table 7.3 show the results of an optimization based on current machines, a Vestas-V90 2.0 MW and a GE 3.6 MW machine. These are the same two turbines used in Chapter 6 to validate the optimization model. In the following examples, fixed capital cost was determined by applying the formulas for rotor and generator costs, equations (4.1) and (4.2), to the published rotor and generator data for the Vestas[34] and GE[14] turbines. This produced a fixed cost of $600,000 for the Vestas, and a fixed cost of $1,111,000, for the GE.

Table 7.2 shows the optimization using $600,000 as the cost constraint. Column 1 shows the annual electrical output of the model using the Vestas configuration, a 45 meter (radius) rotor and a 2.0 MW generator[34]. Column 2 shows the electrical output of the model using a configuration optimized for the wind resource. The rotor and generator sizes for this optimized configuration are shown in Columns 5 and 6. Columns 3 and 4 show the improvement in terms of a fractional increase of annual electrical energy and in terms of additional MW-hrs generated.

Table 7.2: Optimization Results compared to the Vestas-V90 2.0 MW Wind Turbine

		1	2	3	4		5	6
	Average Wind Speed (m/s)	Electricity - Model 45m, 2MW (MW-hr)	Electricity - Optimized Model (MW-hr)	Improvement (Fraction)	Improvement (MW-hr)		Optimized Model Rotor (m)	Optimized Model Generator (kW)
k = 1.8	6	4533	4558	1.006	25		44.72	2100
	7.25	6470	6643	1.027	173		43.57	2400
	8.4	8001	8473	1.059	472		43.18	2500
k = 2.0	6	4412	4444	1.007	32		45.81	1800
	7.25	6513	6618	1.016	105		43.96	2300
	8.4	8215	8598	1.047	383		43.18	2500
k = 2.2	6	4281	4349	1.016	68		45.81	1800
	7.25	6523	6582	1.009	59		44.34	2200
	8.4	8372	8672	1.036	300		43.57	2400

Table 7.3 shows this same information, except as it relates to the GE 3.6 MW machine. The cost constraint is $1,111,000, and the reference case has a 55.5 m rotor and a 3.6 MW generator[14].

Table 7.3: Optimization Results compared to the GE 3.6 MW Wind Turbine

		1	2	3	4		5	6
	Average Wind Speed (m/s)	Electricity - Model 55.5m, 3.6MW (MW-hr)	Electricity - Optimized Model (MW-hr)	Improvement (Fraction)	Improvement (MW-hr)		Optimized Model Rotor (m)	Optimized Model Generator (kW)
k = 1.8	6	7181	7199	1.003	18		55.98	3400
	7.25	10512	10569	1.005	57		54.53	4000
	8.4	13273	13607	1.025	334		53.51	4400
k = 2.0	6	6913	6979	1.010	66		56.26	3300
	7.25	10484	10503	1.002	19		55.26	3700
	8.4	13517	13719	1.015	202		54.53	4000
k = 2.2	6	6646	6814	1.025	168		57.36	2800
	7.25	10411	10415	1.000	4		55.74	3500
	8.4	13682	13800	1.009	118		54.53	4000

These results indicate that current machines are fairly well optimized for the wind speed distributions analyzed. The largest improvement shown was with the Vestas at the k=1.8, V_{avg} = 8.4 wind site. A shift to a 43.18 m rotor and a 2.5 MW generator leads to a 6% improvement in terms of energy captured.

The results indicate that if multiple generators are available for the same rotor size, there is an advantage in picking a generator suited to the wind conditions at the site. This is the case with the Vestas machine. The Vestas turbine comes in two varieties; the Vestas-V90 2.0 MW, and the Vestas-V90 1.8 MW[34]. Analysis shows that at a Class 2 site with *k* values of 2 to 2.2, the 1.8 MW machine is possibly better suited (discounting other factors). In each of the other situations, the 2.0 MW machine is probably the better choice. If a model with a higher generator capacity was offered, the analysis indicates this would be a better match to most of the wind resources. However, the overall gains in total electricity would not be substantial.

Other than the one study[30] discussed in Section 1.5, no references were found in the literature review with regards to relating rotor size to generator size for site-specific wind resources. It is not known how the various turbine manufacturers go about sizing rotor to generator. One possible method is to design around an average wind speed for a common resource. For example, a wind resource with Weibull parameters V_{avg} = 8.4 m/s and k = 2, has a V_{rmc} of 10.9 m/s. Assuming a performance coefficient of 0.5, a 55 meter rotor (radius) will produce roughly 3.6 MW of power at this speed. This matches the GE machine very well. Looking at the Vestas machine, a 45 meter rotor will produce roughly 2.4 megawatts. This is larger than the 2.0 megawatt generator used with the Vestas turbine.

It may be that similar analysis to this study has been carried out, but the studies have not been published. The results of this analysis show that currently available wind turbines seem fairly well designed for wind sites with a Weibull shape parameter near 2. Further analysis should examine resources outside of the k = 1.8 to 2.2 range.

7.3 Optimal Rotor-to-Generator Size

Figures 7.9 thru 7.11 show the optimal rotor size for a given generator size at each of the wind resources examined. The gray lines running from the upper left to the lower right represent a fixed capital cost. The numeric values associated with the gray lines represent the fixed costs in one-hundred-thousand dollar increments, as per the costing formulas used in the study. However, the costing formulas are for a fixed point in time while actual costs are continually changing due to inflation. The purpose of the including the values is only to provide a measure of relative scale.

The optimal relationship is defined as the one that will produce the most electricity at that resource at a given cost. Each of the figures contains two graphs, **a** and **b**. Graph **a** shows the results over the range of the complete study, from a fixed cost of $50,000 to $2,000,000. Graph **b** shows a range where most utility scale wind machines reside today—the 2 to 4 megawatt range. These graphs may be useful to wind farm developers in terms of selecting an appropriate turbine for a given site. While many factors are involved in turbine selection, these graphs should provide some assistance in terms of selecting a turbine with a more favorable rotor-to-generator balance.

a

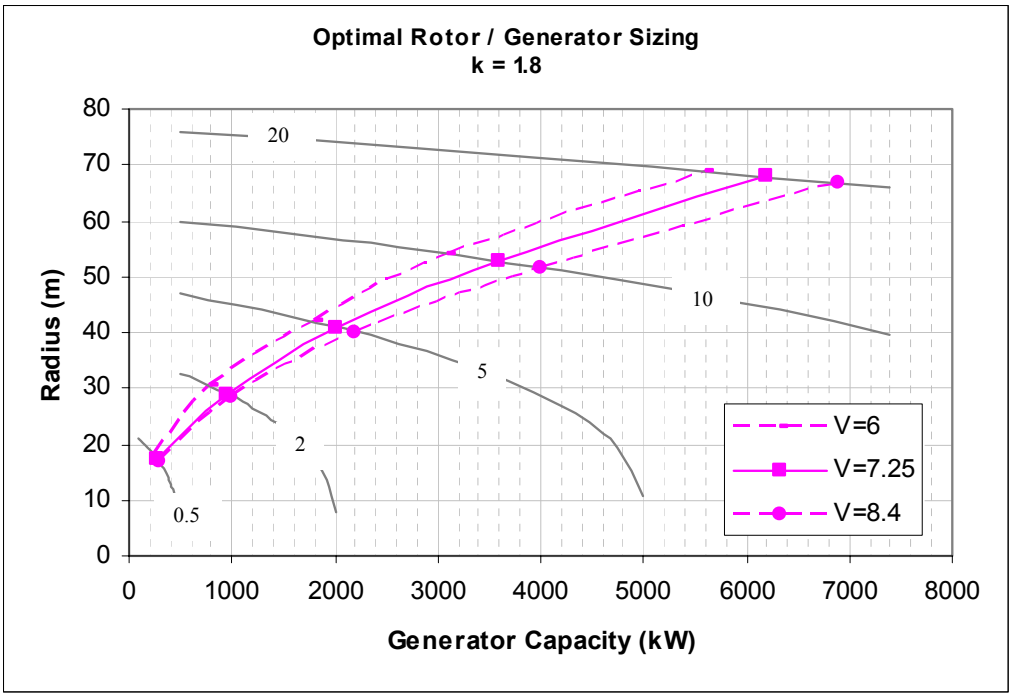

b

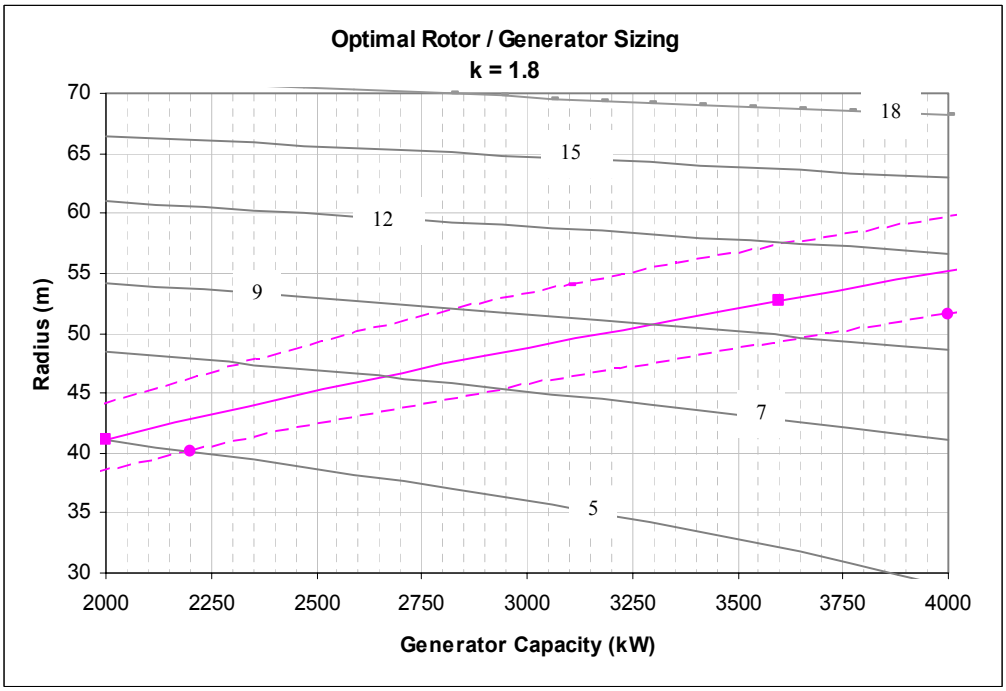

Note: Gray Lines represent lines of Fixed Capital Cost. The associated values are for relative scaling.

Figure 7.9: Optimal Rotor Sizes for various Generator Capacities for a k = 1.8 Wind Resource

a

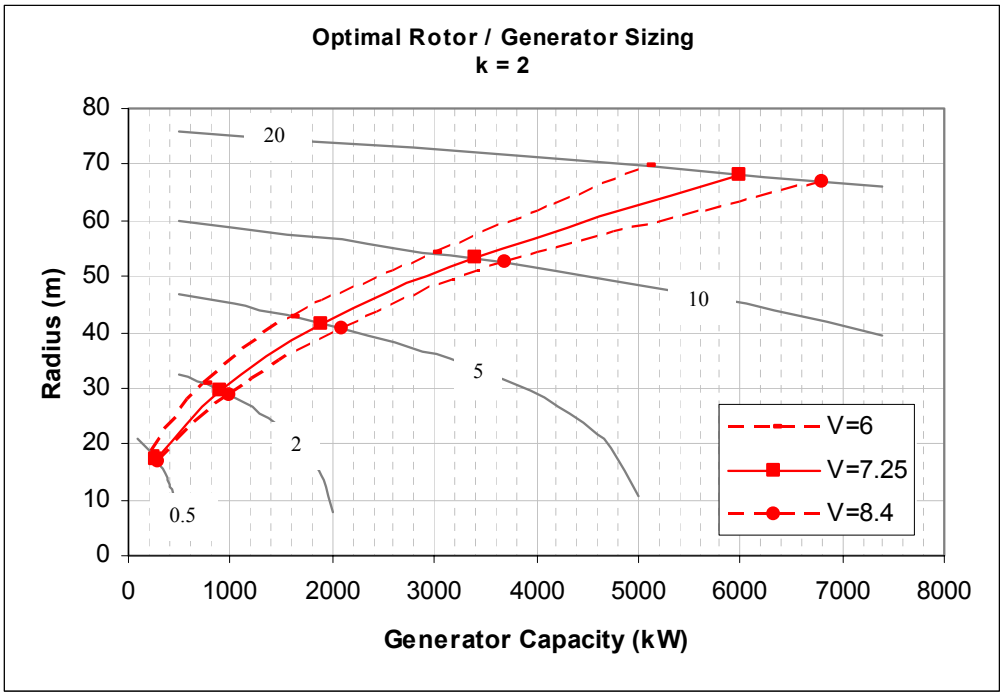

b

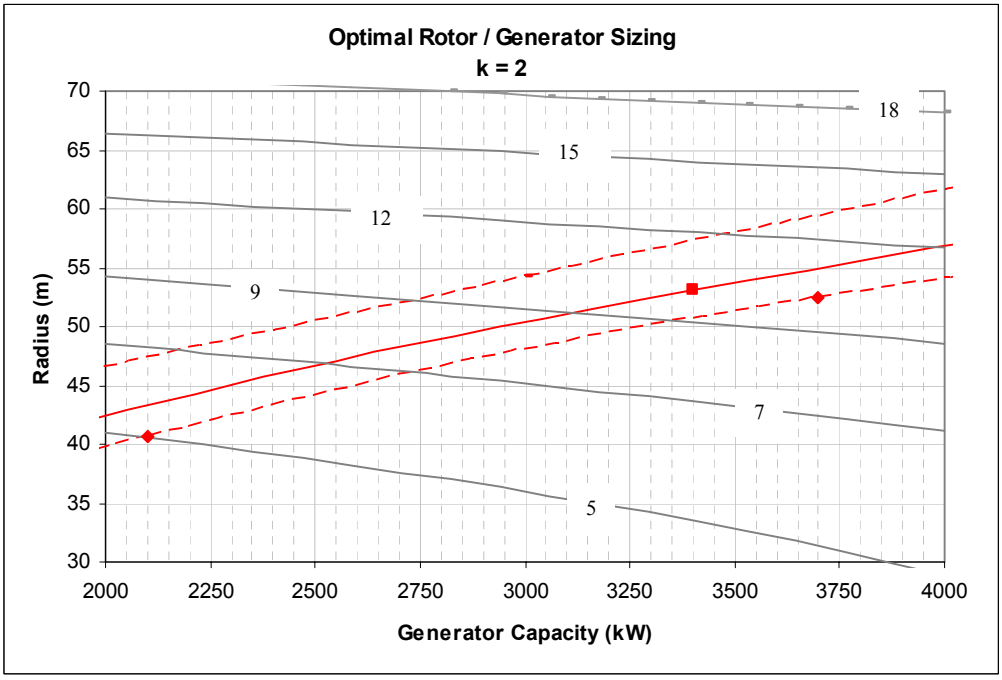

Note: Gray Lines represent lines of Fixed Capital Cost. The associated values are for relative scaling.

Figure 7.10: Optimal Rotor Sizes for various Generator Capacities for a $k = 2$ Wind Resource

a

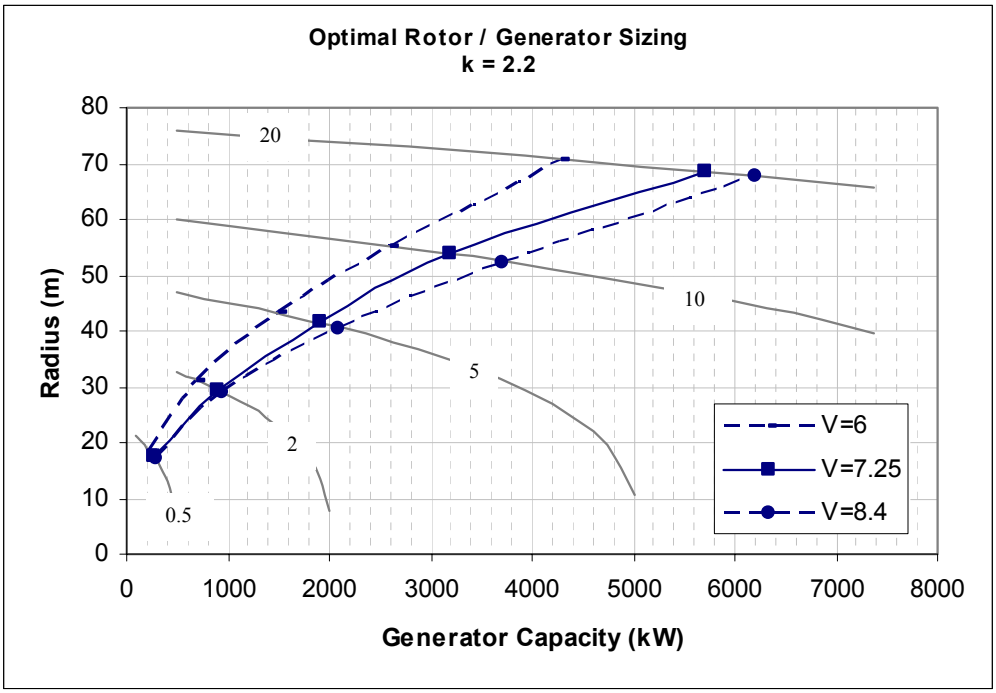

b

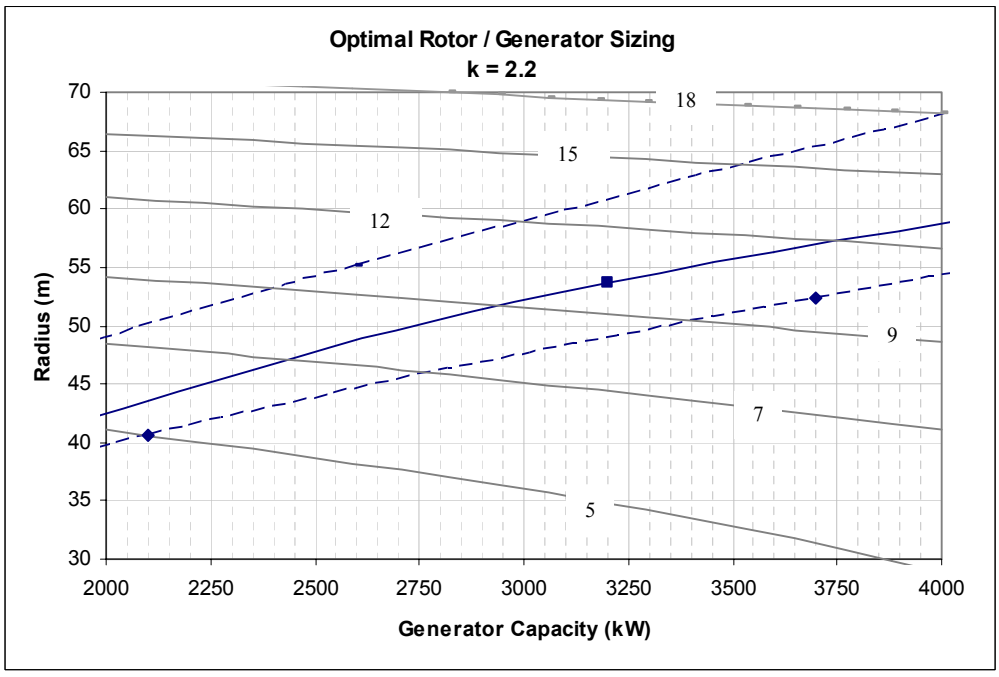

Note: Gray Lines represent lines of Fixed Capital Cost. The associated values are for relative scaling.

Figure 7.11: Optimal Rotor Sizes for various Generator Capacities for a k = 2.2 Wind Resource

7.4 Discussion

The trends seen in Figures 7.3 thru 7.8 result from a complex set of relationships. These are explored in Figure 7.12 and include the following:

- The cubic relationship between power and wind speed (Figure 7.12-a).
- The scaling differences in the cost / size relationships between the rotor and the generator (Figure 7.12-b)
- The various effects of differing Weibull parameters k and V_{avg} (Figure 7.12-c & d).
- The slight difference of output parameters *SA* and *CF* (Figure 7.12-e).

These lead to the following observations about the trends seen in the previous sections.

- The parameter SA and capacity factor are similar measures in that both are functions of rotor size over generator capacity. They are not the same, however, and the differences are exemplified in 7.12-e. SA goes to infinity as rotor size increases, while CF is bounded by one. Although both curves rise, the nature of the rise is different. Capacity factor is also a function of the Weibull distribution in addition to the rotor-to-generator relationship. In most instances SA and CF rise and fall together, but not always. With all other functions held constant, optimum SA falls with an increase in average wind speed, while the corresponding optimum CF rises. The reason for this was discussed in Section 7.1.1
- As the value of k increases with all other parameters held constant, *SA* and *CF* seem to follow each other fairly precisely. This may be a local effect, as the value

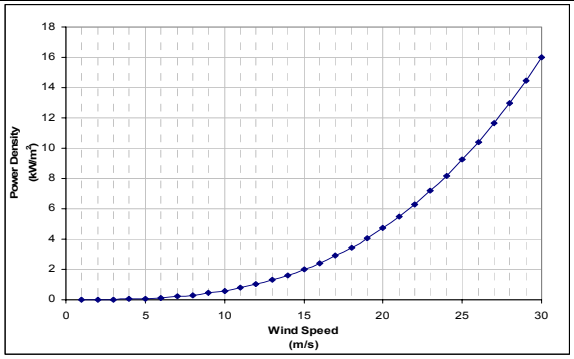

a :Power Density vs. Wind Speed

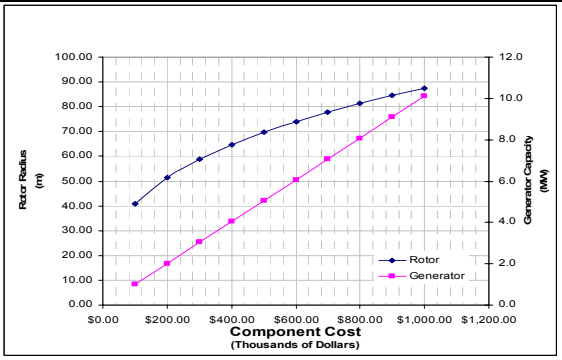

b :Component Cost vs. Size

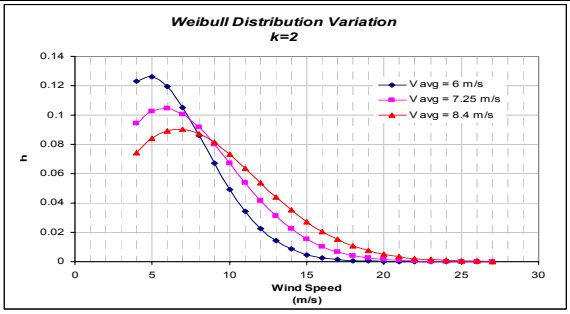

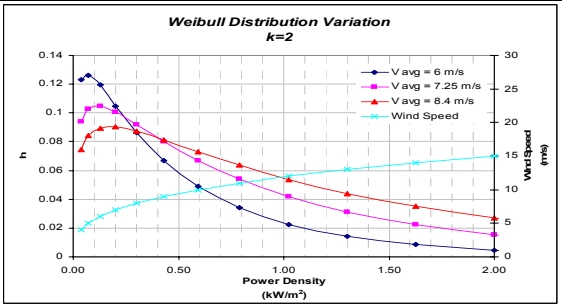

c :Wind Speed Distribution & Power Density Distribution with varying Average Wind Speed

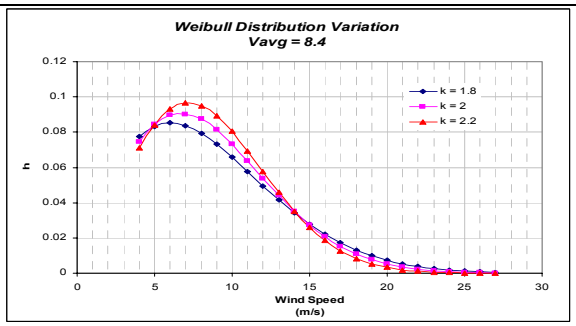

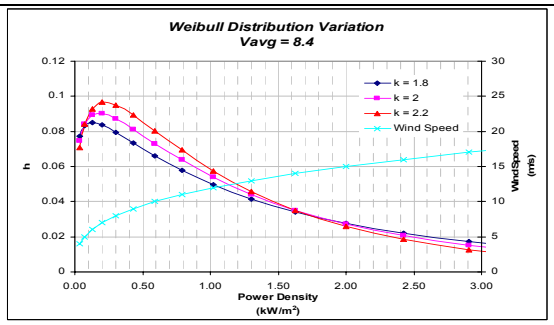

d :Wind Speed Distribution & Power Density Distribution with varying Shape Parameter

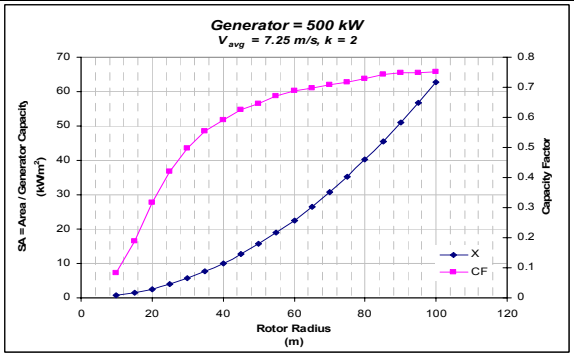

e :Effect of Increasing Rotor Size on *SA* and CF

Figure 7.12: General Trends of Input and Output Parameters

of k was varied only slightly in this study. Theory indicates that increasing k to high values should lead to values of CF approaching unity, and values of SA approaching a value optimized for the average wind speed of the resource. Further investigations are needed, looking at higher k values. Wind sites with values as high as 3 have been considered for wind projects, so it is reasonable to at least study the effect of increasing k to 3.

- As seen in Figure 7.12 c & d, decreasing the value of k has a similar effect as increasing the value of V_{avg}. Both lead to a spreading of the distribution. Likewise, increasing k and decreasing V_{avg} both lead to a narrowing of the distribution. This corresponds to the trends in SA seen in Figure 7.3 and 7.4. SA increases with increasing k, but decreases with increasing V_{avg}. There are differences between Figure 7.12 c & d, however. Increasing k leads to a distribution centered around V_{avg}, and this can be desirable if V_{avg} is high. A turbine can be designed (or selected) that is well optimized for the wind resource. Decreasing V_{avg} leads to distributions that are centered around very low wind speeds which is not desirable. So while the two effects are similar, they are not the same and need to be considered independently.

- The different costing relationships of the rotor and generator have a significant impact on the optimum rotor-to-generator size. As the capital cost of the components increases, optimal SA decreases. A leveling is seen at large capital cost, implying that at a certain size there may be a relationship that more-or-less holds constant from that point forward. This is a bit of a surprise in that one

might expect the opposite; i.e., to see the trend in favor of the generator size accelerating. At very large rotor sizes, one might expect to see virtually all further increases in cost go to the generator. Instead the trend is decelerating. The following provides an explanation:

> For a wind resource with a constant wind speed ($k = \infty$), one could design a turbine with an optimal *SA* independent of cost. The optimal *SA* would be one with a rotor whose power matched the generator capacity at that wind speed. Constant wind speed means a constant power density, and power from the rotor would rise and fall linearly with the size of the rotor. This would correspond directly with increases and decreases in generator size, so *SA* would remain constant. What would change, however, is the cost split between rotor and generator. As the total size of the turbine increased, the fraction of dollars going toward the rotor would rise and the fraction going toward the generator would fall. It seems that this concept is the best explanation for the trends seen in Figures 7.5 and 7.8. *SA* is approaching a cost independent optimum configuration for the wind resource, but the cost ratio is continually shifting toward the rotor. A quick analysis of the data confirms this. At a k =1.8, V_{avg} = 8.4 wind site, the cost breakdown between the rotor and generator at $50,000 capital cost and $2,000,000 capital cost were as follows:

Total Cost	$50,000	$2,000,000
SA	2.97	2.026
Cost of Rotor	$20,300	$1,317,000
Cost of Generator	$29,700	$683,100
$ Rotor / $ Generator	0.684	1.92

> This trend repeats for each of the wind sites examined.

While the general trends shown in Figures 7.3 to 7.8 are consistent, there are characteristics of individual lines that are unexpected and difficult to explain. This is best exemplified by Figures 7.5 and 7.8. Both have data points higher or lower than expected that impact the smoothness of the graphs. This shows up in the other graphs in terms of the concave-up or concave-down nature of the lines. This may be due to a variety of procedural and/or computational errors, but great effort was put forth to check internal and external data, and to validate the overall model. None were found.

The anomalies may be a product of the complex interactions of the various parameters discussed at the beginning of this section. Each of the vertical series of data points in Figures 7.3, 7.4, 7.6 and 7.7 represent a given wind resource. Likewise, each of the lines in Figures 7.5 and 7.8 represent a given wind resource. Each data point represents a unique circumstance—a given capital cost, a cost split between rotor and generator, a *k* value, and an average wind speed. Further analysis looking at values that fall between the values of the parameters studied should provide insight into this.

7.5 Summary of Conclusions

- At a given wind site there is an optimal relationship between rotor and generator size that varies with capital cost (the combined cost of the two components).

- The above relationship leads to optimal capacity factors well below unity. Wind turbine designs with capacity factors above this optimum result in less annual electricity being produced.

- The different cost scaling factors for rotor (cubic) and generator (linear) causes a downward trend in optimal rotor-to-generator size as capital cost increases (at a given wind resource). There is a corresponding downward trend on optimal capacity factor.

- As capital cost increases, capacity factor and the rotor-to-generator size seem to approach constant values. These values are specific for the individual wind resources (Weibull parameters).

- As the capital cost increases, the ratio of dollars spent on the rotor vs. the ratio of dollars spent on the generator increases.

- Increasing the value of shape parameter *k* for a wind resource (while holding the other parameters steady) leads to an increase in the optimal rotor-to-generator size ratio. The corresponding capacity factor also increases.

- Increasing the average wind speed at wind resources while holding the other parameters steady leads to a decrease in the optimal rotor-to-generator size ratio. The corresponding capacity factor, however, increases.

7.6 Implications

- The primary implication of this work is that for large wind turbines greater impact is achieved through variations of generator size vs. variations of rotor size. Simply put, it makes sense for manufacturers to offer multiple generator sizes for

the same wind turbine. Wind farm developers can then select the best generator for their wind resource.

- A useful product of this investigation is the set of graphs in Figures 7.9 thru 7.11. These show the optimal size relationships between rotor and generator for a given wind resource and a given capital cost. While the graphs could aid with the design of wind turbines, it seems the real value is in turbine selection. Wind farm planners can use the graphs to help select the best turbines for their site. Or, when multiple generators are available for a given turbine design, wind farm designers can use the graphs to select the best generator for their site.

7.7 Future Work

There are two obvious ways in which the present study can be expanded:

- The current study examined five different capital cost constraints at nine different wind resources. Some of the trends seen in this study may be better understood if additional trials are performed. Values of k ranging from 1.5 to 3 should be looked at, as well as values between the 1.8, 2, and 2.2 examined in this study. Likewise, values of V_{avg} that fall between and outside of the 6, 7.25, and 8.4 m/s should be examined.

- Research should be conducted to explore the causes of the consistency issues amongst the various curves. While the general trends are consistent, there are anomalies in each of the graphs that have not been explained in the present study.

Additional trials, as described above, may help to understand the nature of these anomalies better.

- A limitation of the current study is that it used the combined cost of only two components as its constraint. It is likely that other components are affected by the rotor-to-generator size relationship, and this would affect the overall results. A future study should try to incorporate other components into the costing relationship. Such a study would be useful both to turbine manufacturers and wind farm developers.

APPENDIX A

PITCH CONTROL

Table A.1: Pitch Angle as a Function of Wind Speed

Wind Speed (m/s)	Pitch Angle (deg)
1	2
2	2
3	2
4	2
5	2
6	2
7	2
8	2
9	2
10	4
11	5
12	7
13	9
14	11
15	12
16	14
17	15
18	16
19	18
20	19
21	20
22	21
23	22
24	23
25	24
26	25
27	26
28	27
29	28
30	29

APPENDIX B

ROTOR DATA

Table B.1: Published C_L and C_D Values for the S809 Aerofoil[26]

Angle of Attack (deg)	S809 Published C_L	S809 Published C_D
-20.1	-0.56	0.3027
-18.1	-0.67	0.3069
-16.1	-0.79	0.1928
-14.2	-0.84	0.0898
-12.2	-0.7	0.0553
-10.1	-0.63	0.039
-8.2	-0.56	0.0233
-6.1	-0.64	0.0131
-4.1	-0.42	0.0134
-2.1	-0.21	0.0119
0.1	0.05	0.0122
2	0.3	0.0116
4.1	0.54	0.0144
6.2	0.79	0.0146
8.1	0.9	0.0162
10.2	0.93	0.0274
11.3	0.92	0.0303
12.1	0.95	0.0369
13.2	0.99	0.0509
14.2	1.01	0.0648
15.3	1.02	0.0776
16.3	1	0.0917
17.1	0.94	0.0994
18.1	0.85	0.2306
19.1	0.7	0.3142
20.1	0.66	0.3186
30	0.705	0.4784
40	0.729	0.6743
50	0.694	0.8799
60	0.593	1.0684
70	0.432	1.2148
80	0.227	1.2989
90	0	1.308

Table B.2: Modified C_L and C_D Values used in the Rotor-to-Generator Size Optimization

Angle of Attack (deg)	Modified C_L	Modified C_D		Angle of Attack (deg)	Modified C_L	Modified C_D
-20	-0.56	0.3027		10	1.03	0.0274
-19	-0.621	0.305		11	1.1	0.0303
-18	-0.67	0.3069		12	1.13	0.09
-17	-0.736	0.2441		13	1.2	0.16
-16	-0.79	0.1928		14	1.27	0.21
-15	-0.819	0.1332		15	1.32	0.285
-14	-0.84	0.0898		16	1.29	0.31
-13	-0.756	0.0691		17	1.27	0.325
-12	-0.7	0.0553		18	1.26	0.385
-11	-0.66	0.046		19	1.25	0.41
-10	-0.63	0.039		20	1.24	0.44
-9	-0.589	0.0299		21	1.211	0.4538
-8	-0.56	0.0233		22	1.186	0.4681
-7	-0.606	0.017		23	1.164	0.4829
-6	-0.64	0.0131		24	1.144	0.4982
-5	-0.519	0.0133		25	1.126	0.514
-4	-0.42	0.0134		26	1.109	0.5302
-3	-0.305	0.0126		27	1.094	0.5469
-2	-0.21	0.0119		28	1.081	0.5639
-1	-0.08	0.0121		29	1.068	0.5814
0	0.05	0.0122		30	1.056	0.5992
1	0.168	0.0119		31	1.045	0.6173
2	0.3	0.0116		32	1.034	0.6358
3	0.414	0.0129		33	1.023	0.6545
4	0.54	0.0144		34	1.013	0.6735
5	0.647	0.0145		35	1.003	0.6928
6	0.79	0.0146		36	0.994	0.7122
7	0.836	0.0153		37	0.984	0.7318
8	0.9	0.0162		38	0.974	0.7516
9	0.956	0.021		39	0.964	0.7715

Table B.2 (Cont.): Modified CL and CD Values used in the Rotor-to-Generator Size Optimization

Angle of Attack (deg)	Modified C_L	Modified C_D		Angle of Attack (deg)	Modified C_L	Modified C_D
40	0.954	0.7916		70	0.476	1.305
41	0.944	0.8116		71	0.454	1.315
42	0.934	0.8318		72	0.431	1.324
43	0.923	0.8519		73	0.409	1.333
44	0.912	0.8721		74	0.385	1.341
45	0.901	0.8922		75	0.362	1.348
46	0.889	0.9123		76	0.338	1.355
47	0.877	0.9322		77	0.315	1.36
48	0.864	0.952		78	0.291	1.365
49	0.852	0.9717		79	0.267	1.369
50	0.838	0.9912		80	0.242	1.373
51	0.824	1.011		81	0.218	1.375
52	0.81	1.03		82	0.194	1.377
53	0.796	1.049		83	0.169	1.378
54	0.78	1.067		84	0.145	1.378
55	0.765	1.085		85	0.121	1.378
56	0.749	1.103		86	0.096	1.376
57	0.732	1.121		87	0.072	1.374
58	0.715	1.138		88	0.048	1.371
59	0.697	1.155		89	0.024	1.367
60	0.679	1.171				
61	0.661	1.187				
62	0.642	1.202				
63	0.623	1.217				
64	0.603	1.231				
65	0.583	1.245				
66	0.562	1.258				
67	0.541	1.271				
68	0.52	1.283				
69	0.498	1.294				

Table B.3: Blade Element Specifications

Blade Element Number	Radial Distance / Radius (Dimensionless)	Chord Length / Radius (Dimensionless)	Twist Angle (deg)
1	0	0.039	0
2	0.144	0.059	0
3	0.167	0.082	30
4	0.192	0.133	27.59
5	0.25	0.128	20.05
6	0.303	0.123	14.04
7	0.357	0.118	9.67
8	0.413	0.113	6.75
9	0.468	0.108	4.84
10	0.522	0.103	3.48
11	0.578	0.098	2.4
12	0.632	0.093	1.51
13	0.687	0.088	0.76
14	0.743	0.083	0.09
15	0.75	0.078	0
16	0.797	0.073	-0.55
17	0.852	0.068	-1.11
18	0.908	0.063	-1.55
19	0.962	0.057	-1.84
20	1	0.052	-2

APPENDIX C

RESULTS FROM THE INDIVIDUAL OPTIMIZATION TRIALS

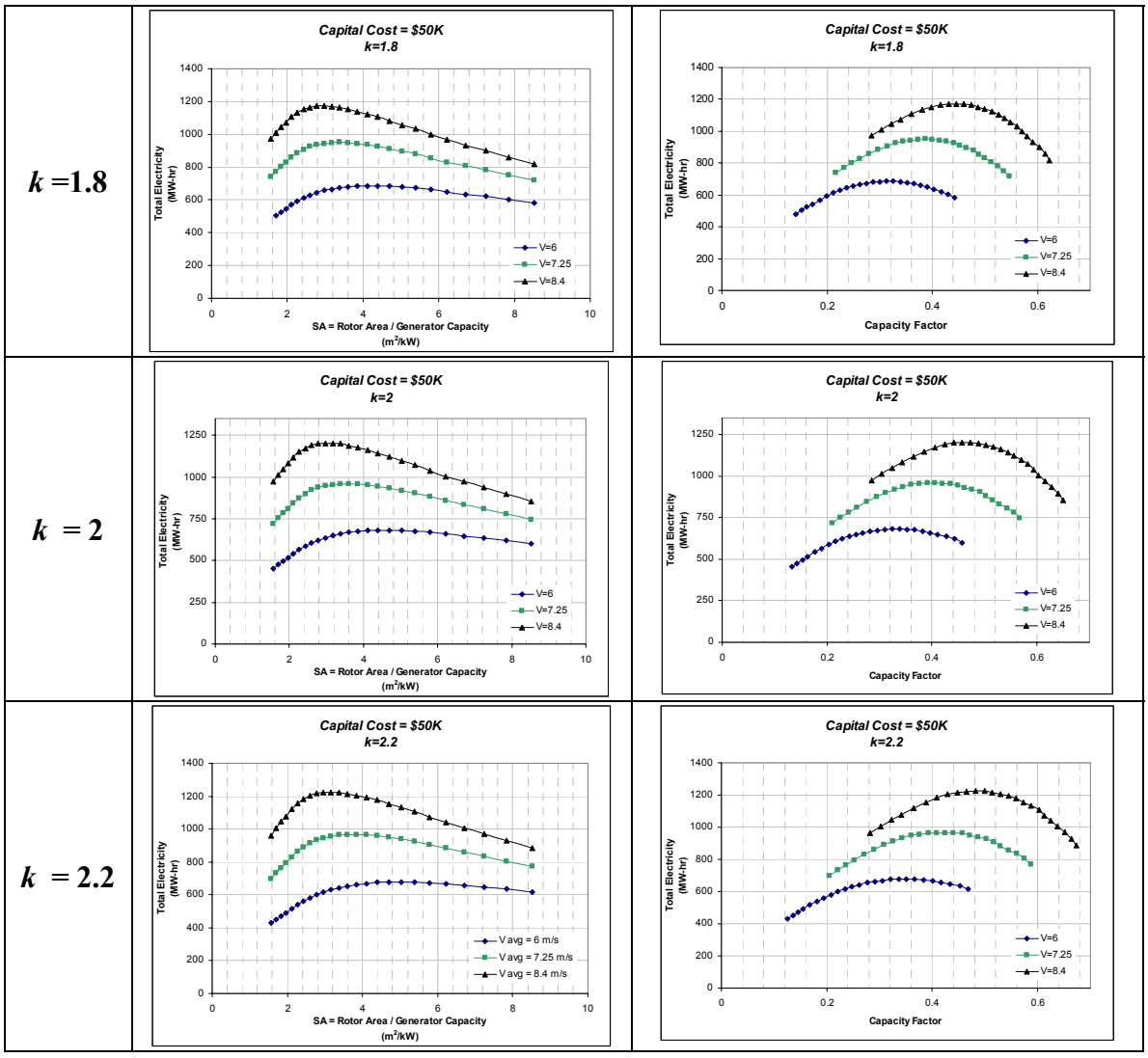

Figure C.1: Trial Results at Fixed Cost of $50,000

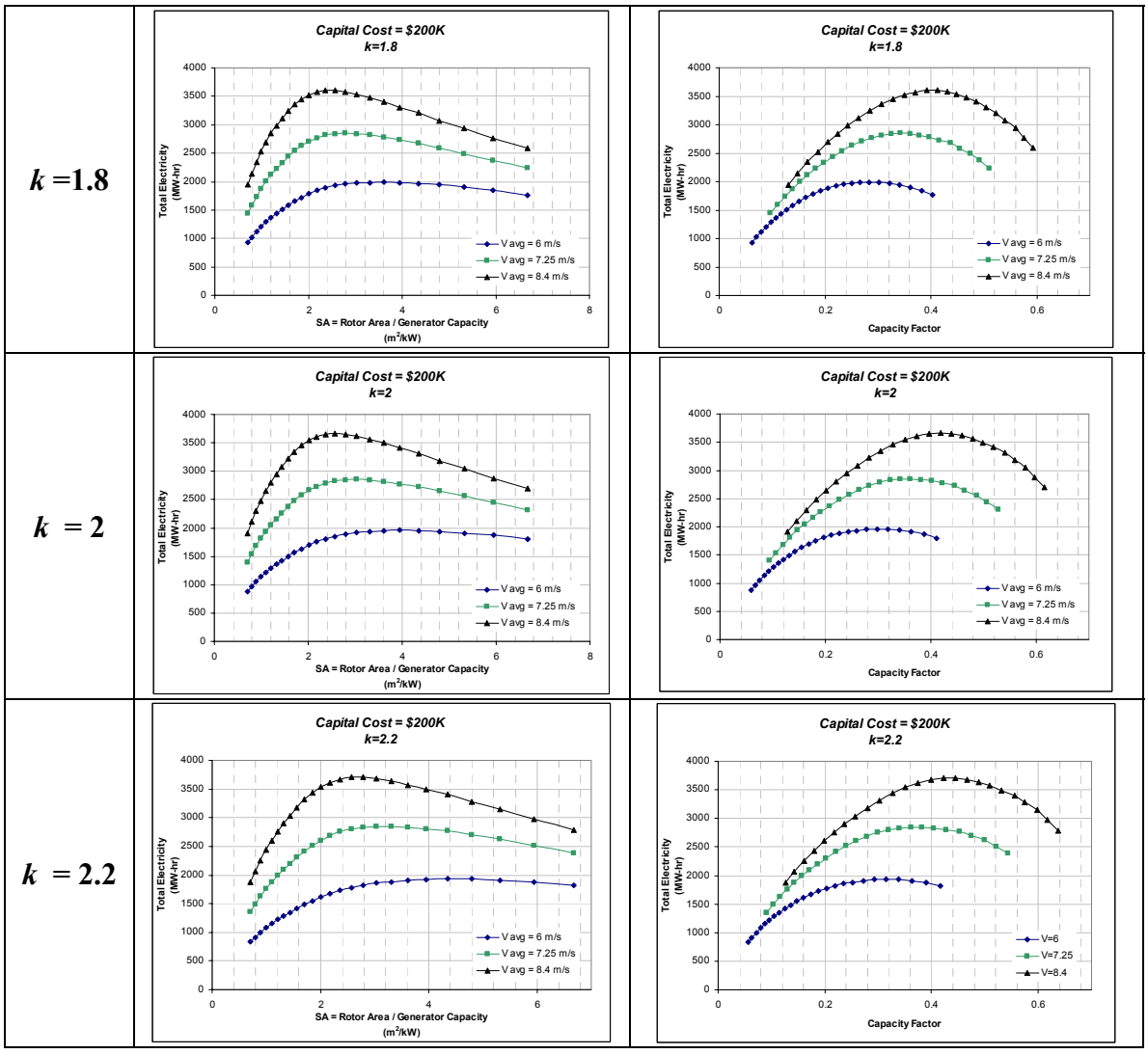

Figure C.2: Trial Results at Fixed Cost of $200,000

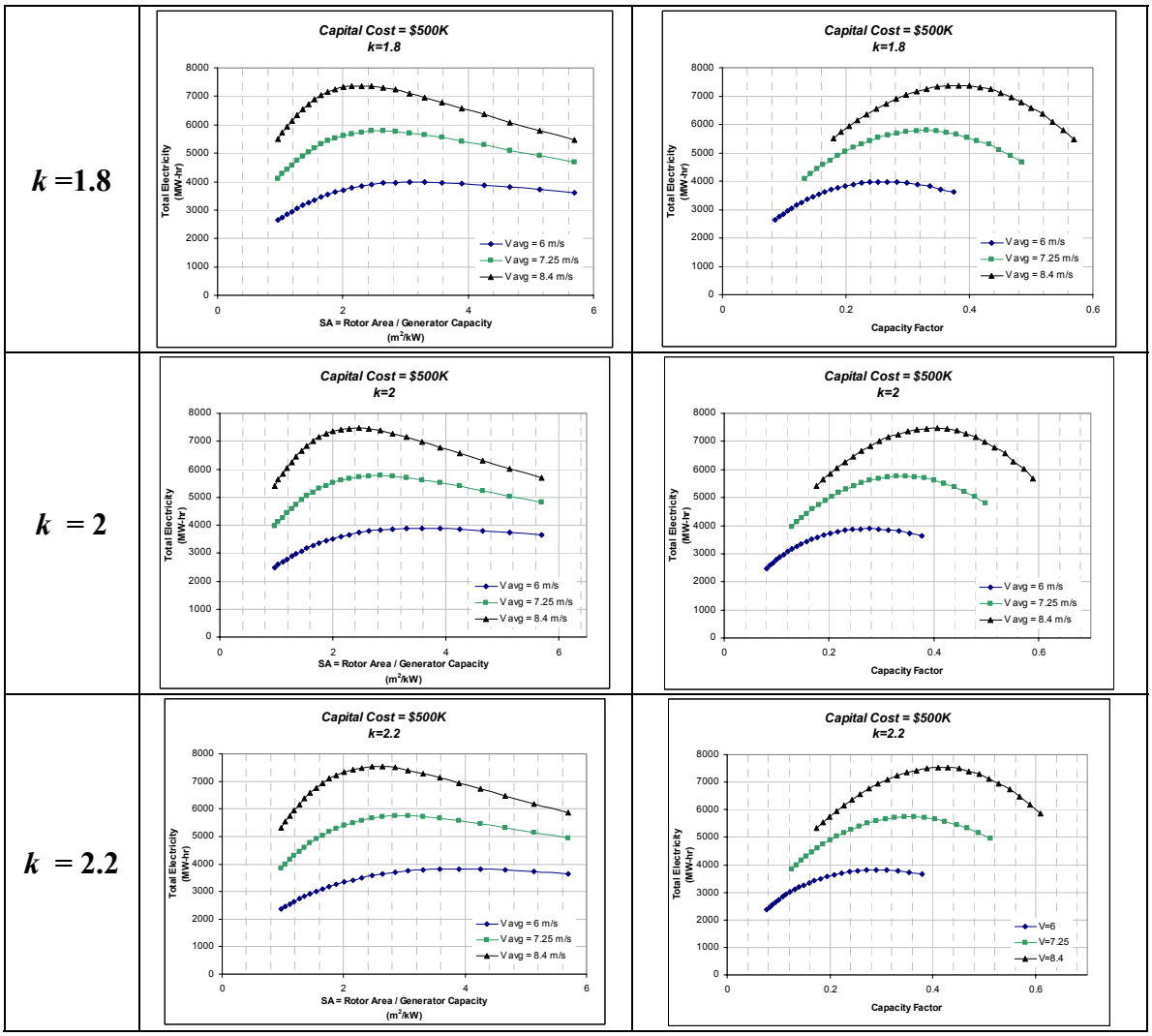

Figure C.3: Trial Results at Fixed Cost of $500,000

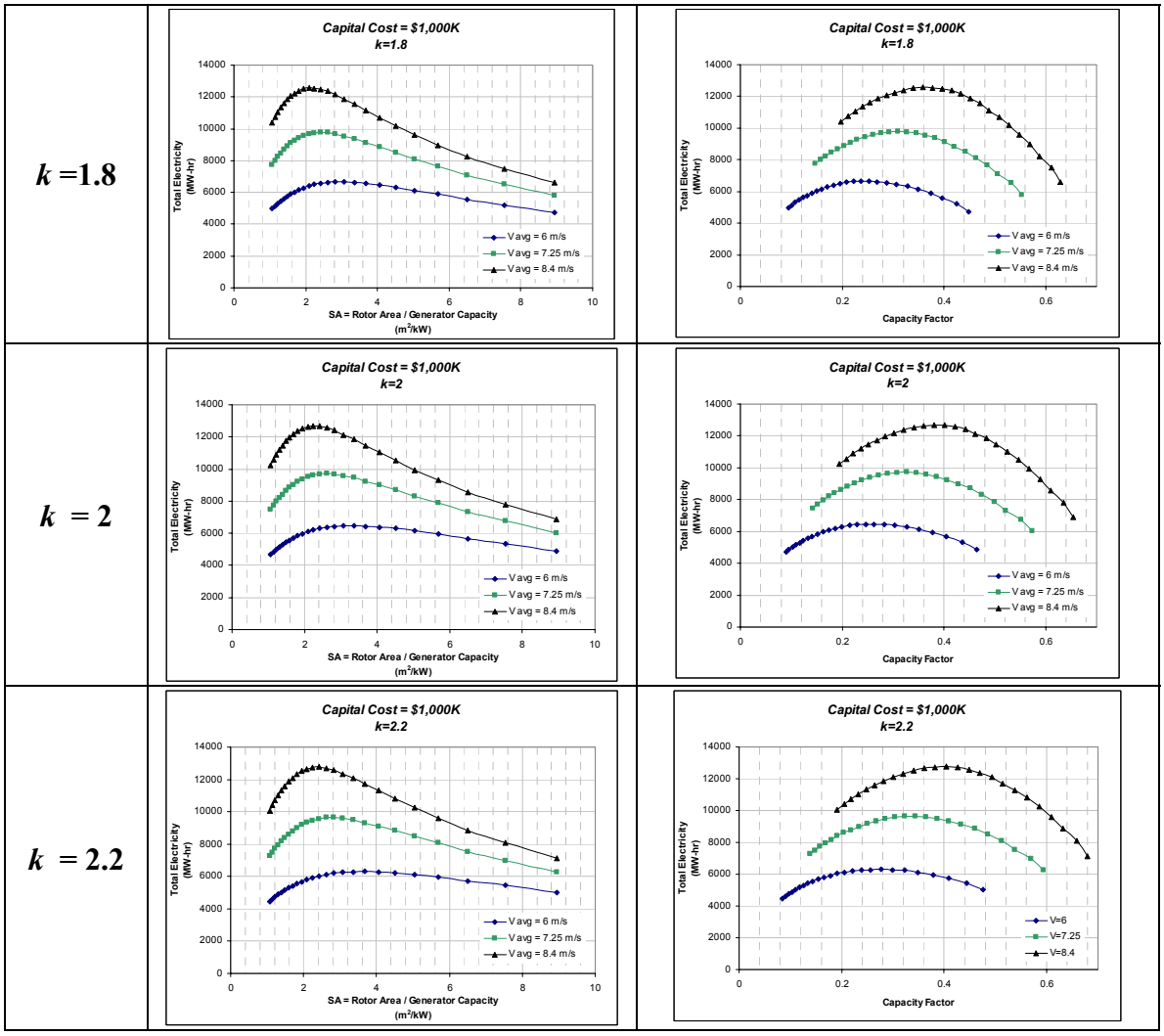

Figure C.4: Trial Results at Fixed Cost of $1,000,000

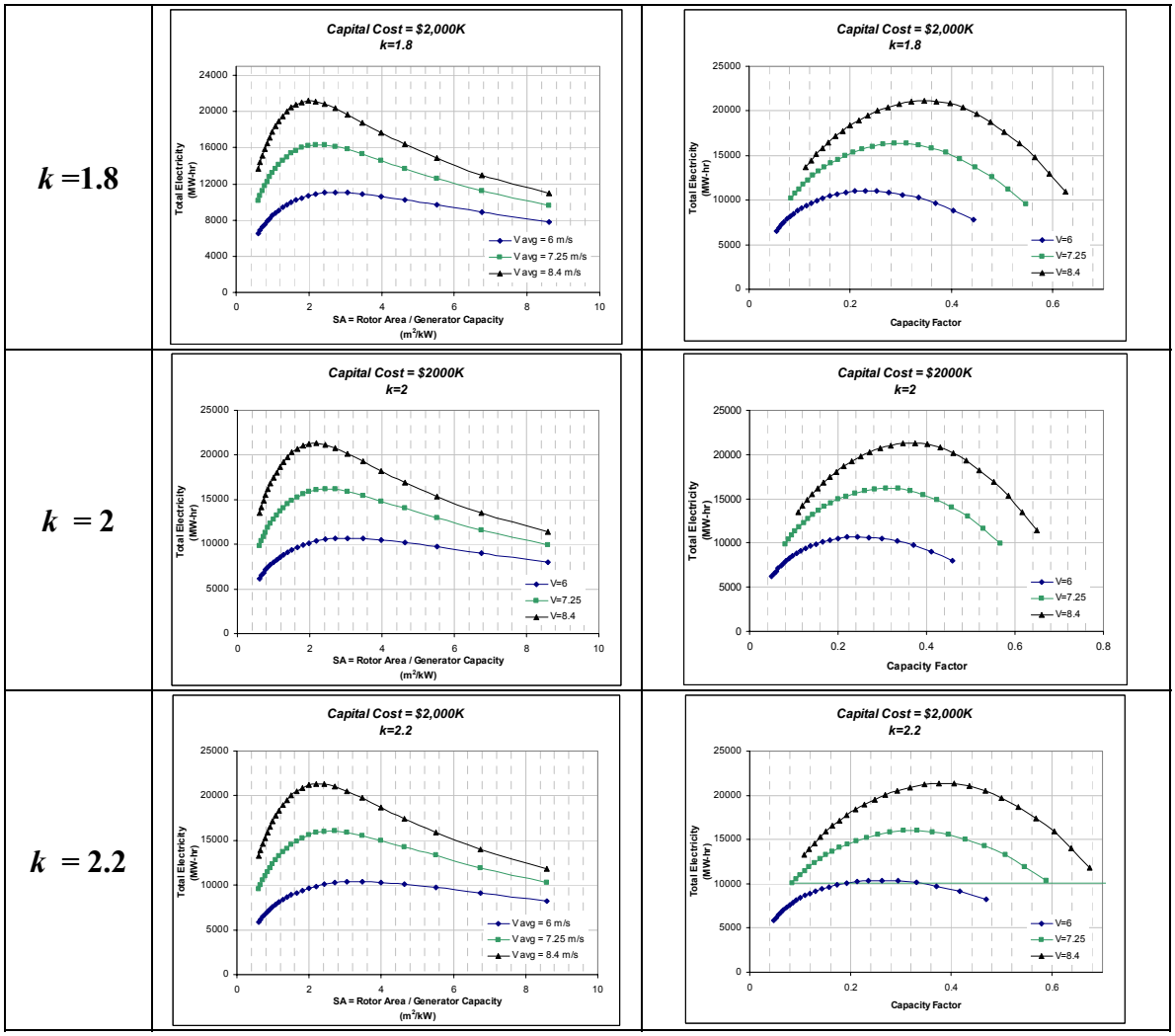

Figure C.5: Trial Results at Fixed Cost of $2,000,000

REFERENCES

[1] Ackermann, T. "European Experience, Offshore Wind Power," presentation to Strategic Energy Initiative, April 21, 2006.

[2] American Wind Energy Association (AWEA). "Annual Industry Rankings Demonstrate Continued Growth of Wind Energy in the United States." http://www.awea.org/news/Annual_Industry_Rankings_Continued_Growth_031506.html (Accessed July 2006)

[3] American Wind Energy Association (AWEA). "Basic Principles of Wind Resource Evaluation." http://www.awea.org/faq/basicwr.html (Accessed July 2006)

[4] American Wind Energy Association (AWEA). "What are the factors in the cost of electricity from wind turbines?" http://www.awea.org/faq/cost.html (Accessed August 2006)

[5] Anderson, John D. "Aircraft Performance and Design." McGraw-Hill, Boston, MA, 1999.

[6] Anon. "Illustrated History of Wind Power Development." http://www.telosnet.com/wind/early.html (Accessed August 2006)

[7] Bell, Benjamin. "An Imagination Breakthrough: Offshore Wind Energy." GE Energy Offshore Wind Presentation, Presented at the Georgia Tech Strategic Energy Initiative workshop *Alternative Energy Technology Innovations: The Coming Economic Boom*, Savannah, GA, 2005.

[8] Billinton, R., and Hua Chen. "Risk Based Optimum Site-Matching Wind Turbine Analysis." Wind Engineering, Vol. 23, No. 6, pp. 341-351, 1999.

[9] Burton, Tony, David Sharpe, Nick Jenkins, and Ervin Bossanyi. "Wind Energy Handbook." John Wiley & Sons Ltd, West Sussex, England, 2001.

[10] Butterfield, S. "Overview of Wind Energy Technology," National Renewable Energy Lab presentation at AGMA/BMA Annual Meeting, Tuscon, AZ, 2006.

[11] Danish Wind Industry Association. "A Wind Energy Pioneer: Charles Brush." http://www.windpower.org/en/pictures/brush.htm (Accessed August 2006)

[12] Department of Energy, Energy Efficiency and Renewable Energy. "History of Wind Energy." http://www1.eere.energy.gov/windandhydro/wind_history.html (Accessed August 2006)

[13] Fuglsang, Peter, and Kenneth Thomsen. "Site-Specific Design Optimization of 1.5-2.0 MW Wind Turbines." Journal of Solar Energy Engineering, Vol. 123, pp. 296-303, 2001.

[14] GE Energy. "3.6 MW Offshore Series Wind Turbine." http://www.gepower.com/prod_serv/products/wind_turbines/en/downloads/ge_36_brochure_new.pdf (Accessed August 2006)

[15] Gerber, Brandon S., James L. Tangler, Earl P. N. Duque, and J. David Kocurek. "Peak and Post-Peak Power Aerodynamics from Phase VI NASA Ames Wind Turbine Data." Journal of Solar Energy Engineering, Vol. 127, pp. 192-199, May 2005.

[16] Giguere, P., and M.S. Selig. "Design or a Tapered and Twisted Blade for the NREL Combined Experiment Rotor." NREL Report SR-500-26173, April 1999.

[17] Gipe, Paul. "Wind Energy Basics – A Guide to Small & Micro Wind Systems." Chelsea Green Publishing Company, White River Junction, VT, 1999.

[18] Glauert, H. "The Elements of Aerofoil and Airscrew Theory." Cambridge University Press, New York, NY, 1947.

[19] Griffin, Dayton A. "WindPACT Turbine Design Scaling Studies Technical Area 1—Composites Blades for 80- to 120-Meter Rotor." NREL Report SR-500-29492, April 2001.

[20] Harrison, Robert, Erich Hau, and Herman Snel. "Large Wind Turbines – Design and Economics." John Wiley & Sons Ltd, West Sussex, England, 2000.

[21] Illsley, John. "History and Archeology of the Ship." Lecture notes, School of History and Welsh History University of Wales, Bangor, http://www.cma.soton.ac.uk/HistShip/shipind.htm (Accessed August 2006)

[22] Jackson, K., C.P. van Dam, and D. Yen-Nakafuji. "Wind Turbine Generator Trends for Site-specific Tailoring." Wind Energy, 8, pp. 443-455, 2005.

[23] Jangamshetti, Suresh H., and V. Guruprasada Rau. "Optimum Siting of Wind Turbine Generators." IEEE Transactions on Energy Conversion, Vol. 16, No. 1, March 2001.

[24] Lavery, Brian. "Ship – The Epic Story of Maritime Adventure." DK Publishing, New York, NY, 2004.

[25] Manwell, J.F., J.G. McGowan, and A.L. Rogers. "Wind Energy Explained – Theory, Design, and Application." John Wiley & Sons Ltd, West Sussex, England, 2002.

[26] National Renewable Energy Laboratories. S809 Aerofoil data downloaded from, http://wind.nrel.gov/designcodes/simulators/wtperf/ (Accessed June 2006)

[27] Patel, Mukund R. "Wind and Solar Power Systems." CRC Press, Boca Raton, FL, 1999

[28] REpower Systems. "REpower 5M." http://www.repower.de/index.php?id=237&L=1 (Accessed August 2006)

[29] Salameh, Ziyad M., and Irianto Safari. "Optimum Windmill- Site Matching." IEEE Transactions on Energy Conversion, Vol. 7, No. 4, December 1992.

[30] Sasi, K.K., and Sujay Basu. "On the Prediction of Capacity Factor and Selection of Size of Wind Electric Generators – a Study based on Indian Sites." Wind Engineering, Vol. 21, No. 2, pp. 74-88, 1997.

[31] Shevell, Richard S. "Fundamentals of Flight." Prentice Hall, Upper Saddle River, NJ, 1989.

[32] Stewart, Susan. "Offshore Wind Resources in the Southeast." Georgia Tech Strategic Energy Initiative Presentation at their workshop *Alternative Energy Technology Innovations: The Coming Economic Boom*, Savannah, GA, 2005.

[33] Tangler, J., and J. David Kocurek. "Wind Turbine Post-Stall Airfoil Performance Characteristics Guidelines for Blade-Element Momentum Methods." NREL Report CP-500-36900, Oct. 2004.

[34] Vestas Wind Systems. "V90-1.8 MW & 2.0 MW – Built on Experience." http://www.vestas.com/pdf/produkter/2006/V90_2_UK.pdf (Accessed August 2006)